^{40}Ar-^{39}Ar LASER MICROPROBE DATING OF MAFIC DYKES AND FAULT ROCKS IN HONG KONG

GEO REPORT No. 206

S.D.G. Campbell & R.J. Sewell

GEOTECHNICAL ENGINEERING OFFICE

CIVIL ENGINEERING AND DEVELOPMENT DEPARTMENT

THE GOVERNMENT OF THE HONG KONG SPECIAL ADMINISTRATIVE REGION

^{40}Ar-^{39}Ar LASER MICROPROBE DATING OF MAFIC DYKES AND FAULT ROCKS IN HONG KONG

GEO REPORT No. 206

S.D.G. Campbell & R.J. Sewell

This report was originally produced in April 2005 as GEO Geological Report No. GR 2/2005

Table of Contents
Table of Contents
Table of Contents
Table of Contents

First published, June 2007

Prepared by:

Geotechnical Engineering Office,
Civil Engineering and Development Department,
Civil Engineering and Development Building,
101 Princess Margaret Road,
Homantin, Kowloon,
Hong Kong.

Table of Contents

Table of Contents

Table of Contents

Table of Contents

PREFACE

In keeping with our policy of releasing information which may be of general interest to the geotechnical profession and the public, we make available selected internal reports in a series of publications termed the GEO Report series. The GEO Reports can be downloaded from the website of the Civil Engineering and Development Department (http://www.cedd.gov.hk) on the Internet. Printed copies are also available for some GEO Reports. For printed copies, a charge is made to cover the cost of printing.

The Geotechnical Engineering Office also produces documents specifically for publication. These include guidance documents and results of comprehensive reviews. These publications and the printed GEO Reports may be obtained from the Government's Information Services Department. Information on how to purchase these documents is given on the second last page of this report.

R.K.S. Chan
Head, Geotechnical Engineering Office
June 2007

Table of Contents Table of Contents Table of Contents Table of Contents

FOREWORD

Following a recommendation in GEO Report No. 118, pilot studies were carried out to investigate the application in Hong Kong of the Argon-Argon (Ar-Ar) method to dating both fault material, and mafic and intermediate dykes. The ^{40}Ar-^{39}Ar dating method is based on the same radioisotope decay system as that used in the K-Ar method of dating. The ^{40}Ar-^{39}Ar method, however, allows all information needed to calculate a sample's age to be determined from the Ar isotopic composition of irradiated samples. The ^{40}Ar-^{39}Ar laser step-heating method was therefore used in this study to date: age(s) of major phases of activity of selected faults; and ages of formation of selected mafic and intermediate dykes.

The study has demonstrated that dating of fault movements is feasible. The main phase(s) of fault activity identified during the study occurred about 70-90 million years ago (Upper Cretaceous). However, the technique appears capable of identifying fault histories in individual samples and younger fault events are also suggested by the data. These include events at 34, 10 and between 3 and 4 million years ago. The technique was not able to identify events more recent than about 3 million years ago. The technique was also successfully applied to the dating of the mafic dykes, the majority of which appear to have been emplaced between 87 and 100 million years ago.

The study was carried out, and the report was compiled, by Dr S.D.G. Campbell and Dr R.J. Sewell. The analyses were performed by the Argon Geochronology Laboratory (AGL), Department of Physics, University of Toronto, Canada. This report draws extensively on reports submitted by the AGL, and by Professors Derek York and Norman Evenson in particular, whose major contributions to the study are gratefully acknowledged.

(H N Wong)
Chief Geotechnical Engineer/Planning

Table of Contents
Table of Contents
Table of Contents
Table of Contents

CONTENTS

Page No.

Table of Contents
Table of Contents
Table of Contents

1. INTRODUCTION

GEO Report No. 118 (Sewell & Campbell, 2001) described various absolute age-dating studies carried out previously in Hong Kong on volcanic and plutonic rocks, superficial deposits and faults. One of the recommendations of the report was that pilot studies should be carried out to investigate the application in Hong Kong of the Argon-Argon (Ar-Ar) method to dating both fault material, and dykes of mafic and intermediate composition. An early pilot application of the Ar-Ar technique in 1993 had attempted to date mafic dykes in Hong Kong, as reported in Sewell & Campbell (2001). However, this had provided ambiguous results, possibly due to the susceptibility of the technique to resetting at temperatures above c.350^{o}C. Therefore further pilot studies were carried out to assess the viability of the technique more fully.

An initial pilot analysis of a single sample of andesite, reported elsewhere in detail (AGL, 1998), used the ^{40}Ar-^{39}Ar laser step heating method to date a single whole-rock chip from a metamorphosed andesite. The sample (HK 856) was obtained from the Tuen Mun Formation in the North-West New Territories of Hong Kong. This sample returned an age of 83.6 $\pm$ 0.4 Ma, which was considered to represent the time of metamorphic overprinting of the rock. Therefore, this demonstrated the potential use of the technique for dating deformation events in general, and possibly also major fault movements. The age spectrum of the sample also showed evidence for a multistage history. This was further confirmed by the analysis of two very small amphibole crystals from the same sample. These were dated at approximately 150 Ma, which are more consistent with Middle to Upper Jurassic emplacement ages for the rock inferred for these rocks (Sewell et al., 2000). While the multistage history would make such material unsuitable for conventional K-Ar dating, this preliminary ^{40}Ar-^{39}Ar dating study suggested that the dating of major fault/dynamic metamorphic events, and emplacement ages of such material was viable.

This report presents the findings of such pilot studies. The analytical work was carried out by the Argon Geochronology Laboratory (AGL) in the Department of Physics, University of Toronto, Toronto, Ontario, Canada, under the direction of Professors Derek York and Norman Evenson. The report draws extensively on reports produced by the AGL (2000a and b), under contract to the Geotechnical Engineering Office, of the then Civil Engineering Department.

2. OBJECTIVES OF THE STUDY

The main objectives of the study were to investigate the application of the ^{40}Ar-^{39}Ar laser step-heating method to dating:

(i) the age of formation of selected Hong Kong mafic and intermediates dykes, and

(ii) the age(s) of major phases of activity of selected faults.

Table of Contents
Table of Contents
Table of Contents
Table of Contents

3. METHODOLOGIES

3.1 General

The ^{40}Ar-^{39}Ar dating method is based on the same radioisotope decay system as that used in the K-Ar method of dating, whereby natural, spontaneous radioactive decay of the potassium isotope ^{40}K, occurs at a known rate to produce the isotope ^{40}Ar. The most fundamental difference between the ^{40}Ar-^{39}Ar and K-Ar methods (Noller et al., 2000) is that the ^{40}Ar-^{39}Ar method allows all the information needed to calculate a sample's age to be determined from the Ar isotopic composition of irradiated samples. In the simplest case, this requires measuring only the relative atomic abundances of ^{40}Ar, ^{39}Ar and ^{36}Ar by mass spectrometry; ^{36}Ar is used, as in K-Ar dating to provide information about non-radiogenic ^{40}Ar, most commonly in making air correction. The measurement of K indirectly via ^{39}Ar is more precise and has better abundance sensitivity (Noller et al., 2000) than most of the commonly used techniques for measuring K in K-Ar dating, and avoids error due to potential homogeneity of K, and thus avoids the need to measure absolute amounts of Ar. The advantages of the ^{40}Ar-^{39}Ar dating method generally outweigh those of the K-Ar method, although the latter is cheaper and faster, and is not subject to recoil of ^{39}Ar atoms produced by the ^{39}K-^{39}Ar reaction (redistribution and/or loss of ^{39}Ar within/from small samples potentially introducing artificial age complexities to age spectra without necessarily affecting the total gas age).

The ability to calculate an age using only Ar isotope data permits the analysis of extremely small samples, including individual crystal phases (e.g. mica, feldspar, pyrite, chlorite), by incremental heating or total fusion. This enables potentially complex histories of formation and deformation (e.g. faulting) to be dated separately within the same samples. The analyses reported here used a laser step-heating incremental technique.

3.2 Mafic Dykes

Dating of basaltic samples has traditionally been carried out by whole rock analysis, rather than by dating of individual mineral phases. Previous work in Hong Kong by Chandy and Snelling (in Allen & Stephens, 1971) used the Potassium-Argon (K-Ar) decay system to determine the ages of 'dolerites', and suggested that two episodes of intrusion were represented: Upper Cretaceous and Palaeocene.

An early pilot application in 1993 of the Ar-Ar technique to date mafic dykes in Hong Kong, reported in Sewell & Campbell (2001), provided ambiguous results, possibly due to the susceptibility of the technique to resetting at temperatures above c.350^{o}C.

For the present study, the dyke material available for analysis (Table 1, Figure 1), was examined under a binocular microscope, after gentle crushing in a mortar. This confirmed that most of the samples were too fine-grained to allow significant mineral phases to be separated. Therefore, most of the irradiated material consisted of whole-rock chips. However, one sample (HK 9842) yielded small pyrite and chlorite and small (0.25 mm diameter) dark mica, as a result of which, dating of pyrite was attempted in one instance.

Table of Contents
Table of Contents
Table of Contents
Table of Contents

3.3 Fault Rocks

There have been comparatively few attempts to use the K-Ar decay to date fault movements. Previous studies have used K-Ar on fault gouge clays, and Ar-Ar on pseudotachylyte (e.g., Kelley et al., 1994; Kralik et al., 1987), but both techniques were applied to material at least 10^7 years old. The challenge of constraining the ages of more recent fault movements, from the more common minerals present in Hong Kong's faulted (commonly schistose and mylonitic) rocks such as those used in this study (Table 1, Figure 1), required new approaches and experimental development.

A twofold approach was adopted:

(i) To indirectly constrain the age of faulting by dating hydrothermal mineralization in the faulted rocks, using the concept that permeable pathways for fluids are often created during active crustal deformation. This strategy was suggested both by the presence of sufficient quantities of pyrite in one of the samples, and by the successful determination of ^{39}Ar and ^{40}Ar in a single cube of this mineral in the parallel work on dykes.

(ii) To directly constrain the age(s) of faulting by identifying extremely small heating events that may be present in the silicate minerals of the faulted rocks. This involved very delicate heating of large samples with a broad beam defocused laser.

4. ANALYTICAL PROCEDURES

To prepare the samples for irradiation, fragments of the appropriate portions of the samples were gently crushed in a mortar and examined under a binocular microscope. Since feldspar is potentially very sensitive to subsequent thermal events, this mineral was separated by hand picking. Several of the fault rock samples yielded feldspar crystals large enough (2-5 mm) to allow very detailed step heating in the low temperature portion of the age spectrum. In addition, fault rock sample HK12078 yielded pyrite grains that were separated in an attempt to date hydrothermal events. However, most of the dyke samples were too fine-grained to allow significant mineral phases to be separated, although HK 9842 yielded small amounts of pyrite and chlorite and a small (0.25 mm diameter) dark mica. Hence, most of the irradiated dyke material consisted of whole-rock chips.

For all samples, the rock chips and crystals were packaged in aluminum foil and loaded into an aluminium canister, together with a number of grains of Fish Creek Tuff sanidine standard (FCT) in the case of the dyke samples, and Taylor Creek Rhyolite sanidine standard (TCR) in the case of the fault rock samples, and irradiated in the McMaster Nuclear Reactor, Hamilton, Ontario, Canada, for a total of 48 Megawatt-hours (approx. 24 hours) for dyke samples and for approximately 0.3 Megawatt-hours (about 10 minutes) for fault rock samples. For the latter samples, a Cd liner was used during the irradiation to avoid production of ^{40}Ar, thus eliminating errors from the corresponding correction.

Table of Contents
Table of Contents
Table of Contents
Table of Contents

All of the samples and standards were then analyzed as part of five separate sample loadings. In each loading, the samples and standards were placed into holes in an aluminum disk and loaded into the ultra-high vacuum sample chamber within the mass spectrometer inlet system. After pumpdown, the sample chamber and gas extraction line were baked at 150˚C for approximately 12 hours for the dyke samples, and 48 hours for the fault rock samples, to achieve low argon blank levels.

The first stage in analysis was to fuse each of the standards in a single heating step, using a 20 watt Spectra-Physics argon-ion laser. The evolved gas was then purified by the combination of a liquid N_2 cold-tra to remove condensable gases and an SAES type 707 Ti-Fe-Zr getter held at 250°C to remove all remaining reactive gases. The remaining noble gas component was inlet into a VG1200 mass spectrometer equipped with an ion multiplier for analysis of argon. The mass spectrometer was operated in static mode, isolated from the pumps during the analysis. All five natural and irradiation-produced argon isotopes (^{36}Ar through ^{40}Ar) were measured in 15 successive cycles over about a twenty-minute period, followed by pumping out of the mass spectrometer. Procedural blanks (in which all steps except the laser heating were followed) were performed before each analysis. The resulting argon isotope measurements were reduced using software developed in-house, which included correction for atmospheric contamination and for interfering nuclear reactions resulting from the irradiation, as well as appropriate statistical analysis of the data, including a detailed treatment of error propagation. The J value (essentially the efficiency of ^{39}Ar production from ^{39}K) was calculated for each standard, using an age of 27.84 Ma for the FCT standard. A weighted average of the J values from all standards was used as the J value for the irradiation.

The samples were analyzed by an identical procedure, except that for the whole rock chips, feldspar separates and three of the pyrites, the gas release was done in a series of heating steps. In each heating step, the laser heated the sample for 30 seconds, followed by the gas purification and analysis steps as above. In successive heating steps the laser power was gradually increased until the sample was fused in the final step.

5. ANALYTICAL RESULTS AND INTERPRETATION

5.1 General

The first-order result of any Ar-Ar analysis is the integrated age calculated from the total sample gas released in all step-heated fractions. This is equivalent to the K-Ar age of the sample. The ages are subject to the usual uncertainties of K-Ar dating, in particular to loss of Ar during secondary heating events. Therefore Ar-Ar data are usually interpreted by use of the conventional age spectrum plot of cumulative ^{39}Ar release *vs.* apparent age. The apparent ages are calculated assuming that all of the initial trapped Ar in the sample is atmospheric in composition. If this assumption does not hold, or if recoil of ^{39}Ar during sample irradiation is significant, then the $^{36}Ar/^{40}Ar$ *vs.* $^{39}Ar/^{40}Ar$ correlation diagram is considered to be to be a more precise and flexible tool for interpretation.

5.1.1 Remarks on Whole-rock and Feldspar Analyses

The direct dating approach to more recent fault movements requires a sensitive

Table of Contents
Table of Contents
Table of Contents
Table of Contents

potassium-rich chronometer to search for a possible weak, friction-related, heating signal. In principle, a near-zero age, suggestive of a very recent event, may be registered in domains at the surface of the crystal, where the ^{40}Ar built up by previous millions of years of ^{40}K decay is most easily lost. If a near-zero event can be extracted in the laboratory when a crystal is sequentially heated to higher temperatures, these surface regions should degas in the lowest temperature fractions before the more tightly held K-Ar domains from the interiors of the crystal diffuse out. On the age-spectrum, the record of this event may be recognized by a pattern of fractions, climbing from a near-zero age in the first releases of ^{39}Ar, up to an age more characteristic of the bulk of the sample.

Different mineral components in a rock will react differently to such subtle and transient heating events, and the K-feldspar is typically one of the most easily disturbed radiogenic systems, in particular for Ar-Ar analysis. Therefore, this characteristic pattern was looked for in large single feldspars from three samples, and large whole-rock chips from two of the remaining samples that did not yield appropriate feldspars. These samples were carefully step-heated, focusing on their very low temperature gas releases, to determine: if a pattern climbing from ~0 Ma existed, and; to determine the proportion of the low-age region in the crystal, to assess the magnitude of the effect that a possible signal would have on a mineral in the fault rock.

In typical step-heating analyses in Ar-Ar dating, where perhaps 10 steps may normally be taken, the lowest temperature fraction will therefore comprise about 10% of the total ^{39}Ar released, and will represent a mixture of all the gas extractable up to that point. However, any low-age signals, if present, would probably amount to only a few percent at most. Furthermore the absolute error in age determination is normally a direct function of the amount of argon being measured. Therefore to measure low ages on small proportions of the total sample argon, with reasonably small relative errors, quite large total samples would need to be used. These samples must be heated gently and as uniformly as possible, with a broad-beam, defocused laser beam.

The samples used were single crystals or rock chips, 2-5 mm in diameter. These required long clean-up times to handle the additional gas load, which in turn increased the analytical blanks. These analyses required very careful attention to both the blanks and sample analyses to make precise and accurate measurements of the small quantities of ^{39}Ar and the ^{40}Ar/^{36}Ar ratios.

5.1.2 Remarks about Pyrite Analyses

Like many minerals that do not contain potassium, but which may host K-bearing inclusions (*e.g.*, quartz), pyrite is likely to show very low diffusion rates for K, and probably for Ar as well. This would imply that, once the pyrite has formed, the K and Ar of the inclusions would remain relatively firmly trapped within the pyrite crystal, and that the K-Ar age of the inclusions would therefore be resistant to thermal resetting.

A complication for Ar-Ar dating is that tiny, K-rich inclusions, hosted within a K-free pyrite phase, could be highly subject to redistribution of ^{39}Ar by recoil during irradiation. When samples are irradiated with fast neutrons in a nuclear reactor to produce ^{39}Ar from ^{39}K, the products are a ^{39}Ar nucleus and a proton. The proton is violently ejected from the ^{39}Ar

Table of Contents
Table of Contents
Table of Contents
Table of Contents

nucleus, causing that nucleus to recoil from the original position of the ^{39}K parent, for a distance of about 0.1mm through the crystal lattice. If the sample contains a microstructure of the order of 0.1mm in size (such as exsolution structures in feldspars, or tiny inclusions), this recoil can carry the product ^{39}Ar atom between K-rich and K-poor sites in the sample. This destroys the correlation between ^{40}Ar produced by radioactive decay in nature and ^{39}Ar produced from K in the reactor, the correlation on which the Ar-Ar method depends.

5.2 Dyke Samples

Four whole rock samples of mafic dykes (HK1651, HK9728, HK9842 and HK10981) were analysed.

The age-spectra of the four dyke whole-rocks proved to be complexly discordant and difficult to interpret using conventional age-spectrum diagrams. Much of this discordance is likely to have resulted from ^{39}Ar redistribution between the fine-grained minerals within the samples. Such recoil-induced redistribution destroys the coupling between ^{39}Ar (the surrogate for the parent ^{40}K) and ^{40}Ar (the daughter) and renders ages calculated from the resulting ^{40}Ar/^{39}Ar ratios meaningless. In addition to internal redistribution of ^{39}Ar, such recoil-affected samples may also be subject to overall loss of ^{39}Ar, causing their integrated ages to be biased upwards. However recent research on dating of fine-grained sediments (Hu et al., 1998) has shown how to recognise the effects of recoil on the Ar correlation diagram. In many cases, horizontal line segments joining successive points can identify recoil-afflicted data. Accordingly, the isochron plot was used to interpret the complex step-heating data of these analyses. In order to follow the often complex trajectories of successive fractions on the correlation diagram, it was necessary to analyse an unusually large number of step-heated fractions of the whole-rock samples. Interpretation of the isotope data for the minerals was more straightforward and is reported as plateau plots or integrated ages. In both age plateaux and isochrons, a sequence of successive gas fractions are usually required to lie on a single plateau or isochron, within analytical error. In several cases, however, fractions were excluded from the calculation because of excessive scatter from the trend; such cases are indicated in the discussion below and in Table 2.

Summaries of the analytical data for one mica and four whole rock analyses are contained in Appendix A. The data are displayed graphically in Figures 2 to 14 (In Fig. 2, as in the other Figures, the fractions are labelled by their sequential fraction numbers, as given in Appendix A), and summarized in Table 2.

5.2.1 HK1651

HK1651 was obtained from a 1 m wide mafic dyke, intruding the Tsing Shan Granite (age c.159 Ma (Sewell et al., 2000)) in the North-West New Territories. The whole-rock fragment was analyzed in 42 heating steps and yielded the youngest integrated age of the dykes, at 74.7 $\pm$ 0.3 Ma (see Table 2). Its age spectrum (Fig. 2) is quite complex. Over much of the ^{39}Ar release, the ages gently rise to about 75 Ma, very close to the integrated age. The overall impression is of a relatively young sample (approximately 70-80 Ma), but it is difficult purely from the age spectrum to interpret the behaviour of this sample. However, Fig. 2 shows the spectrum divided into regions of varying Ar-isotope behaviour, as inferred

Table of Contents
Table of Contents
Table of Contents
Table of Contents

from examination of the argon correlation diagram.

On the $^{39}Ar/^{40}Ar$ *vs.* $^{36}Ar/^{40}Ar$ plot, the data display three separate linear segments that yield progressively higher ages (Fig. 3). Two are confined to relatively low temperatures and appear within the first ~20% of the sample's total ^{39}Ar release. Fractions 1-6 (omitting fraction 2) fit an isochron corresponding to an age of 59.8 ± 4.3 Ma. The initial $^{40}Ar/^{36}Ar$ of this isochron is 375 ± 17, significantly higher than the atmospheric $^{40}Ar/^{36}Ar$ ratio of 295.5, represented by the label "Nier" on the $^{36}Ar/^{40}Ar$ axis (Fig. 3). This isochron could represent a relatively low-temperature event at about 60 Ma which reset the less retentive sites in the whole rock, without completely degassing the radiogenic ^{40}Ar already accumulated (hence the high initial $^{40}Ar/^{36}Ar$ ratio).

Fractions 7 to 11 form a roughly horizontal array on the correlation diagram (Fig. 3), and could therefore represent the effects of recoil redistribution of ^{39}Ar in this fine-grained whole rock. Since recoil can move ^{39}Ar between phases, but does not affect the ^{36}Ar and ^{40}Ar, it produces a horizontal shift along the $^{39}Ar/^{40}Ar$ axis in the diagram.

Fractions 12 to 16 form the second linear segment (Fig. 4) and give a significantly older isochron age of 70.1 ± 0.4 Ma with an initial $^{40}Ar/^{36}Ar$ of 294 ± 8, indistinguishable from atmosphere. Since the initial ratio is atmospheric, these fractions appear as a short plateau on the age spectrum (Fig. 2). These are followed by fractions 17 to 19, lying along a line segment extending at an angle to the isochron, from fraction 16 as a pivot point. Although resembling the "ambichrons" described by Hu et al. (1998), and labelled as such on Fig. 2, it is too short to attach any significance to.

The largest single portion of the gas released (representing ~40% of the total ^{39}Ar), in fractions 21 to 33 (Fig. 2), appears to represent recoil. In Fig. 5, these fractions show erratic horizontal motion (the signature of recoil) between the 70.1 Ma isochron and an older 75.1 Ma isochron formed by fractions 34 to 39 (omitting fraction 37). These high-temperature fractions define the third linear segment, and give an isochron age of 75.1 ± 0.8 Ma, a result that is within analytical uncertainties of the integrated age of 74.7 ± 0.3 Ma for this sample. The initial $^{40}Ar/^{36}Ar$ ratio, at 353 ± 73, is not distinguishable from that of the atmosphere.

The coincidence of the integrated and final, high-temperature isochron ages (Table 2) suggests that this may be the age of formation of this sample, and that recoil redistributed ^{39}Ar in the sample, but produced no net loss of ^{39}Ar. Alternatively, but perhaps less probably, this age could represent a metamorphic event in which the resetting of the argon systematics was total, leaving no vestige of any earlier event in the argon record.

5.2.2 HK9728

The whole-rock sample HK9728 was obtained from a 1 m wide dyke intruding the High Island Formation (age c. 140 Ma (Sewell et al., 2000)) in the North-East New Territories. This sample had the highest integrated age of the four whole rocks in this study, at 105.3 ± 0.5 Ma. On the age spectrum (Fig. 6), the high integrated age results from a step-like rising of ages over about the last third of the ^{39}Ar release. This corresponds to a change from a high-Ca/K phase or phases, contributing the earlier portion of the spectrum, to

Table of Contents
Table of Contents
Table of Contents
Table of Contents

a low-Ca/K material, providing the step-like portion. It is possible that the steps represents an event at ≥160 Ma, followed by almost total loss of argon from the rock at about 100 Ma. However the correlation diagram provides another view of these data.

The data form a V-shaped pattern on the $^{39}Ar/^{40}Ar$ vs. $^{36}Ar/^{40}Ar$ plot (Fig. 7). Fractions 3 to 7 (omitting fraction 6) form a straight-line segment in the upper arm of the V, and give an apparent age of 99.8 ± 0.5 Ma with an initial $^{40}Ar/^{36}Ar$ of 297 ± 6. The lower arm of the V is made up of higher temperature fractions (9 to 15). However, rather than being perfectly linear, this arm curves gently upward, giving it an ambiguous status. A line can be fitted to these data in several plausible ways. For instance, fractions 9 to 16, excluding fraction 15, yielded an age of 93.8 ± 1.9 and an initial $^{40}Ar/^{36}Ar$ of 715 ± 41 (Table 2). The $\Sigma S/(n\text{-}1)$, a measure of goodness of fit, is close to its expected value of 1.0 (Table 2). A subset of these, fractions 10 to 12, very closely fit a line (Fig. 7) giving an age of 87 ± 12 Ma and an initial $^{40}Ar/^{36}Ar$ of 908 ± 295 (Table 2). These two isochrons are mutually consistent, because the shorter segment of fractions 10 to 12 yields higher errors in both age and initial ratio (because of the greater uncertainty in extrapolating this short segment to intercept the two axes). Both isochron ages are younger than the integrated age of 105.3 ± 0.5 Ma. However the apparent curvature of fractions 9 to 16, if it is real, suggests the involvement of at least three reservoirs rather than the two required by the isochron model, which may not therefore be strictly applicable.

5.2.3 HK9842

HK9842 was obtained from a 1 m wide dyke cross-cutting rhyolite dykes (age c. 146 Ma, Sewell et al., 2000)) from the northeast of Lantau Island. This sample was the only one from which useful mineral separates were obtained. In addition to the whole rock, which was analyzed in 40 heating steps, individual grains of dark mica, pyrite and chlorite were analyzed. The mica, despite its very small size (0.25 mm diameter) was analyzed in eight heating steps. The other two minerals were too small in size and too low in K to step heat, and were analyzed by one-step total fusion.

In spite of the detailed step heating of the whole rock fragment into a total of 40 fractions, this sample showed very few convincing lineations on the $^{39}Ar/^{40}Ar$ *vs.* $^{36}Ar/^{40}Ar$ plot (Fig. 8). Most of the fractions (corresponding to more than 60% of the ^{39}Ar) appear to have been affected by ^{39}Ar recoil, as shown by erratic horizontal trajectories and the absence of linear segments on the correlation diagram. For this reason, the best age estimate may be given by its integrated age of 91.0 ± 0.4 Ma. However, because of the possibility of overall loss of ^{39}Ar during irradiation, minerals separated from the rock may provide more reliable ages. Single-crystal integrated ages for pyrite and chlorite are 88 ± 11 (P22-119) and 80.8 ± 4.9 (P22-120) Ma, respectively (Table 2). These are K-poor phases and had to be fused in single shots. On the other hand, although mica separated from the rock (P22-107) was very small, it could be step-heated to yield eight age fractions. The mica age spectrum (Fig. 10) displays a plateau (fractions 2 to 4) constituting 63% of the ^{39}Ar released, and corresponding to an age of 108.3 ± 1.6 Ma. This result is in close agreement with the integrated age for the mica of 106.2 ± 1.7 Ma. However, small micas in this size range may also be subject to ^{39}Ar recoil loss, which would increase their apparent Ar-Ar age. On Figure 10, two curved lines are sketched, suggesting the resemblance of this mica to the “two-faced” mica discussed by York & Lopez-Martinez (1986), and indicating diffusional loss of argon.

Table of Contents
Table of Contents
Table of Contents
Table of Contents

5.2.4 HK10981

Sample HK10981 was obtained from a 1 m wide dyke intersected in a borehole on Ma Wan Island. The dyke formed the margin of a quartzphyric rhyolite dyke (age c. 146 Ma (Sewell et al., 2000)). A whole rock sample was heated in 18 steps, and gave an integrated age of 96.2 ± 0.4 Ma. The age spectrum, while appearing more straightforward than the other whole rocks (Fig. 11), shares with HK9728 the upward-rising portion at the end of the spectrum (Fig. 6). Although the rise is less marked than in HK 9728, the similarity of the two samples extends to their correlation diagrams.

Step-heated fractions of whole rock form an isotopic pattern on the $^{39}Ar/^{40}Ar$ *vs.* $^{36}Ar/^{40}Ar$ plot (Figs. 12 and 13) that is reminiscent of the V distribution of whole rock HK9728 (Fig. 7). Fractions from the low-temperature arm of the V (fractions 4-6) give an age of 89.3 ± 0.9, with an initial ratio within 2σ of that for the atmosphere, at 403 ± 56. Nine high temperature fractions (10-18) give an isochron age of 86.6 ± 1.8 Ma with a distinctly elevated initial $^{40}Ar/^{36}Ar$ of 998 ± 163. Both ages are significantly younger than the integrated age of 96.2 ± 0.4 Ma.

5.2.5 Summary

A summary histogram of all whole rock and mineral ages for the dykes is presented in Figure 14. Each age contributes equal area Gaussian to the total. The width of the Gaussian, and so its height, reflects the error of that age. These result are considered further in Section 6.

5.3 Fault Rock Samples

Five samples of fault rocks (HK3419, HK7284, HK7729, HK12078 and HK12086), were analysed.

Unlike the situation for the dykes that were analysed, the correlation diagrams for the fault rocks offered no additional insight into the most recent, low-temperature events, on which the study focussed. In particular, as the study was looking for very faint traces of relatively subtle events (compared to the more pervasive heating events usually recorded in Ar-Ar analysis), it was necessary to interpret the data on a step-by-step basis, rather than in a broader search for plateaux or correlation lines. Therefore the interpretations presented must be regarded as tentative. Apparently, no previous study had attempted to recover such faint traces of recent, low-temperature events. Given this, and the absence of independent dating of possible fault activity by other techniques, the information recovered from these samples should be regarded only as suggestive. Nevertheless it is felt that the results are indicative of the potential of the methods used, if applied in a more extensive and controlled study.

The data and interpretations are presented in a case-by-case format, beginning with the data for pyrite crystals separated from HK12078, and then the step-heating data for the whole rocks and minerals from the five samples analyzed.

Table of Contents
Table of Contents
Table of Contents
Table of Contents

Summaries of the analytical data for one pyrite, three K-feldspars, and two whole rock analyses, are contained in Appendix B. The data are displayed graphically in Figures 15 to 31, and summarized in Tables 3 to 5.

5.3.1 Pyrite from HK12078

Pyrite is not a conventional material for K-Ar analysis; the only published study known prior to this study were from earlier work by the AGL, but carried out by pre-laser techniques (York et al., 1982). However a single-crystal pyrite had been analysed by laser fusion in the dyke portion of this study, which produced the first known single-crystal Ar-Ar analysis of pyrite. Since pyrite mineralization may occur in the hydrothermal environment associated with fluid movement along faults, its potential in dating fault activity was explored.

Pyrite is not a K-bearing phase, and any significant potassium (with its daughter argon) must be sited in inclusions within the pyrite crystals. The occurrence of such inclusions is not guaranteed. Also, their abundance and nature could vary on a crystal to crystal basis, as could the actual formation time of pyrite grains. Therefore, single-crystal analysis is a logical tool to explore pyrite geochronology. The measured Ar-Ar age of the inclusions should correspond to that of their host pyrite.

Separated pyrite cubes from HK12078, an altered coarse-grained granite (the Sha Tin Granite) from a fault in the Rambler Channel, ranged from 0.2 to 0.7 mm in diameter. Twelve single grains were analysed, of which nine were fused in a single step and 3 were subjected to step-heating analysis. Because of the small amounts of gas released from the pyrite samples, only one grain yielded as many as nine steps; the other two grains gave only 2 and 5 steps respectively. The age spectra of the step-heated pyrites were not very coherent, and are considered to have been largely affected by recoil, with possible effects of multiple generations of pyrite and/or inclusions. Therefore the gas fractions from the individual steps were mathematically combined to yield integrated age data for the step-heated pyrites. Table 4 shows the single-step and integrated ages for the 12 pyrite crystals. The weighted mean age of 11 of the crystals, deduced from their total fusion ages and their integrated ages from the 3 step-heating runs, is 78.5 ± 2.8 Ma. The single outlier, P23-21 has a significantly younger total-gas age of 44.2 ± 2.1 Ma.

The ages of the 12 pyrites are summarized in Figure 15. This plot is an age histogram in which each of the 12 ages and its associated error is used to generate a corresponding bell-shaped gaussian probability density curve. Each curve encloses the same area, so that a small error yields a narrow but high gaussian curve, while a large error gives a broad but low curve. The curve plotted in Figure 15 was then generated by summing the 12 individual gaussian curves to yield a complex curve which shows the overall distribution of ages and errors in the population. For instance, the outlier at 44.2 ± 2.1 Ma shows up as an almost isolated gaussian at the left of the Figure, and demonstrates the shape and size of a single gaussian contributor to the sum.

No single-step pyrite or significant gas fraction within the step-heated pyrites yielded an age of less than 35 Ma. Thus, although the pyrite ages significantly post-date the presumed crystallization of the Sha Tin Granite at 146 Ma (Sewell et al., 2000), no sulphide generations could be attributed to relatively recent faulting episodes.

Table of Contents
Table of Contents
Table of Contents
Table of Contents

5.3.2 HK7284

A whole rock sample was obtained from HK7284, a weakly sheared coarse ash crystal tuff from the Tai Mo Shan Formation. The results from the first six steps of a step-heating run are shown in Figure 16. The errors in age are relatively large, and while two of the steps are within 2σ of zero age, all of the age steps are well within 2σ of 90 Ma. The large errors result from the surprisingly small amount of Ar extracted from the sample, although by the end of the sixth step, the sample had been significantly heated. This sample therefore appeared to show no evidence of young (a few Ma) ages as was seen in other samples (see below), and further study, including completion of the step-heating run, was not pursued.

5.3.3 K-Feldspar from HK12086

The age spectrum of feldspar (P23-137) extracted from HK 12086, a strongly sheared coarse-grained granite (Sha Tin Granite) from the Tolo Channel Fault, is shown in Figure 17, and an expanded view of the first 6.4% of the released ^{39}Ar in Figure 18. (The expanded spectrum here and in subsequent Figures still has an abscissa labelled from 0 to 1, but the fraction of ^{39}Ar in the expanded diagrams is given in the upper right corner.) The spectrum climbs from within 1σ of zero (12 ± 14 Ma) in the first fraction (0.3% of ^{39}Ar) to 35 Ma in the first 6.4% of evolved ^{39}Ar (Fig. 18). Within this interval, small amounts of ^{39}Ar are present in the first 3 fractions and form an age plateau within their respective errors (plateau age = 17 ± 12 Ma). However, their corresponding ^{40}Ar/^{36}Ar ratios are not significantly more radiogenic than present atmosphere, and the relatively large uncertainties in the small ^{39}Ar signals preclude precise age determination for this portion of the spectrum.

Significant quantities of radiogenic ^{40}Ar (*i.e.*, sample ^{40}Ar/^{36}Ar ratios distinguishable from the present atmospheric ratio of 295.5, and therefore ages distinguishable from zero) are first detected starting at fraction 4, which yields an age of 31 ±6 Ma. Most of the spectrum is in the region of 60-80 Ma, consistent with ages frequently observed in these samples (*cf.* below). The meaning of the rise to 180 Ma in the final fraction is obscure, but may reflect a recoil component.

5.3.4 K-Feldspar from HK12078

Over 99% of the age spectrum of a K-feldspar (P23-20), extracted from HK 12078, an altered coarse-grained granite (Sha Tin Granite) from a fault in the Rambler Channel, lies at ages of 60 Ma or more, rising across the spectrum to ages around 70 Ma (Figure 19). This sample therefore appears to be virtually unaffected by younger events. Nonetheless, the first step, representing only 0.08% of the total evolved ^{39}Ar, gives an age 4 ± 8 Ma (Figure 20). Note that any conventional Ar-Ar analysis would utterly fail to reveal any sign of this tiny initial low-age fraction.

The very steep rise to an approximate age plateau is precisely the type of spectrum we would expect of a sample transiently and only moderately heated during fault movement. The tiny size of the initial, low-age gas fraction points up the challenge of accurately measuring such minute quantities of argon. Despite the fact that this first fraction is indistinguishable from zero age, the value of 4 ± 8 Ma is interesting in terms of the ages yielded by the following two samples.

Table of Contents
Table of Contents
Table of Contents
Table of Contents

5.3.5 K-Feldspar from HK3419

The age spectrum of a feldspar extracted from the fault rock within the Tai Mo Shan Formation at the base of a thrust fault, shows the most extended low-age portion of any of the samples studied (Figure 21). The first three fractions have $^{40}Ar/^{36}Ar$ ratios that are significantly higher than modern atmosphere, but their ^{39}Ar levels are only slightly higher than those of the blank, and thus their ages are poorly constrained. In all, these three fractions represent less than 0.2% of the total sample ^{39}Ar. The three subsequent fractions 4-6 yield significantly more ^{39}Ar (amounting to 4.6% of the total) and uniform ages averaging to 4.12 ± 0.19 Ma. They thus form a rather precise mini-plateau prior to the climb to older ages, starting with fraction 7 (Figure 22).

Almost 70% of the ^{39}Ar in this sample lies in a slightly ragged plateau around the ubiquitous 80 Ma age (Figure 21; the drop in age in the final 1% may well be a recoil effect). But despite the reasonably well-defined plateau, this sample has lost considerable radiogenic argon. Furthermore, the shape of the age spectrum is not that of a simple diffusional loss, as can be seen from the broad low-age region. Rather than a smooth rise from low ages to the plateau, over 10% of the sample ^{39}Ar is released with ages less than 10 Ma. This tends to support the reality of the low-age plateau at about 4 Ma.

5.3.6 Whole Rock from HK7729

The spectrum of whole rock sample**,** extracted from a mylonite within the Tai Mo Shan Formation at the base of the Tiu Tang Lung Thrust, rises to an age greater than 90 Ma after only 2.9% of the ^{39}Ar was released (Figure 23). The very low-temperature interval prior to 90 Ma consists of 9 steps that climb in age in a discontinuous fashion. The first fraction has a $^{40}Ar/^{36}Ar$ ratio within error of the atmospheric value and gives an apparent age within error of zero. The ensuing 4 fractions form a short plateau with an age of 3.0 ± 0.2 Ma, after which the spectrum jumps to ~8 Ma in the next two fractions (Figure 24). Two fractions around 30 Ma comprise less than 0.5% of the sample ^{39}Ar, after which the age rises sharply to over 90 Ma (Figure 23).

The initial region of this spectrum bears a strong resemblance to that of the HK3419, from the same formation, but from a different fault zone, except that the initial portion is compressed by about a factor of ten in ^{39}Ar. If feldspar within this whole-rock sample is responsible for the behaviour, it demonstrates that feldspar is indeed a sensitive recorder of low-temperature events.

The unusual bowl-shape of the central part of the age spectrum should not be taken too literally. This sample contained massive amounts of argon, and in order to measure its total ^{39}Ar content, the mass spectrometer was operated in ranges far in excess of the calibrated levels. Therefore, while the proportions of total sample ^{39}Ar are at least approximately correct, the isotopic ratios and therefore the ages are highly suspect in the very large middle fractions (at least fractions 12-16). As fraction sizes again approached the smaller, better-calibrated region, the ages again approach 90 Ma. Nevertheless this polymineralic whole rock may exhibit some real anomalies in its behaviour.

Table of Contents
Table of Contents
Table of Contents
Table of Contents

6. CONCLUSIONS

Ar-Ar dating of the whole rocks and minerals from the dykes yielded four possible whole-rock and five possible mineral ages between 60 and 108 Ma (Table 2). Their distribution is plotted on Figure 14, which displays the ages as the sum of gaussian curves of identical areas for each analysis. The solid area represents the whole-rock ages, and the superimposed outlined area, the mineral ages.

The youngest sample in the study was HK1651, for which all three possible ages, and the integrated age, are younger than any ages produced from the other samples. The oldest of these ages is about 75 Ma. Whether this represents an emplacement age or the time of pervasive metamorphism cannot be directly determined.

The oldest age in any of the samples is recorded by the mica, which gives a plateau age of 108 Ma. This may provide the best estimate of dyke emplacement, although there is a strong possibility of recoil loss of ^{39}Ar in such small biotite. If this age is excluded, along with those from HK1651, the remaining ages cluster between 87 and 100 Ma for the whole rocks, with the chlorite age bringing the range down to 81 Ma if the minerals are included. There is therefore little direct evidence from the argon system for any events older than about 100 Ma affecting these rocks. Either they were emplaced by this time, or pervasive metamorphism had wiped out virtually all trace of their emplacement age. However, it is also possible that all of the ages reflect overprinting events. Regardless, the record of two or more ages in a single whole rock sample shows that these dykes have been strongly affected by metamorphism. Metamorphic disturbance is also suggested by the dip to 86 Ma from the plateau age of 108 Ma in the mid-to high temperature portion of the mica age-spectrum (York & López-Martinez, 1986). A similar event appears to be recorded by the chlorite and pyrite, which also give ages significantly younger than the mica plateau. However, the significance of Ar-Ar ages in the chlorite and pyrite are uncertain.

The very low concentrations of K in pyrite and chlorite make single-grain dating of these phases difficult. The first Ar-Ar dating of pyrite (York et al., 1982) used bulk separates from Archean rock, and showed that the age corresponded to the time of major orogeny. Pyrite from HK9842 represented the first known analysis of a single crystal, and although its age is imprecise, because of the extremely small gas evolved from a tiny cube, it corresponds to the chlorite age and may similarly record metamorphism in the dyke.

The interpretation of the whole-rocks shows that, in spite of pervasive discordance apparent in the age-spectra, well-defined ages can be obtained from three of the four whole rocks, using the isochron diagram. In each sample, the proportion of the step-heating data forming lineations on this plot appeared to be inversely proportional to the amount of recoil-affected data. The most heavily affected sample, HK9842, having almost three-quarters of its fractions being affected by recoil, yielded no definitive line segments. The isochron ages from the straight line segments of the whole rock data range from 60 to 87 Ma. Ages derived from high temperature segments for three of the dykes correspond roughly with the chlorite/pyrite peak, possible reflecting the same overprinting episode (Figure 14). If this is the case, then the whole-rocks have experienced significant resetting of their K-Ar systems, and/or easily reset K-rich minerals dominate their mineralogy.

Table of Contents
Table of Contents
Table of Contents
Table of Contents

Five samples from fault zones were examined, particularly to determine whether any signature of relatively recent events could be found in the Ar-Ar systematics. Since this was the first study of its kind, it was necessary to explore innovative approaches. One approach, using pyrite crystals found in one sample, attempted to date hydrothermal activity presumed to be associated with the fault zone, and yielded no ages younger than about 30 Ma. The other approach, using very subtle age data contained in the first few percent of argon released during laboratory heating, was far more encouraging. Four of the samples showed evidence of a 34 Ma event. The 34 Ma event appears to accord well with an important tectonic event in the region, marking the ignition of sea-floor spreading in the South China Sea. Two samples also showed evidence of events at about 10 and 3-4 Ma. These may well represent the effects of tectonic activity along these faults at these times.

The age-spectra of the four fault rock samples dominated by >50 Ma fractions indicative of their early evolution, also contained low temperature portions that pass close to zero-age. This shows that the low temperature portions of these fault rocks are capable of recording their much more recent geological history in addition to their igneous/metamorphic crystallization ages. The imprint of these late-stage events appears to be very minor: for three of the samples, this near-zero-age portion comprising less than 2% of the total sample ^{39}Ar volume. The individual step ages of the low temperature portions of the age spectra are summarized for each sample in Figures 25-28 (which are age histograms of the type used above for the pyrite data shown in Figure 15). In Figure 29, these low-temperature steps are summed for all four of the samples, while Figure 30 shows an enlarged view of the first 20 Ma of Figure 29.

The climbing patterns of younger ages often seen on plateau diagrams for K-feldspar frequently conform to models of diffusion loss of Ar. However, the low-temperature portions of these samples do not resemble the expected smoothly climbing patterns characteristic of diffusive Ar loss. Instead, the profiles display an apparently significant step structure (Figure 31, which displays the low-temperature portions of the four age spectra on one diagram). Thus, despite very different fractions of gas release being involved, all four samples show pronounced discontinuities at about 34 Ma (illustrated by a dotted line in Figure 31). The two Tai Mo Shan Formation samples both display similar breaks at about 10 Ma and 3-4 Ma (also indicated by dotted lines in Figure 31). These features are summarized in Table 5.

In summary, with respect to the fault rocks:

(i) A small but significant event at about 34 Ma is recorded by all four fault rocks. This age approximates to the age of opening (sea-floor spreading) of the South China Sea.

(ii) The most significantly affected material analyzed (as shown by the proportion of total argon released; Table 5) was the K-feldspar from the vicinity of the Tuen Mun Fault. Whether this was due to its location with respect to this fault, or due to mineralogical controls, or whether the Tuen Mun Fault was more active at that time than the other three faults, will require further work to resolve.

Table of Contents
Table of Contents
Table of Contents
Table of Contents

(iii) Events at 10 and 3-4 Ma are seen in the samples from both the Tuen Mun Fault and Tiu Tang Lung Thrust, but not in the materials from the Tolo Channel Fault or the fault in the Rambler Channel. This may indicate that only the Tuen Mun Fault and the Tiu Tang Llung Thrust were active in those episodes.

In three out of four of the age spectra, the first gas fractions that contain measurable ^{39}Ar also gave ^{40}Ar/^{36}Ar ratios within error of the atmospheric value. This pattern is consistent with more recent, late Pleistocene to Holocene, fault activity. The effect of this activity on these minerals is too weak to constrain temporally at this point. However, in future it may be possible to increase the signal by sampling closer to fault planes, or to reduce background noise by improved analytical techniques.

In conclusion, it is suggested that these measurements indicate strongly that valuable evidence of relatively recent fault movements may be encoded in the very smallest fractions of argon released in step-heating analyses, and that further, more detailed studies are warranted.

7. REFERENCES

Allen, P.M and Stephens, E.A. (1971). Report on the Geological Survey of Hong Kong. Institute of Geological Sciences, London, 107 p.

Argon Geochronology Laboratory (AGL) (1998). Report to Hong Kong Geological Survey on ^{40}Ar/^{39}Ar Laser Microprobe Dating of Samples of HK856. Department of Physics, University of Toronto, Ontario, Canada, 6 p.

Argon Geochronology Laboratory (AGL) (2000a). Report to Hong Kong Geological Survey on ^{40}Ar/^{39}Ar Laser Microprobe Dating of Samples from Hong Kong. Phase II: Mafic Dykes HK1651, HK9728, HK9842 and HK10981. Department of Physics, University of Toronto, Ontario, Canada, 32 p.

Argon Geochronology Laboratory (AGL) (2000b). Report to Hong Kong Geological Survey on ^{40}Ar/^{39}Ar Laser Microprobe Dating of Samples from Hong Kong. Phase III: Fault Rocks HK3419, HK7284, HK12077, HK12078 and HK12086. Department of Physics, University of Toronto, Ontario, Canada, 42 p.

Hu, Q., Evensen, N.M., Smith, P.E. & York, D. (1998). A world in a grain of sand: regional metamorphic history from ^{40}Ar/^{39}Ar laser probe analyses of Proterozoic sediments from the Canadian shield, Precambrian Research, Vol. 91, pp 287-294.

Kelley, S.P., Reddy, S.M. & Maddock, R. (1994). Laser-probe ^{40}Ar/^{39}Ar investigation of a pseudotachylyte and its host rock from the Outer Isles Thrust, Scotland. Geology, Vol. 22, pp 443-446.

Kralik, M., Klima, K. & Riedmüller, G. (1987). Dating fault gouges. Nature, Vol. 327, pp 315-317.

Table of Contents Table of Contents Table of Contents Table of Contents

Noller, J.S., Sowers, J.M. & Lettis, W.R. (2000). Quaternary Geochronology, Methods and Applications. American Geophysical Union, Washington DC, 582 p.

Sewell, R.J. & Campbell, S.D.G. (1981). Absolute Age Dating of Hong Kong Volcanic and Plutonic Rocks, Superficial Deposits, and Faults. GEO Report No. 118, Geotechnical Engineering Office, Civil Engineering Department. 153 p

Sewell, R.J., Campbell, S.D.G., Fletcher, C.J.N., Lai, K.W. & Kirk, P.A. (2000). The Pre-Quaternary Geology of Hong Kong. Geotechnical Engineering Office, Civil Engineering Department, Government of HKSAR. 181 p.

York, D. & López-Martinez, M. (1986). The two-faced mica. Geophysical Research Letters, Vol.13, part 9, pp 973-975.

York, D., A., Masliwec, P., Kuybida, J.A., Hanes, C.M., Hall, W.J., Kenyon, E.T.C., Spooner, E.T.C. & Scott, S.D. (1982). $^{40}Ar/^{39}Ar$ dating of pyrite. Nature, Vol. 300, No. 5887, pp 52-53.

Table of Contents

Table of Contents

Table of Contents

Table of Contents

LIST OF TABLES

Table of Contents
Table of Contents
Table of Contents

Table 1 - Samples from Hong Kong Geological Survey Rock Archive Analyzed in this Study

HK No	East	North	Sheet	Final Name	Locality
HK1651	811945	825620	5SE	DOLERITE	SIU LANG SHUI
HK9728	856700	825150	8SE	BASALT	HIGH ISLAND FORMATION
HK9842	821660	820200	10NW	LAMPROPHYRE	PENNY’S BAY
HK10981	824011	822973	10NE	BASALT	MA WAN
HK856	814270	828889	5SE	TUFF	TUEN MUN
HK3419	831700	842710	3NW	TUFF MYLONITE	KONG NGA PO
HK7284	833625	842020	3NW	FINE ASH LITHIC CRYSTAL METATUFF	HA SHAN WAI WAT
HK7729	842770	841170	3SE	SCHISTOSE METATUFF	WU KAU TANG
HK12078	830065	822390	10NE	GRANITIC MYLONITE	RAMBLER CHANNEL FAULT
HK12086	837583	827241	7SE	GRANITIC MYLONITE	SHATIN BH-3, DEPTH:34.42 - 34.62

Table of Contents
Table of Contents
Table of Contents
Table of Contents

Table 2 - Ar-Ar Data for Four Hong Kong Mafic Dykes

HK Sample No.	U of T Sample No.	Sample Type	No. of steps	Integrated Age	$^{37}Ar/^{39}Ar$	Points Fitted (N)	Isochron Age (Ma)	$^{40}Ar/^{36}Ar$ Initial	$\frac{\Sigma S}{(n-2)}$
HK1651 (in Tsing Shan Granite, NW New Territories)	P22-413	WR	42	74.7 ± 0.3	0.482 ± 0.002	1-6 (del.2) (5) 12-16 (5) 34-39 (del.37) (5)	59.8 ± 4.3 70.1 ± 0.4 75.1 ± 0.8	375 ± 17 294 ± 8 353 ± 73	0.41 0.55 0.34
HK9728 (in High Island Fm., NE New Territories)	P22-116	WR	16	105.3 ± 0.5	1.136 ± 0.003	3-7 (del.6) (5) 9-16 (del.15) (7) 10-12 (3)	99.8 ± 0.5 93.8 ± 1.9 87 ± 12	297 ± 6 715 ± 41 908 ± 295	1.28 1.19 0.06
HK9842 (cross-cuts rhyolite dykes, NE Lantau)	P22-108 P22-107 P22-119 P22-120	WR Mica Pyrite Chlor	40 8 1 1	91.0 ± 0.4 106.2 ± 1.7 88 ± 11 80.8 ± 4.9	0.754 ± 0.001 0.234 ± 0.006 11.0 ± 0.1 46.9 ± 0.4	2-4 (3)*	108.3 ± 1.6*	63%^{39}Ar*	
HK10981 (qtzphyric dyke margin Ma Wan)	P22-327	WR	18	96.2 ± 0.4	0.829 ± 0.003	4-6 (3) 10-18 (9)	89.3 ± 0.9 86.6 ± 1.8	403 ± 56 998 ± 163	0.17 0.37

Notes. *= calculated for plateau

Table of Contents
Table of Contents
Table of Contents
Table of Contents

Table 3 - Summary of Analyses of Fault Rocks

HK No.	Fault	Host Rock	Host Age	Sample Rock Type	Analysis	Type	Steps
HK3419	Base of Tuen Mun thrust	Tai Mo Shan Fm.	164 Ma	Mylonite	P23-124	Plagioclase	38 [30]
HK7284		Tai Mo Shan Fm.	164 Ma	weakly sheared crystal tuff	P23-125	WR	6 (partial)
HK7729	Base of Tiu Tang Lung thrust	Tai Mo Shan Fm.	Early Cret.	schistose metatuff mylonite	P23-126	WR	24 [22]
HK12078	Fault in Rambler Channel	Sha Tin Granite	146 Ma	altered granite	P23-06	Pyrite	1
					P23-08	Pyrite	1
					P23-20	K feldspar	25 [23]
					P23-21	Pyrite	1
					P23-22	Pyrite	1
					P23-23	Pyrite	1
					P23-24	Pyrite	1
					P23-25	Pyrite	1
					P23-36	Pyrite	1
					P23-37	Pyrite	2
					P23-38	Pyrite	1
					P23-39	Pyrite	5
					P23-40	Pyrite	10 [9]
HK12086	Tolo Channel Fault	Sha Tin Granite	146 Ma	strongly sheared	P23-137	Plagioclase	22 [18]
						Total	141 [124]

Table of Contents
Table of Contents
Table of Contents
Table of Contents

Table 4 - Ar-Ar Data for Single Pyrite Crystals from Fault Rock HK12078

Sample No.	No. Steps	Integrated Age
P23-06	1	88 ± 14
P23-08	1	85 ± 37
P23-21	1	*44.2 ± 2.1*
P23-22	1	74 ± 13
P23-23	1	77.5 ± 3.9
P23-24	1	77.3 ± 6.3
P23-25	1	66 ± 9
P23-36	1	78 ± 8
P23-37	2	92.4 ± 3.0
P23-38	1	84.9 ± 2.8
P23-39	5	94 ± 7
P23-40	9	70.6 ± 1.8
weighted mean	11	78.5 ± 2.8

Table of Contents
Table of Contents
Table of Contents
Table of Contents

Table 5 - Low-temperature Events Recorded in Hong Kong Fault Samples

Host Rock	Fault	HK Sample No.	Material Analyzed	3-4 Ma event		10 Ma event		34 Ma event	
				f	f_c	f	f_c	f	f_c
Tai Mo Shan Fm.	Tuen Mun Fault	HK3419	K-Fdsp	4.4	4.6	4	14	9	26
	Tiu Tang Lung Fault	HK7729	WR	1.2	1.2	1.3	2.5	0.3	2.9
Sha Tin Granite	Fault in Rambler Channel	HK12078	K-Fdsp					0.7	0.8
	Tolo Channel Fault	HK12086	K-Fdsp					1.1	1.8

Legend:

f percent of total ^{39}Ar in this age fraction
f_c cumulative percent of total ^{39}Ar, including this age fraction

Table of Contents
Table of Contents
Table of Contents
Table of Contents

LIST OF FIGURES

Table of Contents
Table of Contents
Table of Contents

Table of Contents
Table of Contents
Table of Contents

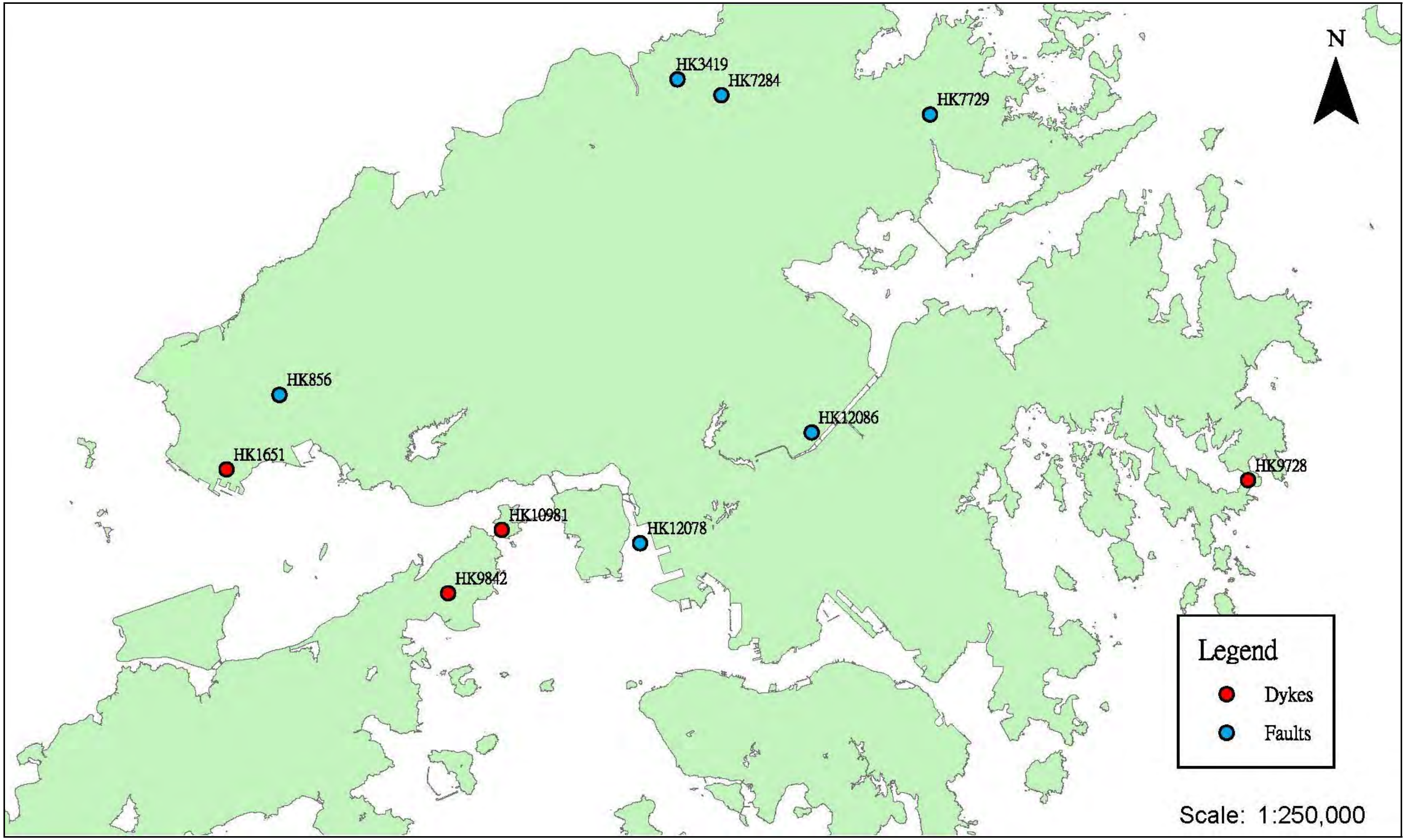

Figure 1 - Locations of Mafic Dyke and Fault Rock Samples Used in Study

Table of Contents
Table of Contents
Table of Contents
Table of Contents

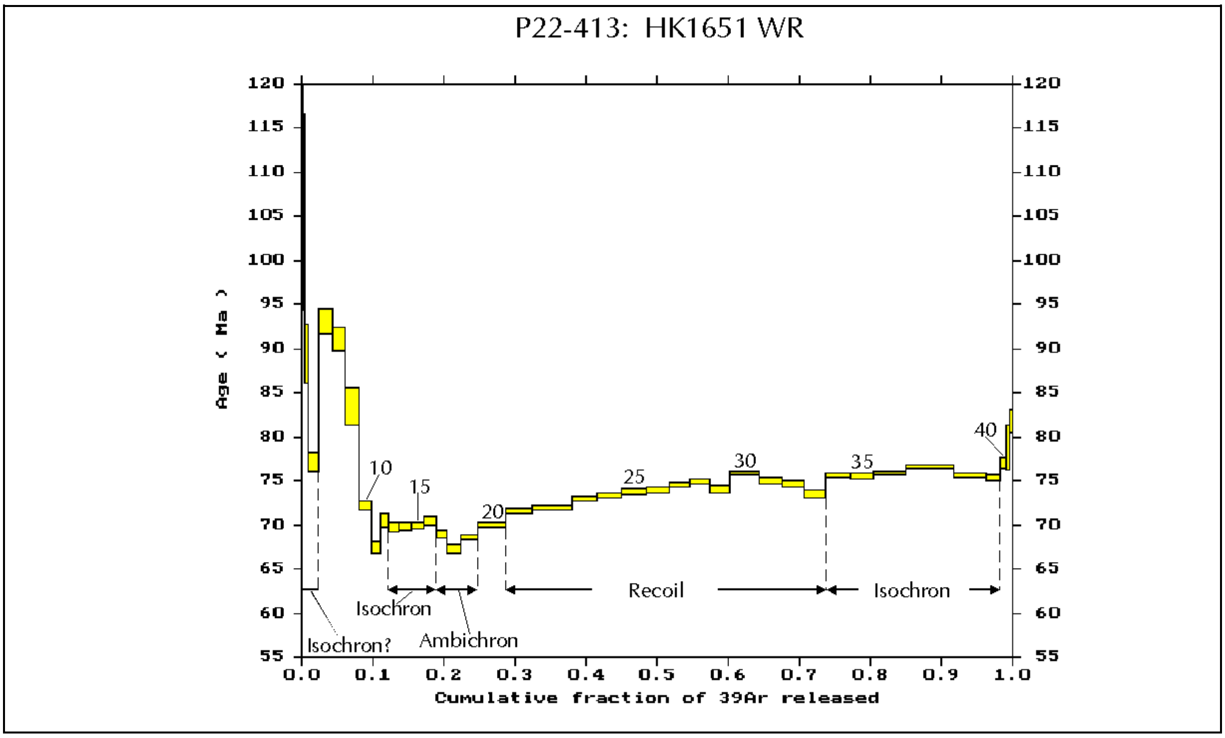

Figure 2 - Argon Age Spectrum of Mafic Dyke HK1651 Whole Rock. Numbers Identify Individual Gas Fractions. On Basis of Correlation Diagrams (Figures 3-5) Portions of Spectrum Are Identified as Isochrons or Ambichrons (Respectively Lines of Negative or Positive Slope), or Resulting from Recoil of ^{39}Ar (Horizontal Lines).

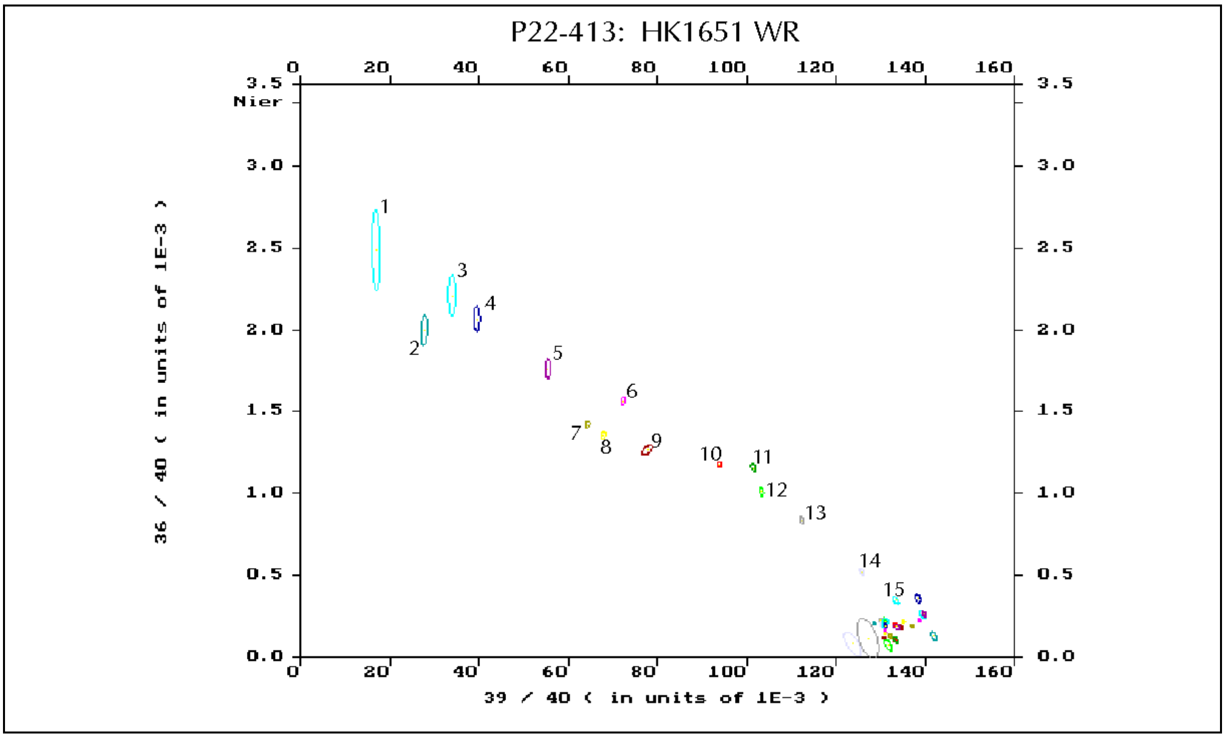

Figure 3 - ^{36}Ar/^{40}Ar vs. ^{39}Ar/^{40}Ar Correlation Diagram of Mafic Dyke HK1651 Whole Rock. “Nier” Represents Composition of Modern Atmosphere. Numbers Identify Individual Gas Fractions (See also Figure 4).

Table of Contents
Table of Contents
Table of Contents
Table of Contents

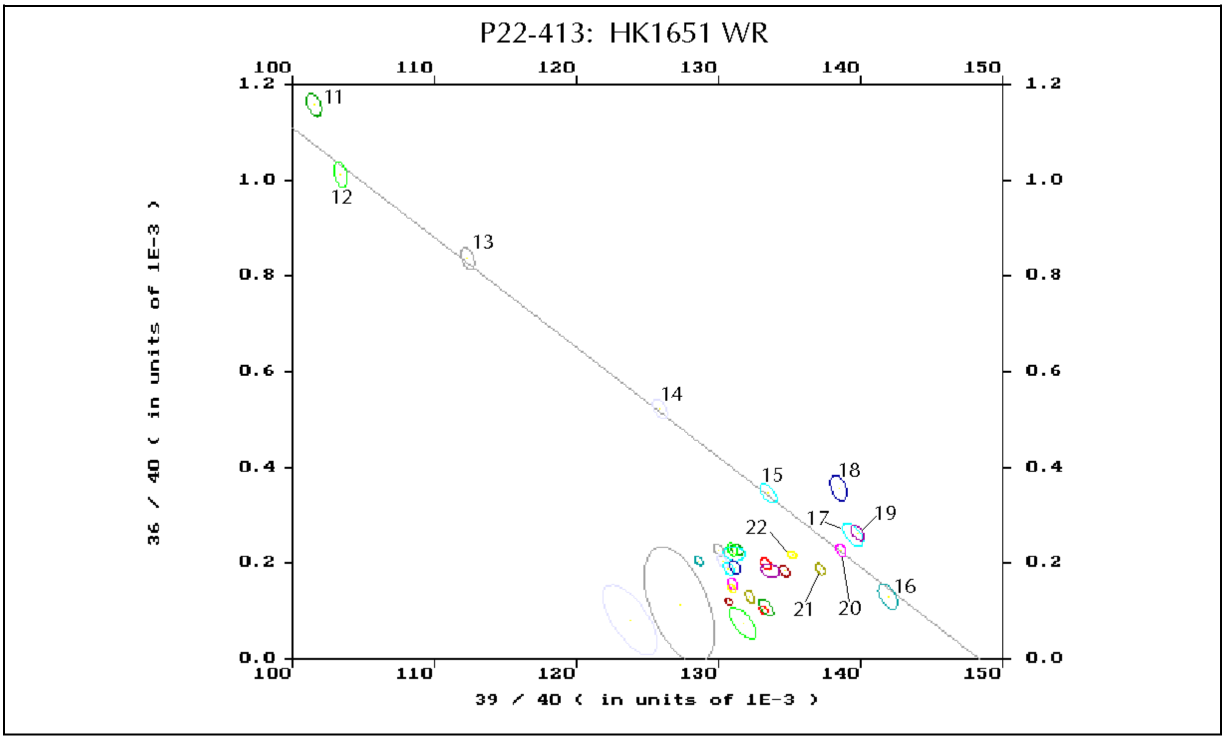

Figure 4 - Detail of Figure 3 for Fractions 11-42 (See also Figure 5). Isochron Fitted to Points 12-16 Yields Age of 70.1 ± 0.4 Ma (See Table 2).

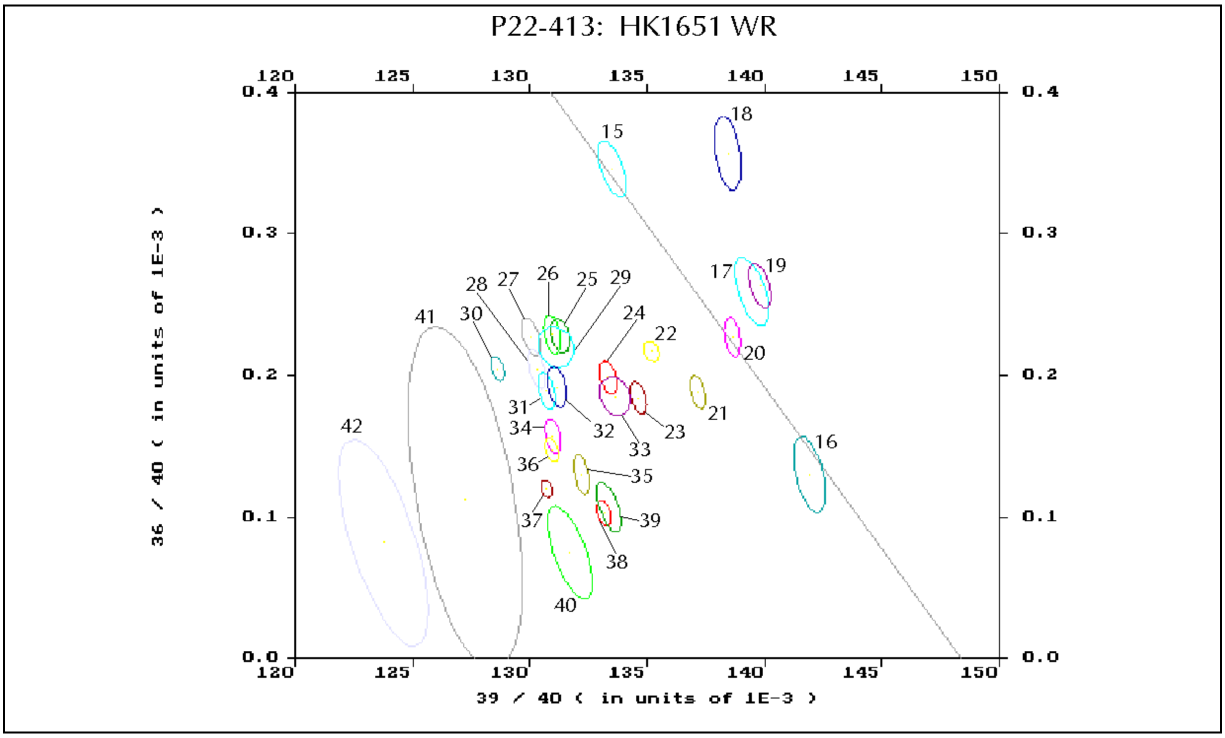

Figure 5 - Detail of Figure 3 for Fractions 15-42 (see also Figure 4)

Table of Contents
Table of Contents
Table of Contents
Table of Contents

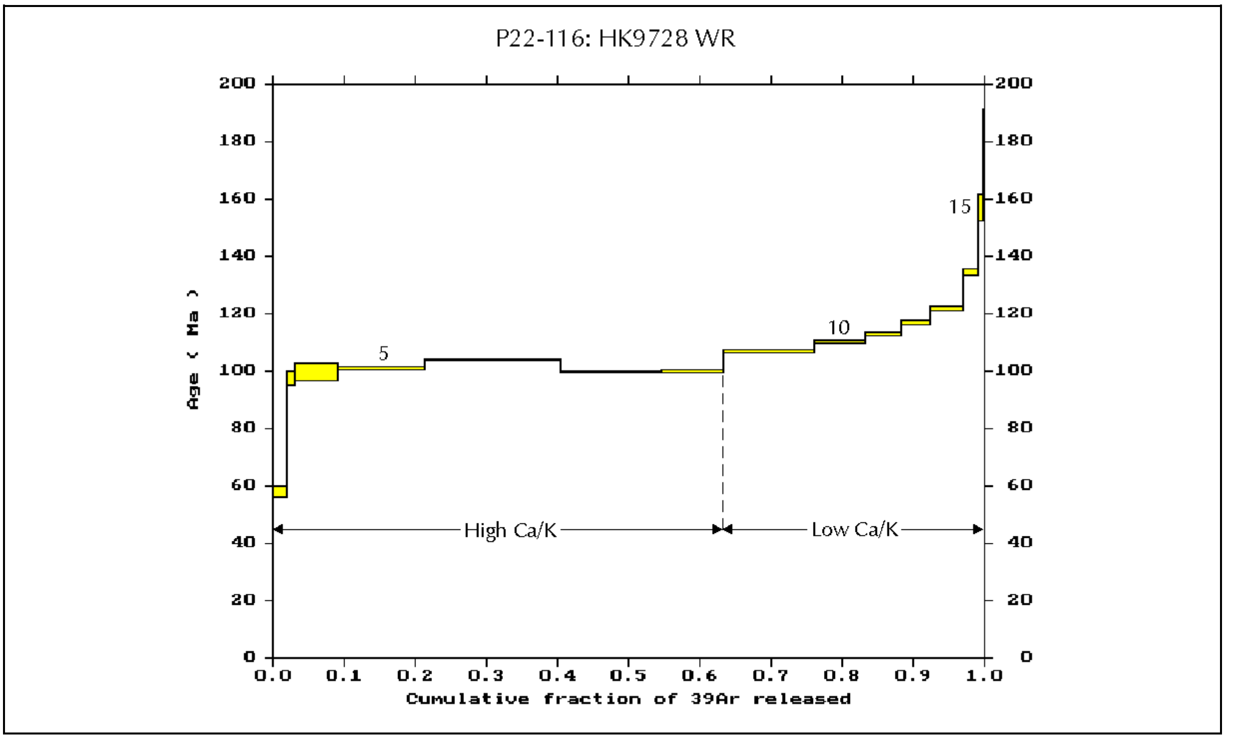

Figure 6 - Argon Age Spectrum of Mafic Dyke HK9728 Whole Rock. Numbers Identify Individual Gas Fractions. Regions of Ar Release from High and Low Ca/K Phases, as Indicated by $^{37}Ar/^{39}Ar$ Ratios, Are Labelled.

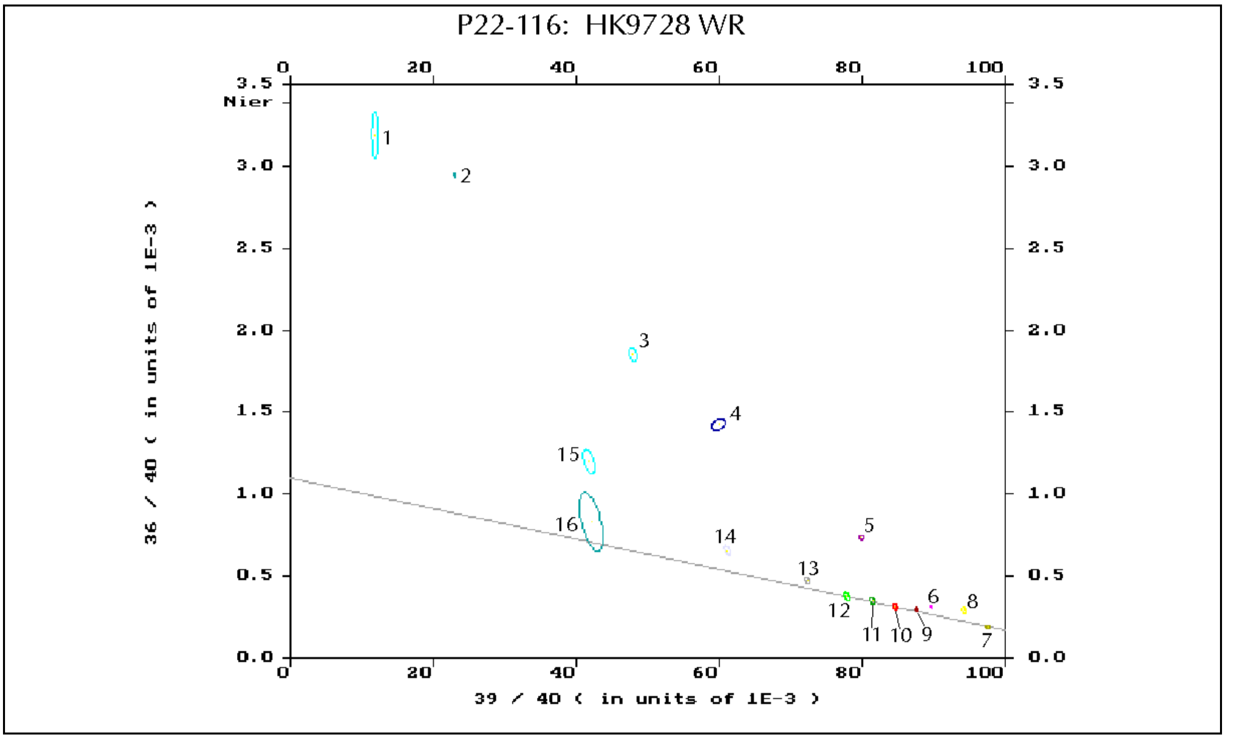

Figure 7 - $^{36}Ar/^{40}Ar$ vs. $^{39}Ar/^{40}Ar$ Correlation Diagram of Mafic Dyke HK 9728 Whole Rock. “Nier” Represents Composition of Modern Atmosphere. Numbers Identify Individual Gas Fractions. Note V-shaped Array of Points. Isochron Fitted to Points 10-12 Yields Age of 87 ± 12 Ma (See Table 2).

Table of Contents
Table of Contents
Table of Contents
Table of Contents

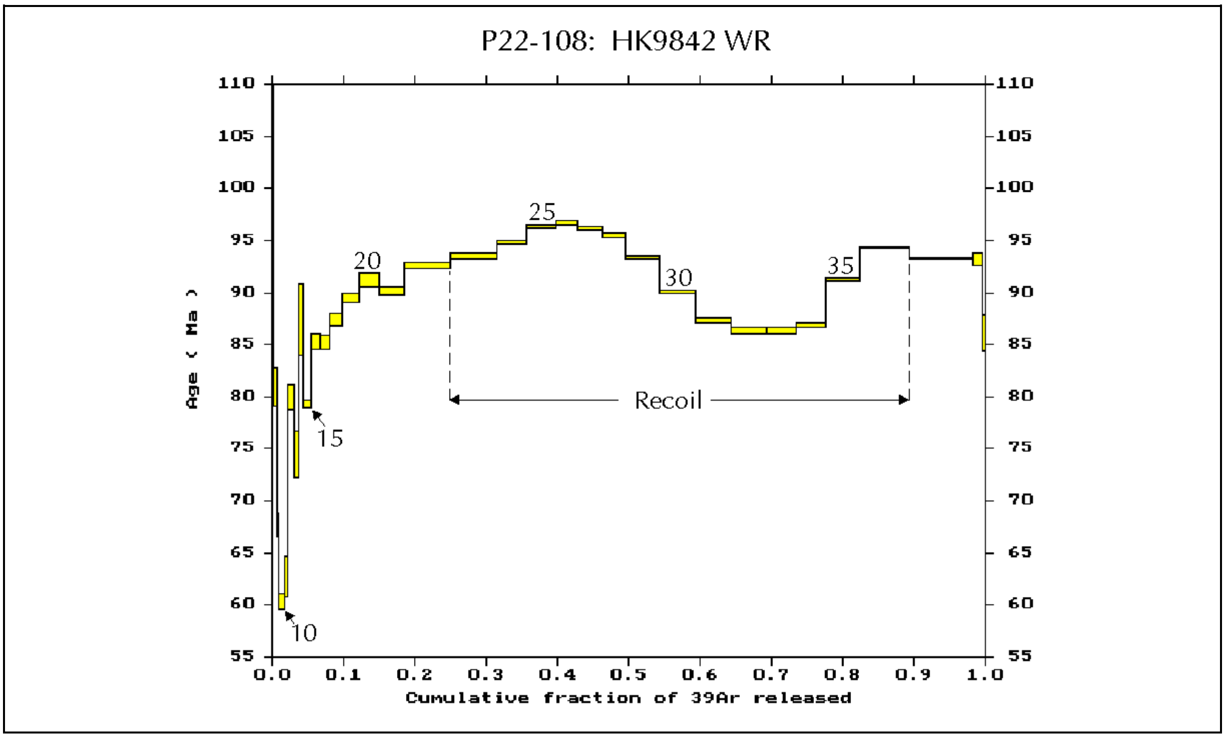

Figure 8 - Argon Age Spectrum of Mafic Dyke HK9842 Whole Rock. Numbers Identify Individual Gas Fractions. Region of Ar Release from Highly Recoil-affected Phases Is Labelled.

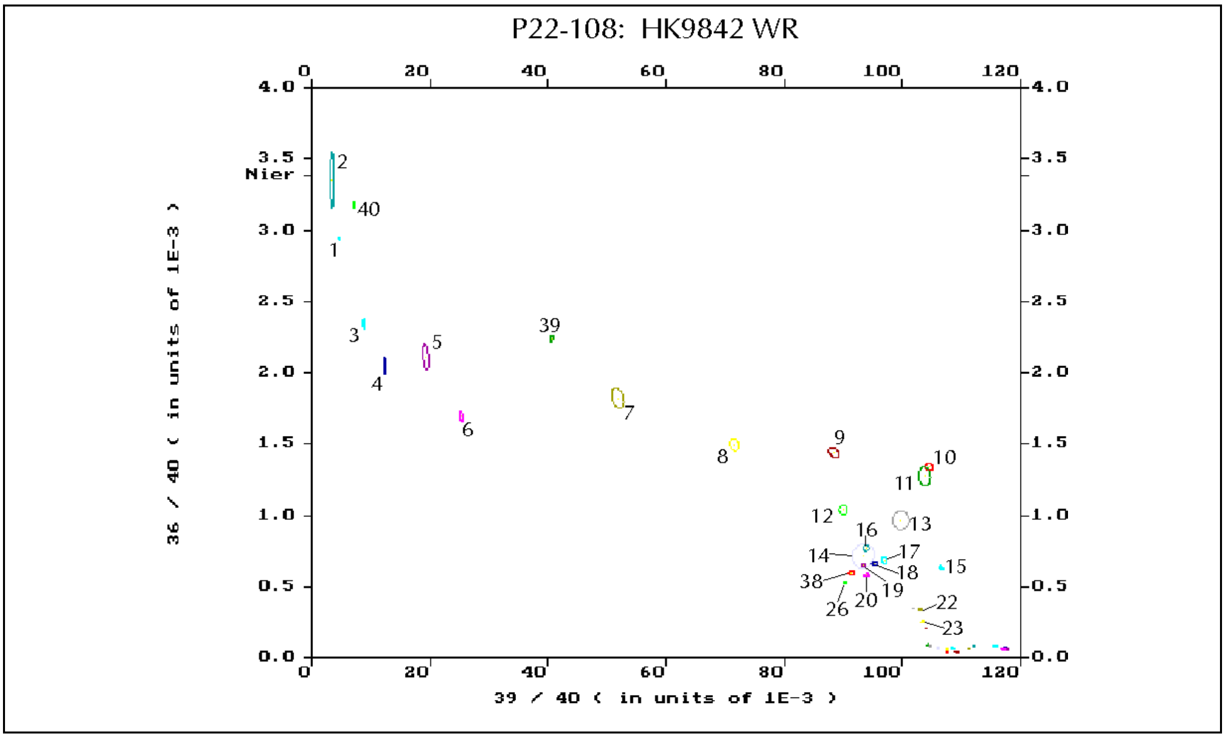

Figure 9 - $^{36}Ar/^{40}Ar$ vs. $^{39}Ar/^{40}Ar$ Correlation Diagram of Mafic Dyke HK9842 Whole Rock. "Nier" Represents Composition of Modern Atmosphere. Numbers Identify Individual Gas Fractions, except in Region of Ar Release from Highly Recoil-affected Phases, in Lower Right Hand of Figure. Note Late Fractions Revert towards Modern Atmosphere.

Table of Contents
Table of Contents
Table of Contents
Table of Contents

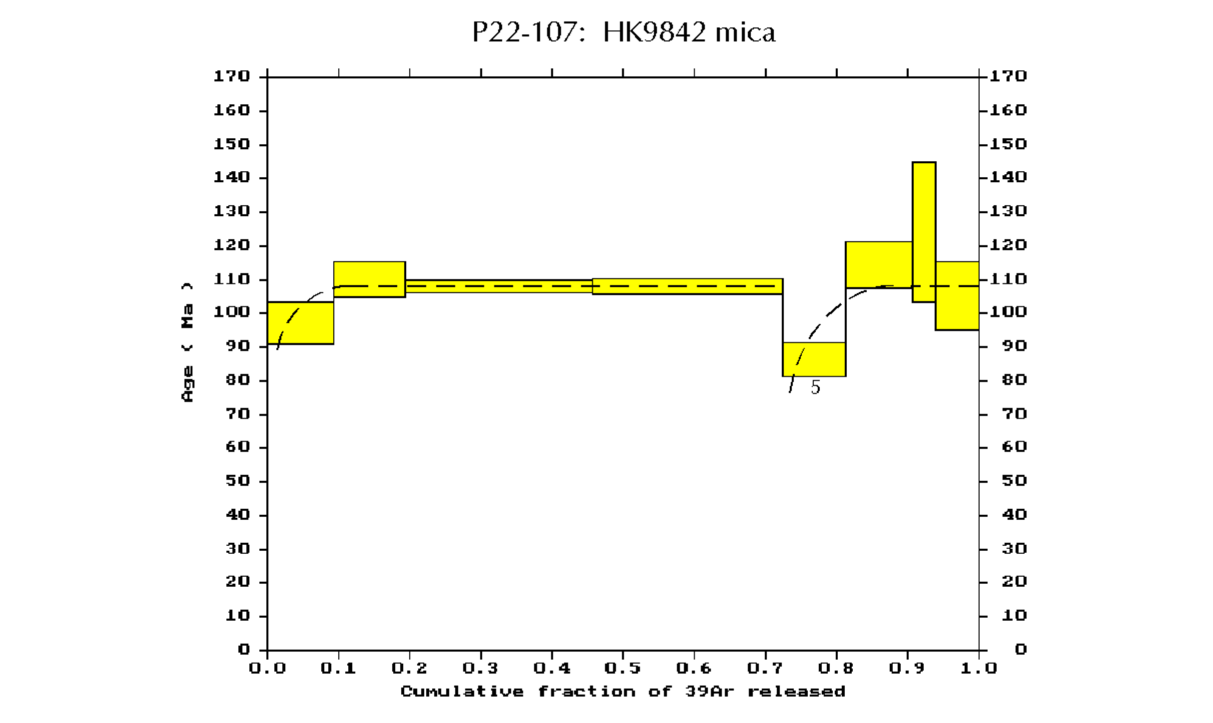

Figure 10 - Argon Age Spectrum of Mica from Mafic Dyke HK9842. Number Identifies Fifth Gas Fraction. Dashed Lines Suggest Two-phase Ar-retention (cf. York & Lopez-Martinez, 1986).

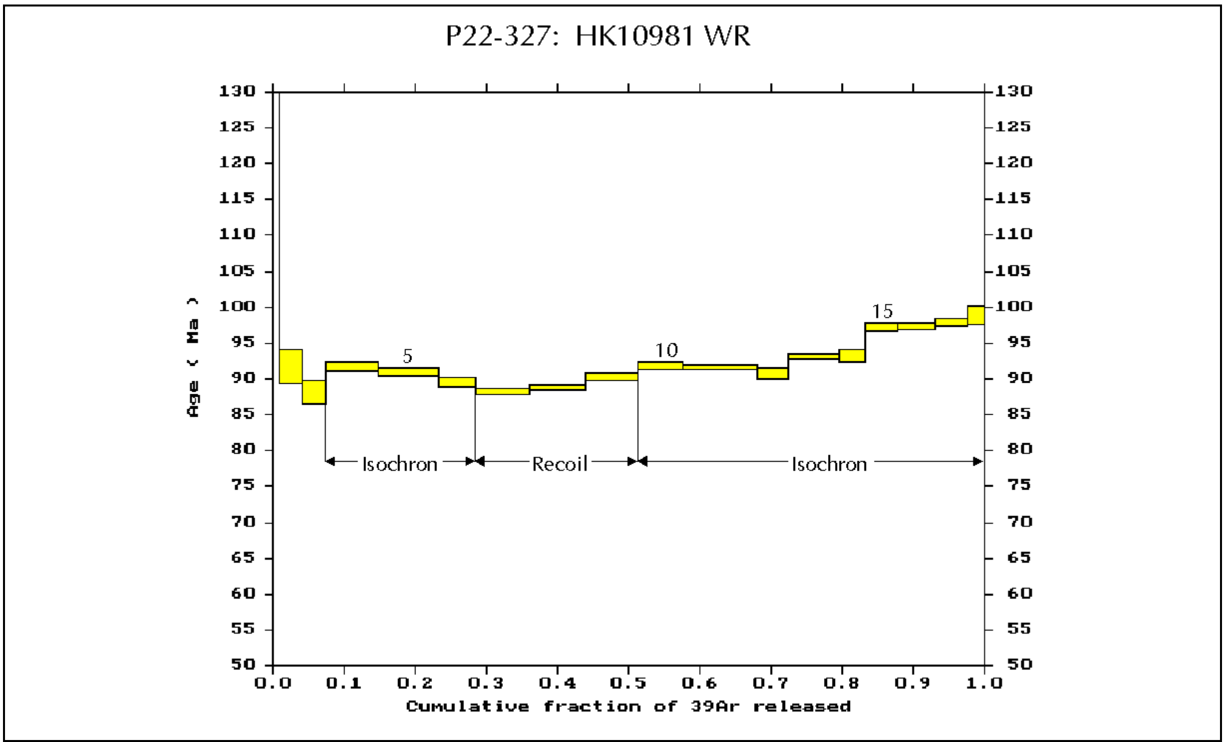

Figure 11 - Argon Age Spectrum of Mafic Dyke HK10981 Whole Rock. Numbers Identify Individual Gas Fractions. Interpretation Based on Correlation Diagrams (Figures 12-13) as for Figure 2.

Table of Contents
Table of Contents
Table of Contents
Table of Contents

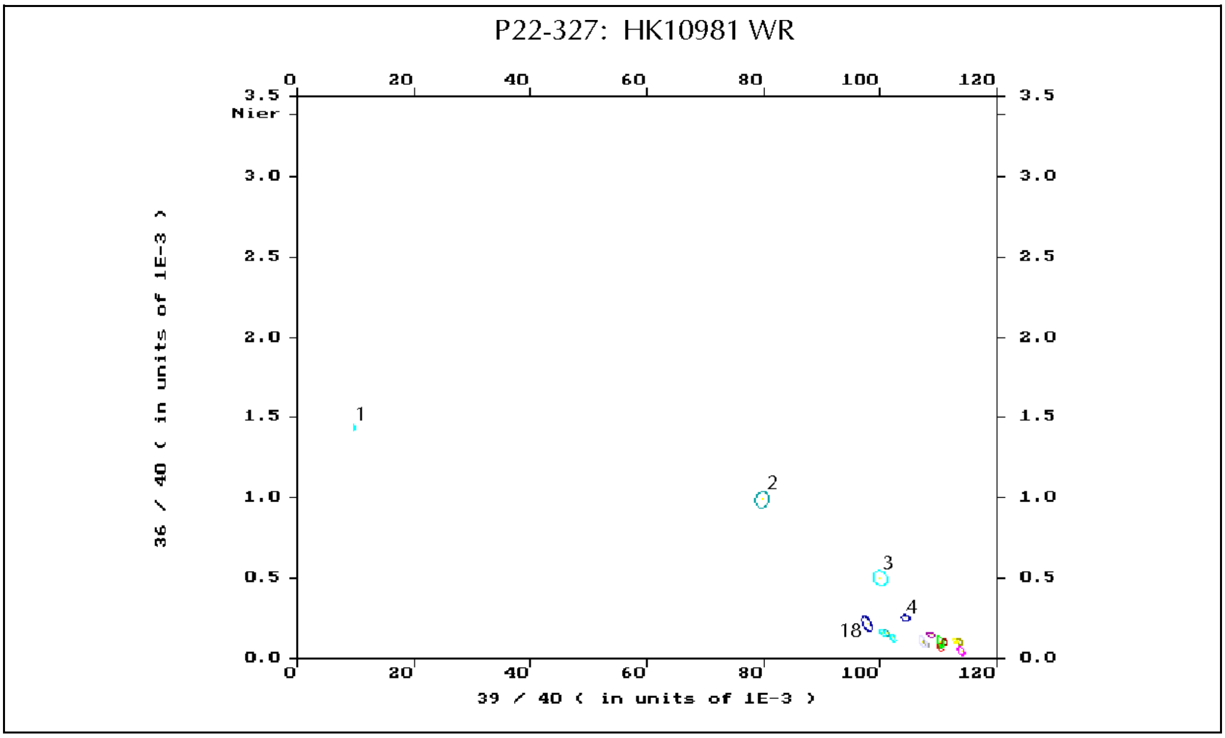

Figure 12 - $^{36}Ar/^{40}Ar$ vs. $^{39}Ar/^{40}Ar$ Correlation Diagram of Mafic Dyke HK10981 Whole Rock. "Nier" Represents Composition of Modern Atmosphere. Numbers Identify Individual Gas Fractions 3-18 (See also Figure 13).

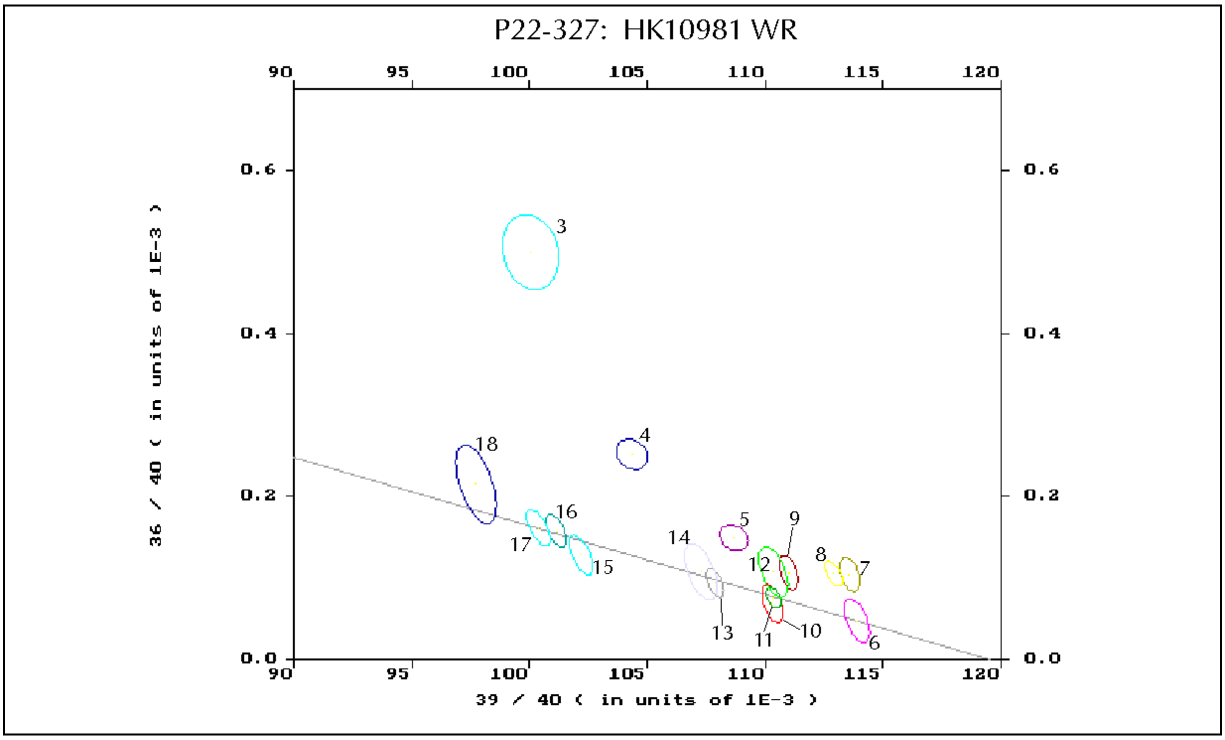

Figure 13 - Detail of Figure 11 for Fractions 3-12. Note V-shaped Array of Points, as on Figure 7. Isochron Fitted to Points 10-18 Yields Age of 86.6 ± 1.8 Ma (See Table 2).

Table of Contents
Table of Contents
Table of Contents
Table of Contents

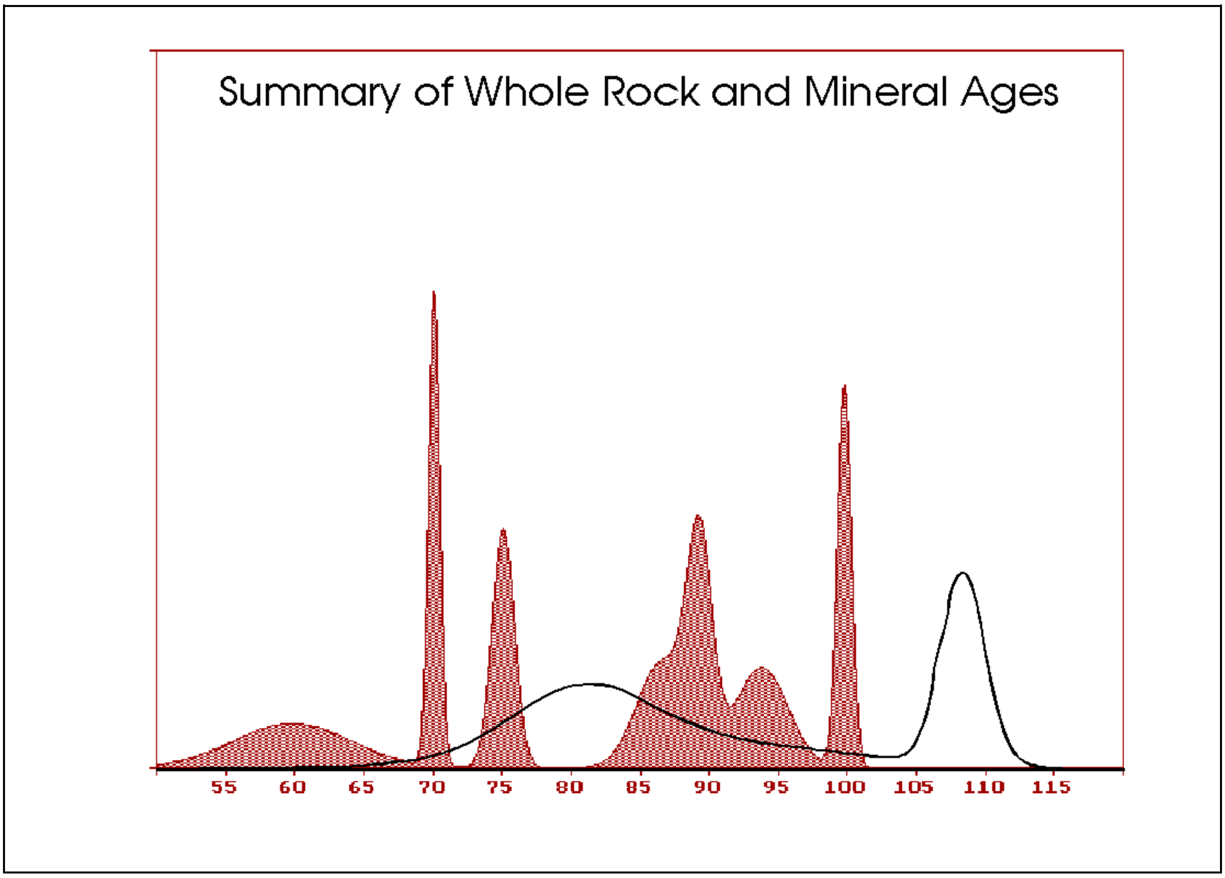

Figure 14 - Summary Histogram of All Mafic Dyke Whole-Rock and Mineral Ages. Each Age Contributes Equal Area Gaussian to Total, Width of Gaussian (and so its Height) Reflects Error of that Age.

Table of Contents
Table of Contents
Table of Contents
Table of Contents

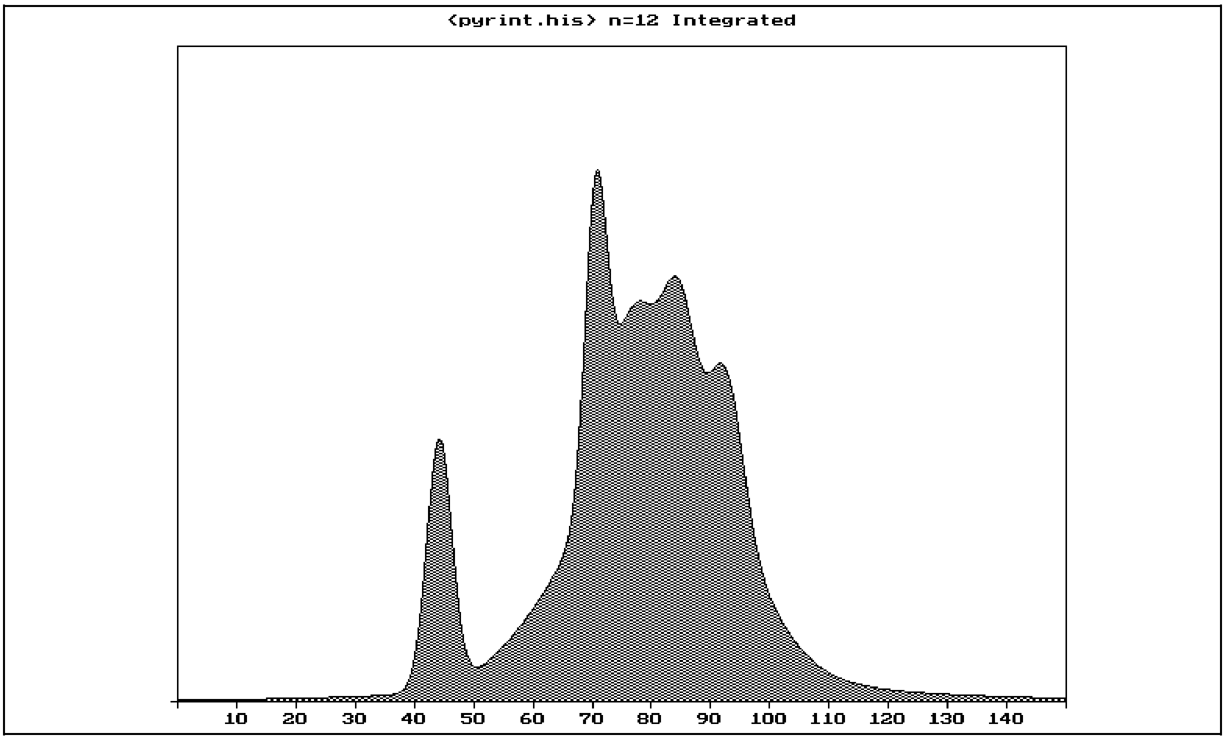

Figure 15 - Summary Histogram of Pyrite Ages for Fault Rocks. Each Age in Table 3 Contributes Equal Area Gaussian to Total, Width of Gaussian (and so its Height) Reflects Error of that Age.

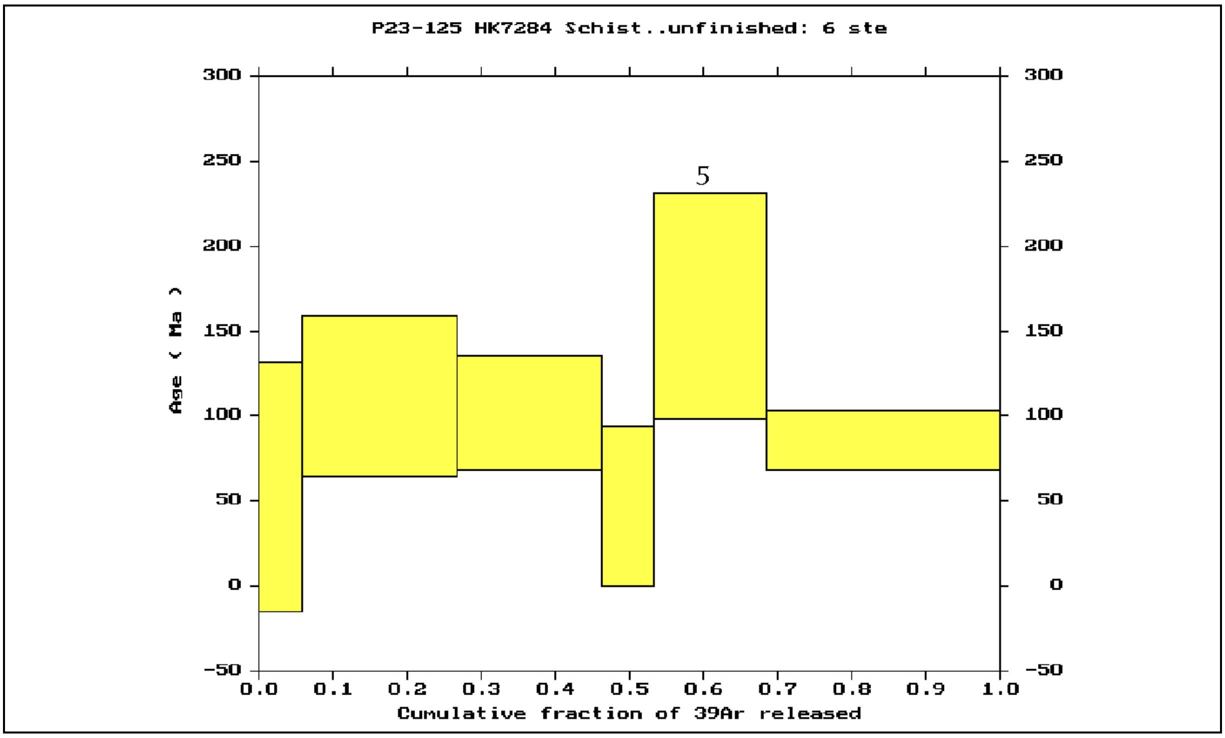

Figure 16 - Argon Age Spectrum of Initial Fractions of Fault Rock HK7284 Whole Rock. Number Identifies Fifth Gas Fraction. Spectrum Shows No Sign of Young, Low-temperature Events

Table of Contents
Table of Contents
Table of Contents
Table of Contents

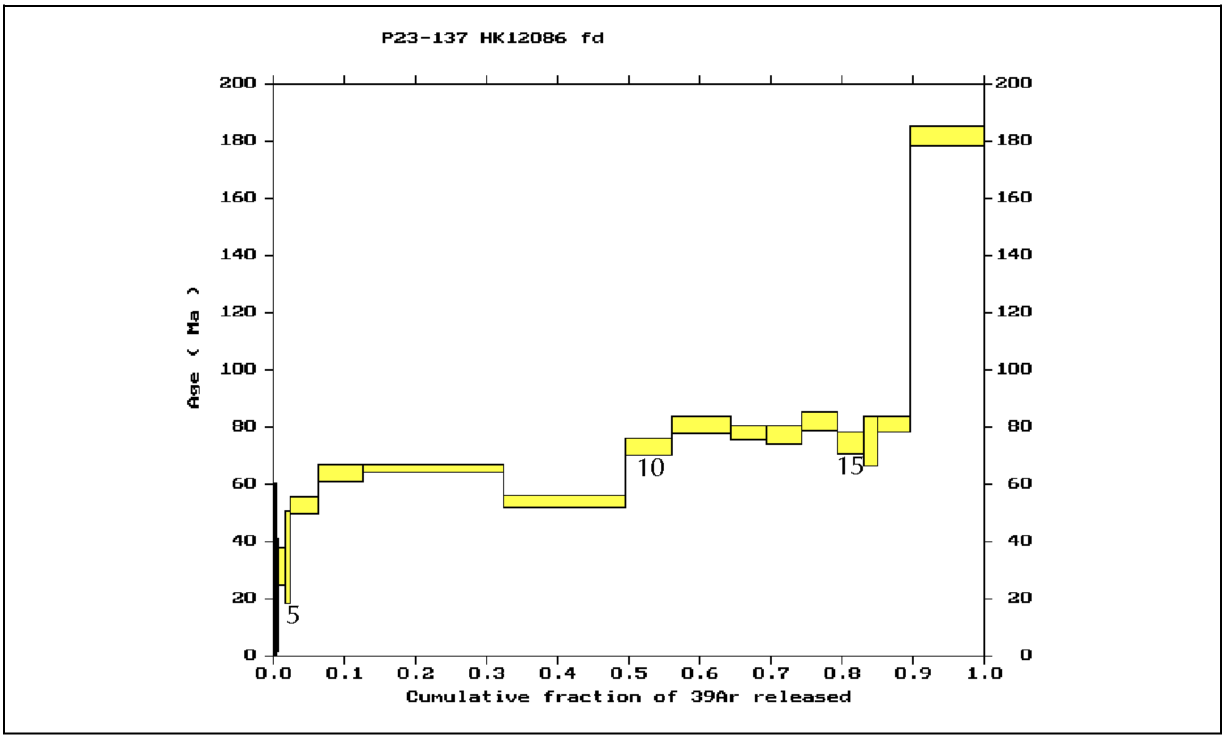

Figure 17 - Argon Age Spectrum of Feldspar in Fault Rock HK12086. Numbers Identify Individual Gas Fractions. (See also Figure 18).

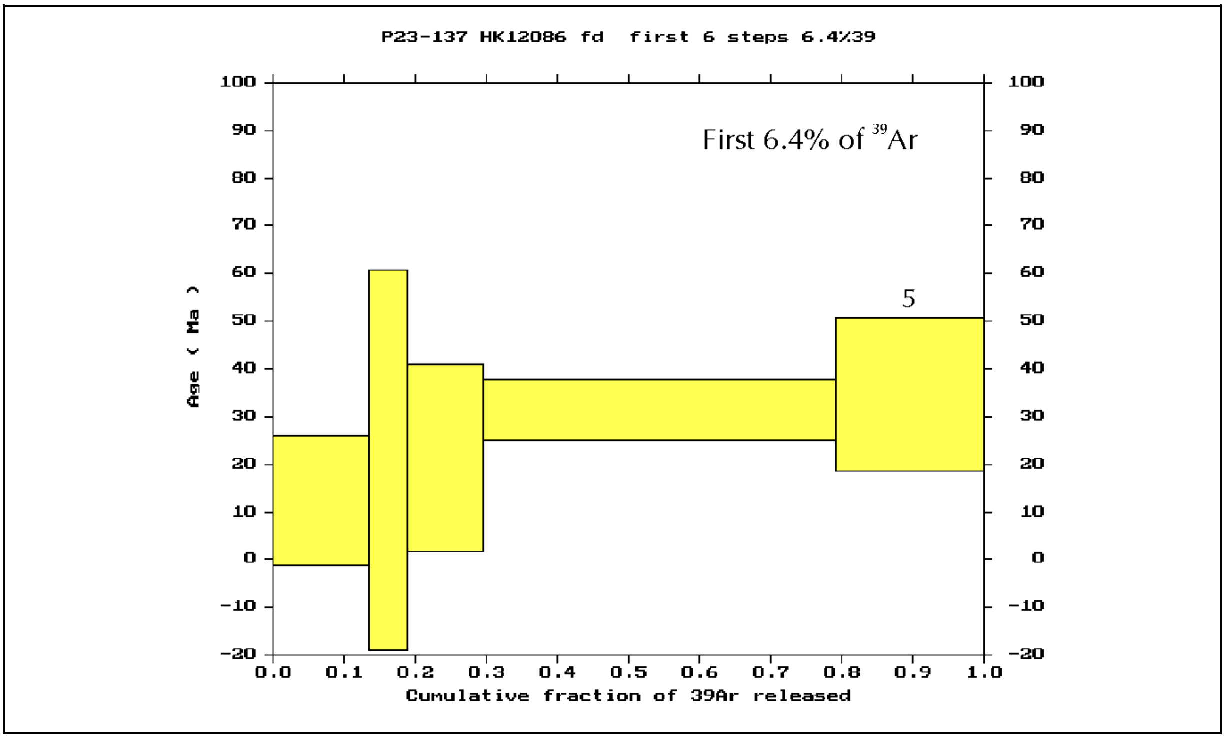

Figure 18 - Detail of Figure 17, Showing Fractions 1-5, Representing First 6.4% of Sample ^{39}Ar.

Table of Contents
Table of Contents
Table of Contents
Table of Contents

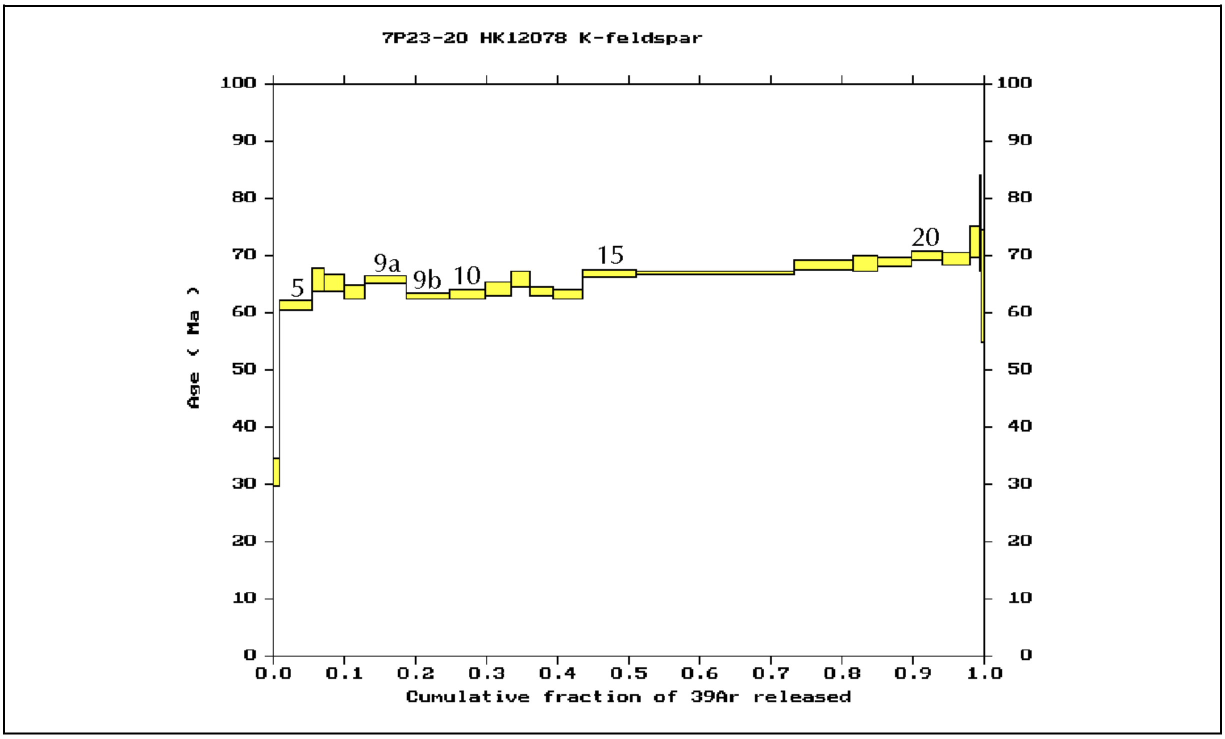

Figure 19 - Argon Age Spectrum of K-Feldspar in Fault Rock HK12078. Numbers Identify Individual Gas Fractions. (See also Figure 20)

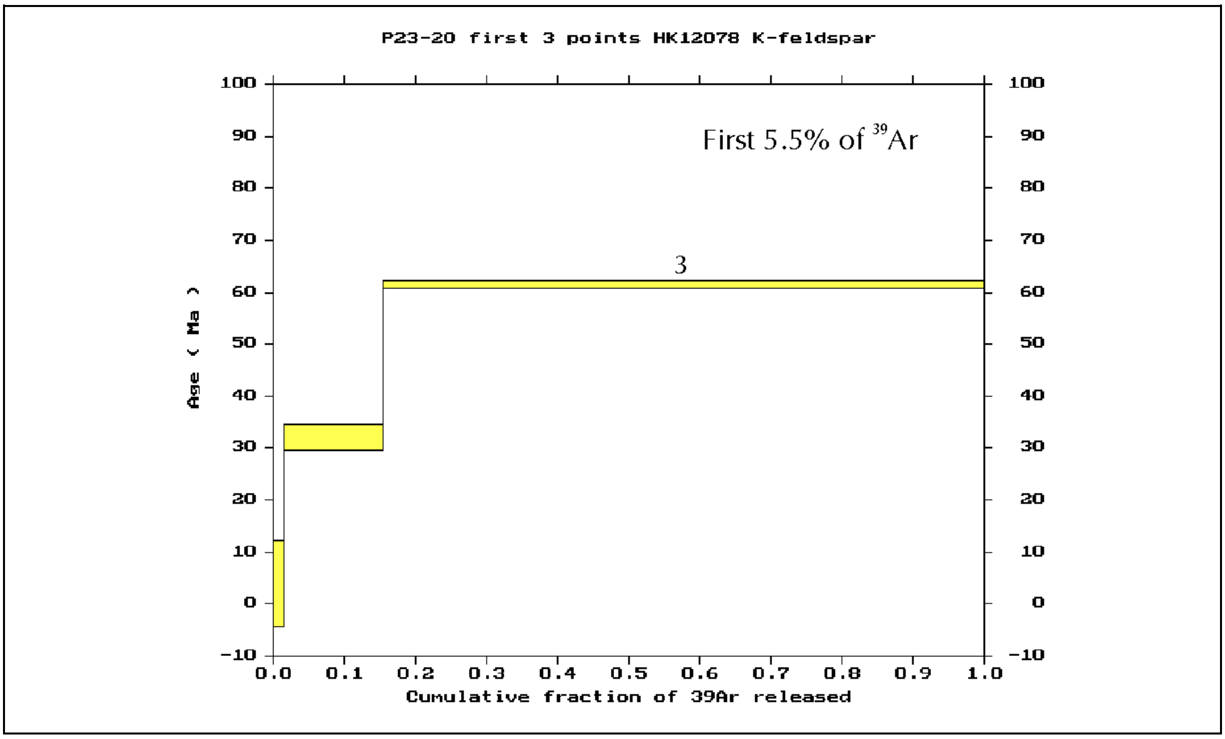

Figure 20 - Detail of Figure 19, Showing Fractions 1-3, Representing First 5.5% of Sample ^{39}Ar.

Table of Contents
Table of Contents
Table of Contents
Table of Contents

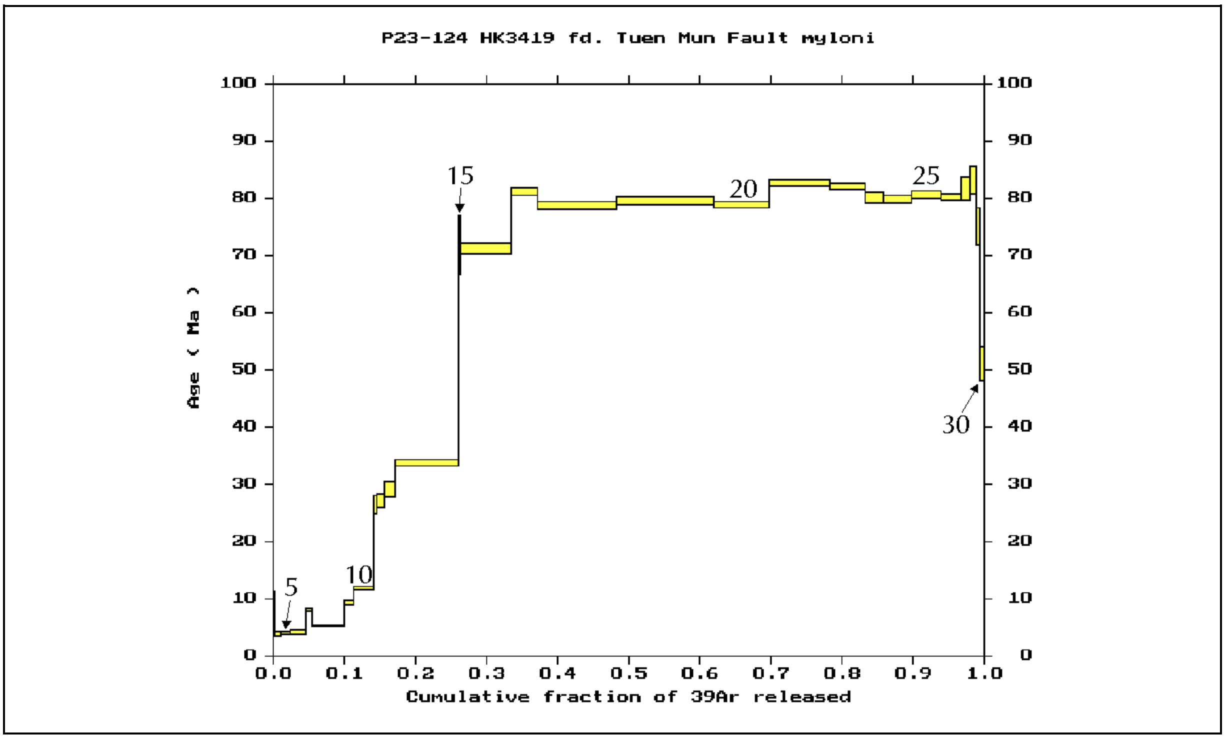

Figure 21 - Argon Age Spectrum of K-Feldspar in Fault Rock HK3419. Numbers Identify Individual Gas Fractions. (See also Figure 22).

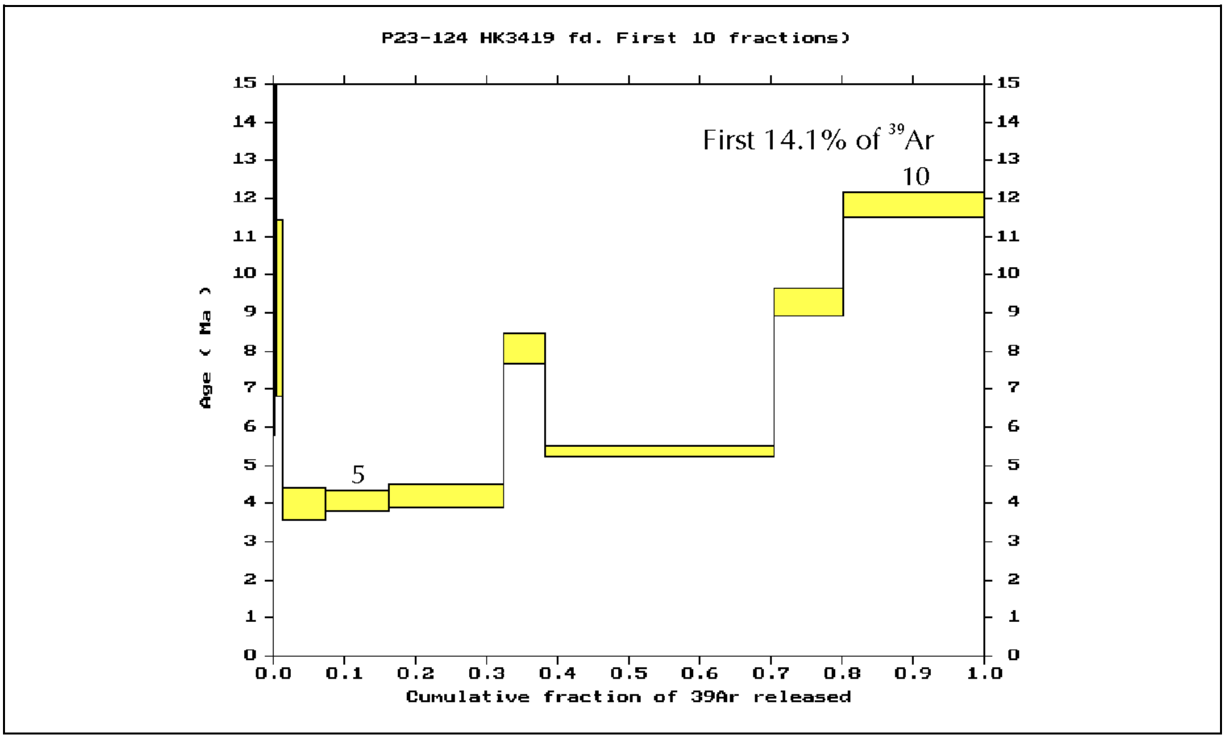

Figure 22 - Detail of Figure 21, Showing Fractions 1-5, Representing First 14.1% of Sample ^{39}Ar.

Table of Contents
Table of Contents
Table of Contents
Table of Contents

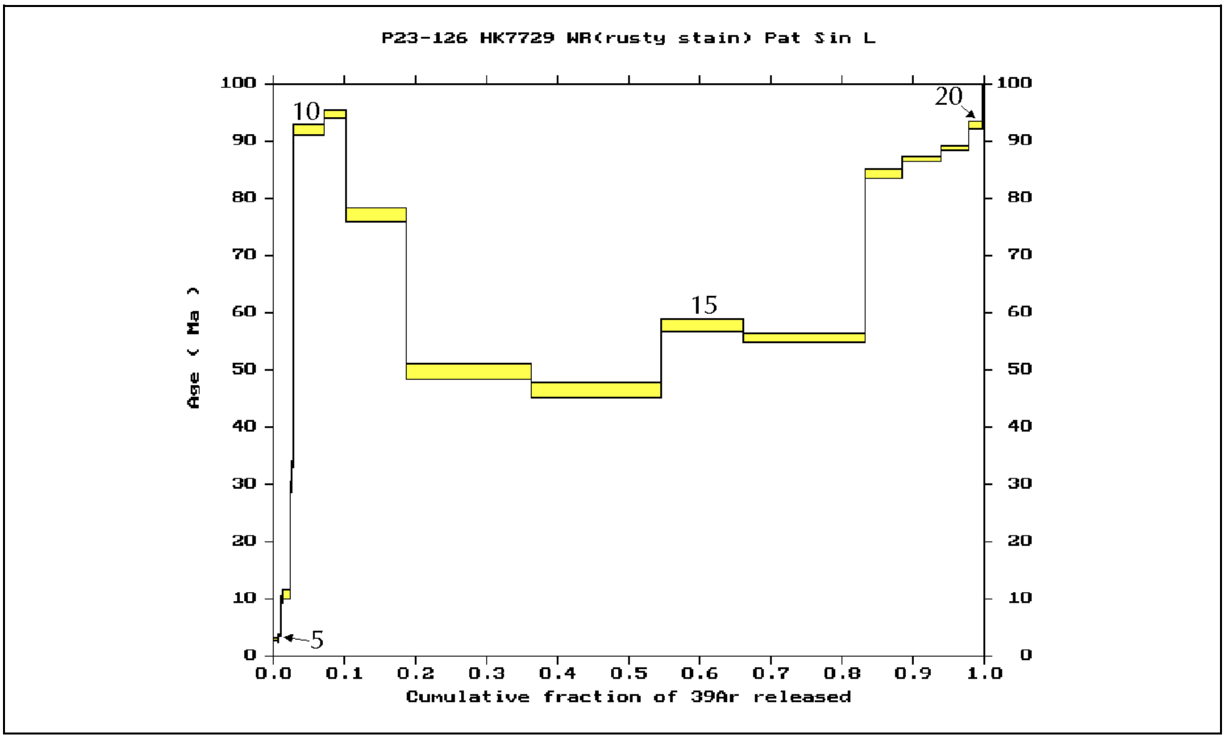

Figure 23 - Argon Age Spectrum of Fault Rock HK7729 Whole Rock. Numbers Identify Individual Gas Fractions. (See also Figure 24).

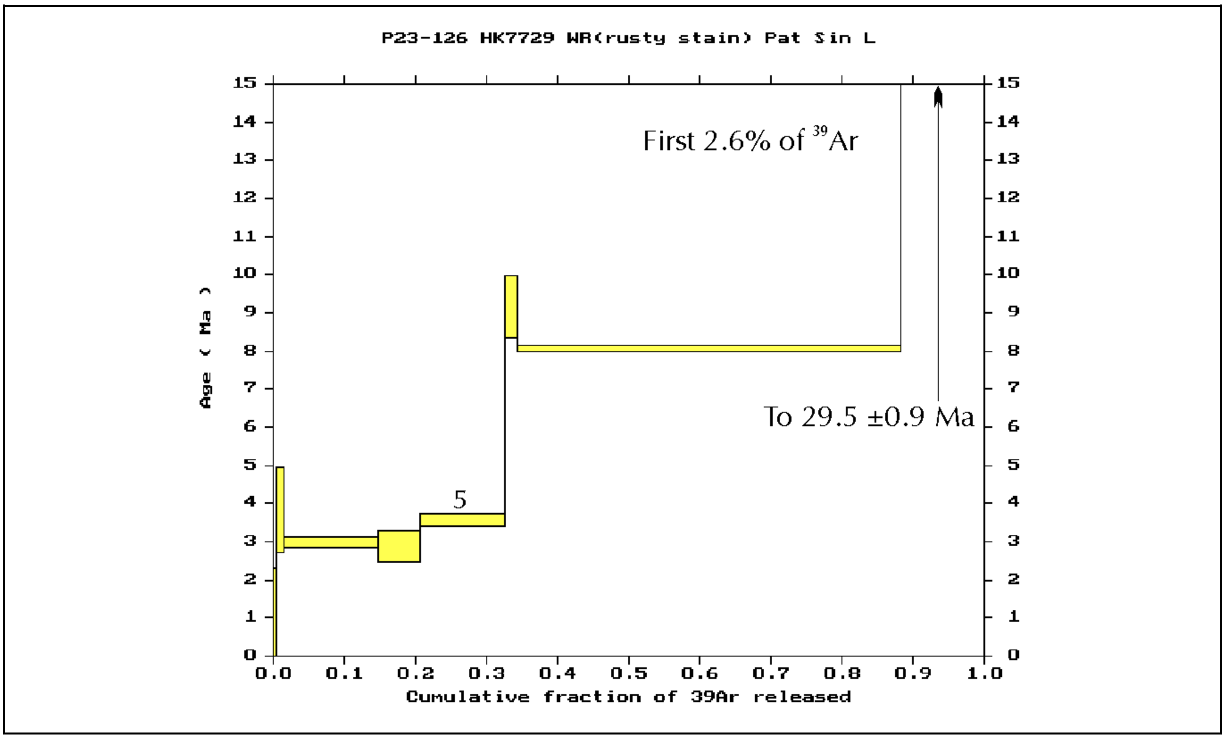

Figure 24 - Detail of Figure 23, Showing Fractions 1-9, Representing First 2.6% of Sample ^{39}Ar. Number Identified Fifth Gas Fraction. Fractions 8 and 9 Are off Vertical Scale

Table of Contents
Table of Contents
Table of Contents
Table of Contents

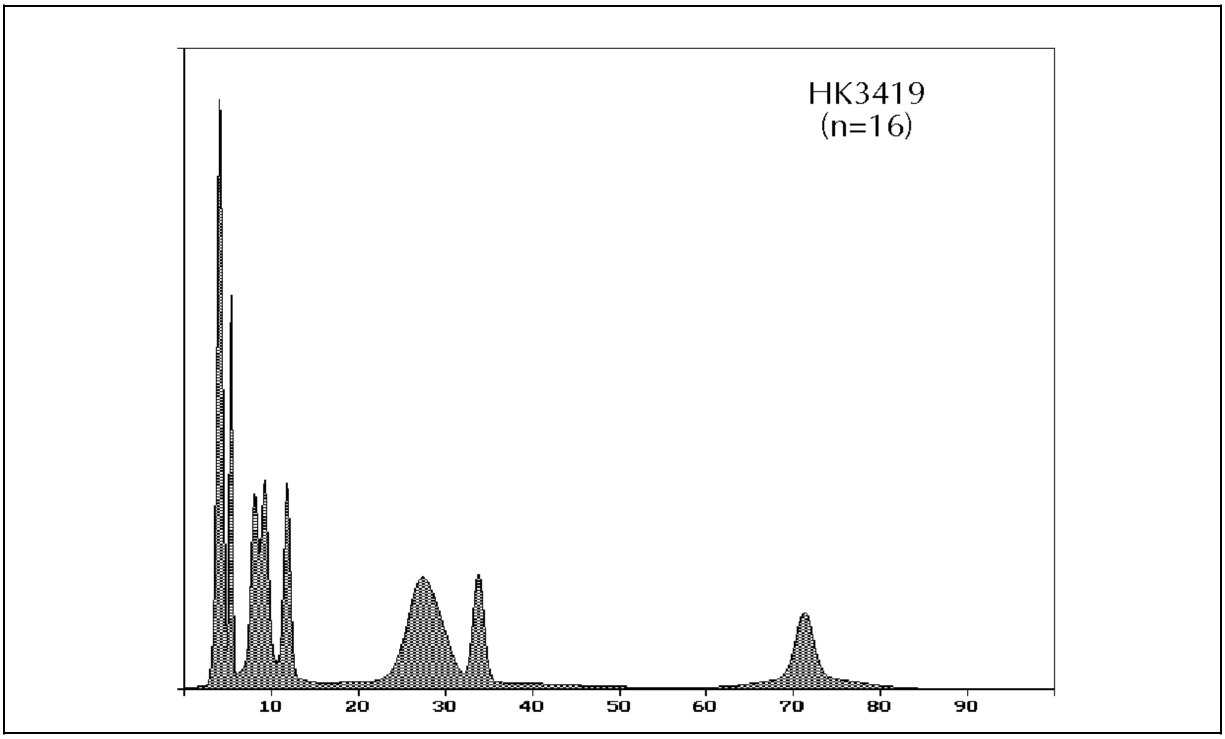

Figure 25 - Summary Histogram of Ages of First 16 Ar Fractions in Feldspar from Fault Rock HK3419. Age Interpretation as for Figure 14.

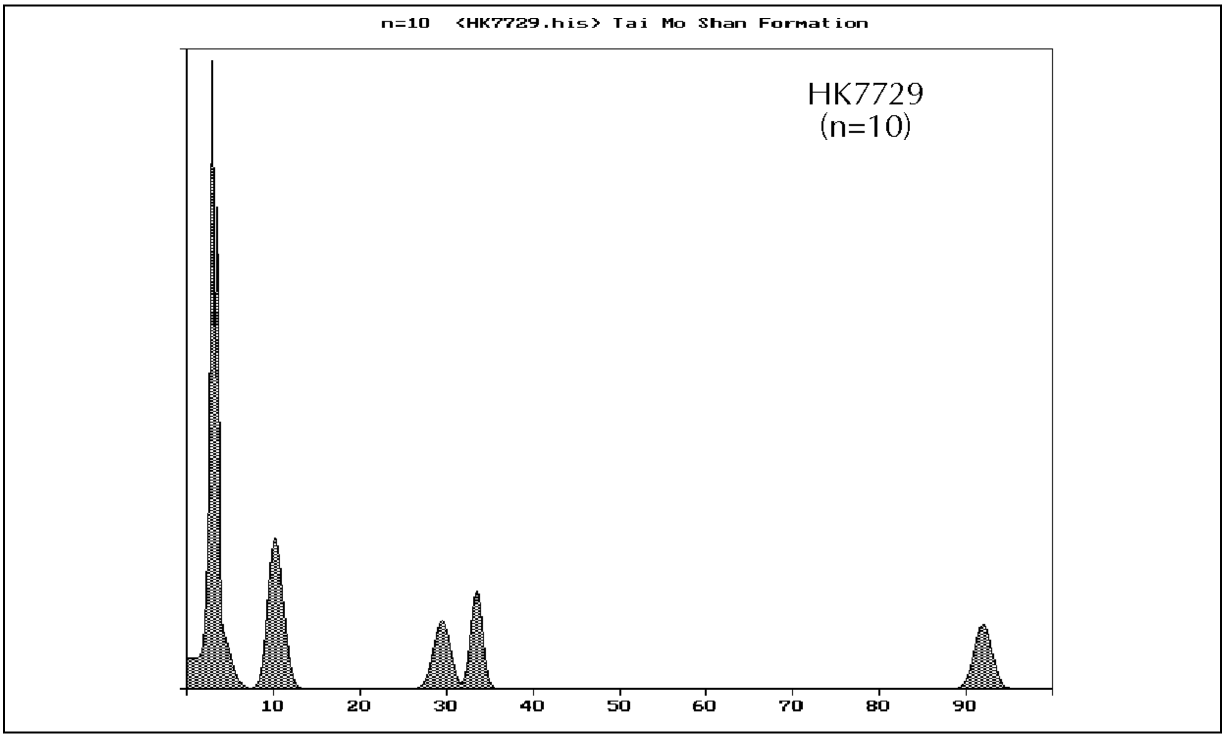

Figure 26 - Summary Histogram of Ages of First 10 Ar Fractions in Feldspar from Fault Rock HK7729. Age Interpretation as for Figure 14. Horizontal Scale as for Figure 25.

Table of Contents
Table of Contents
Table of Contents
Table of Contents

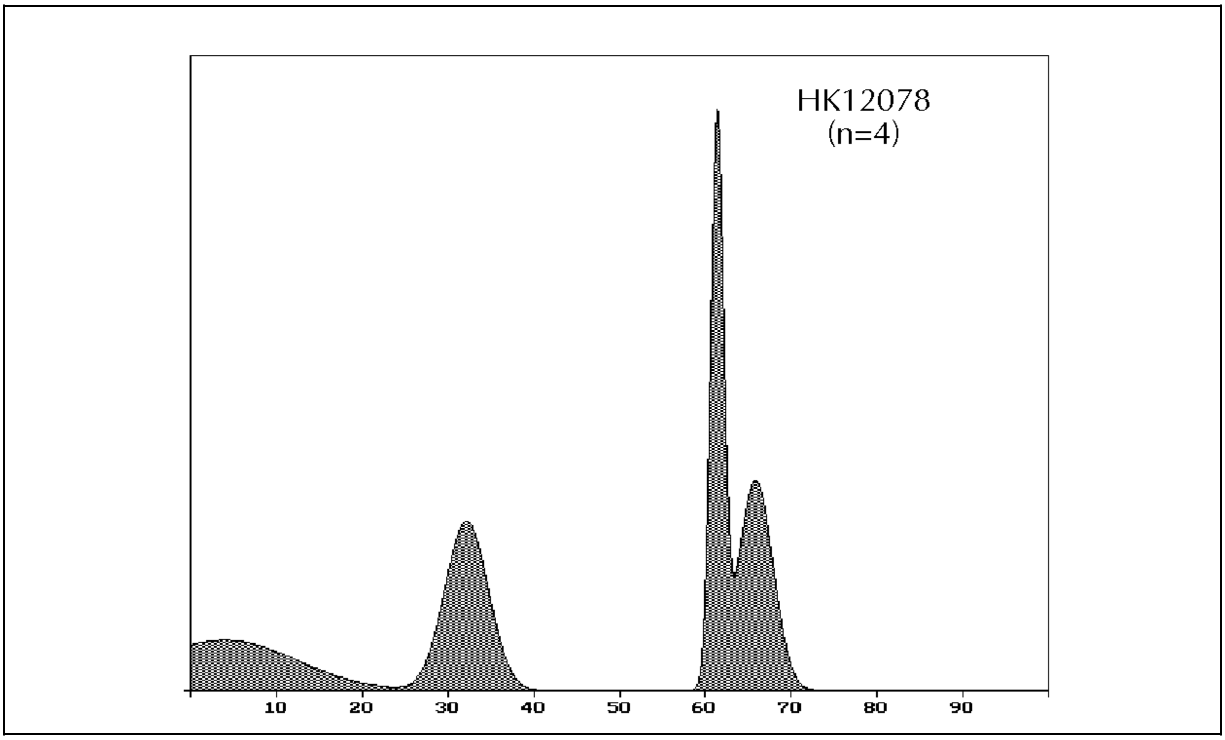

Figure 27 - Summary Histogram of Ages of First 16 Ar Fractions in Feldspar from Fault Rock HK12078. Age Interpretation as for Figure 14. Horizontal Scale as for Figure 25.

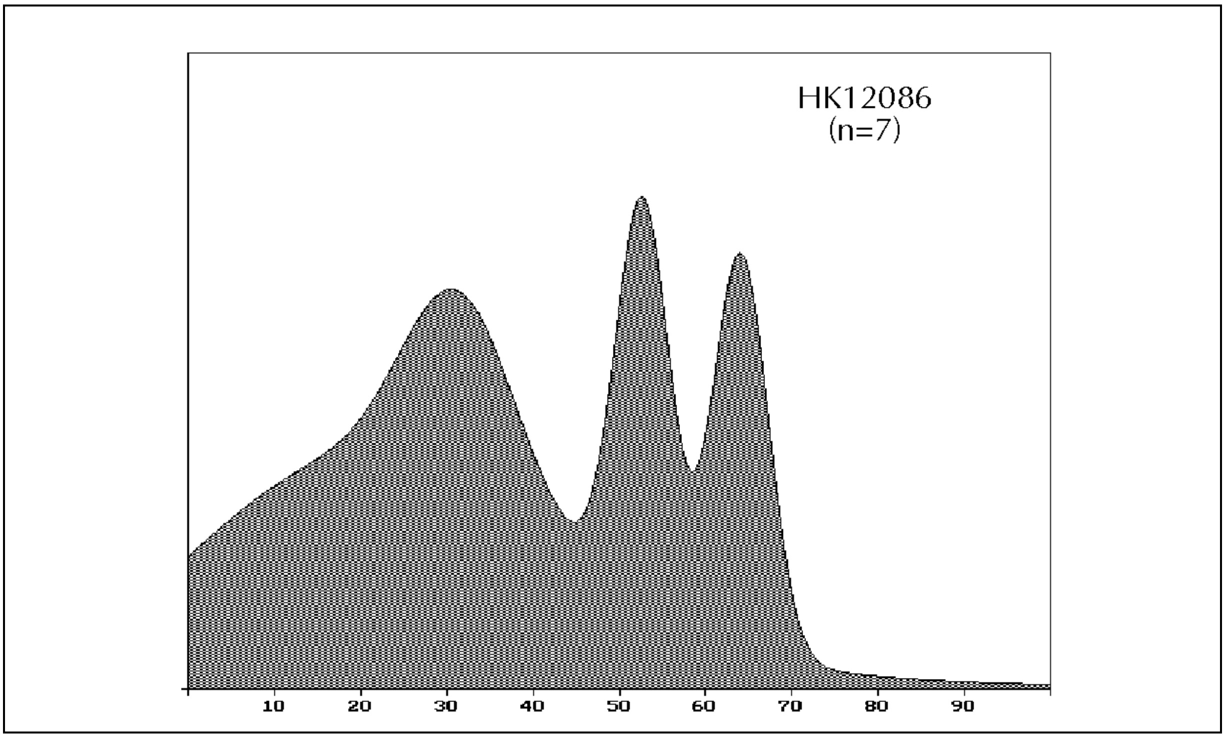

Figure 28 - Summary Histogram of Ages of First 16 Ar Fractions in Feldspar from Fault Rock HK12086. Age Interpretation as for Figure 14. Horizontal Scale as for Figure 25.

Table of Contents
Table of Contents
Table of Contents
Table of Contents

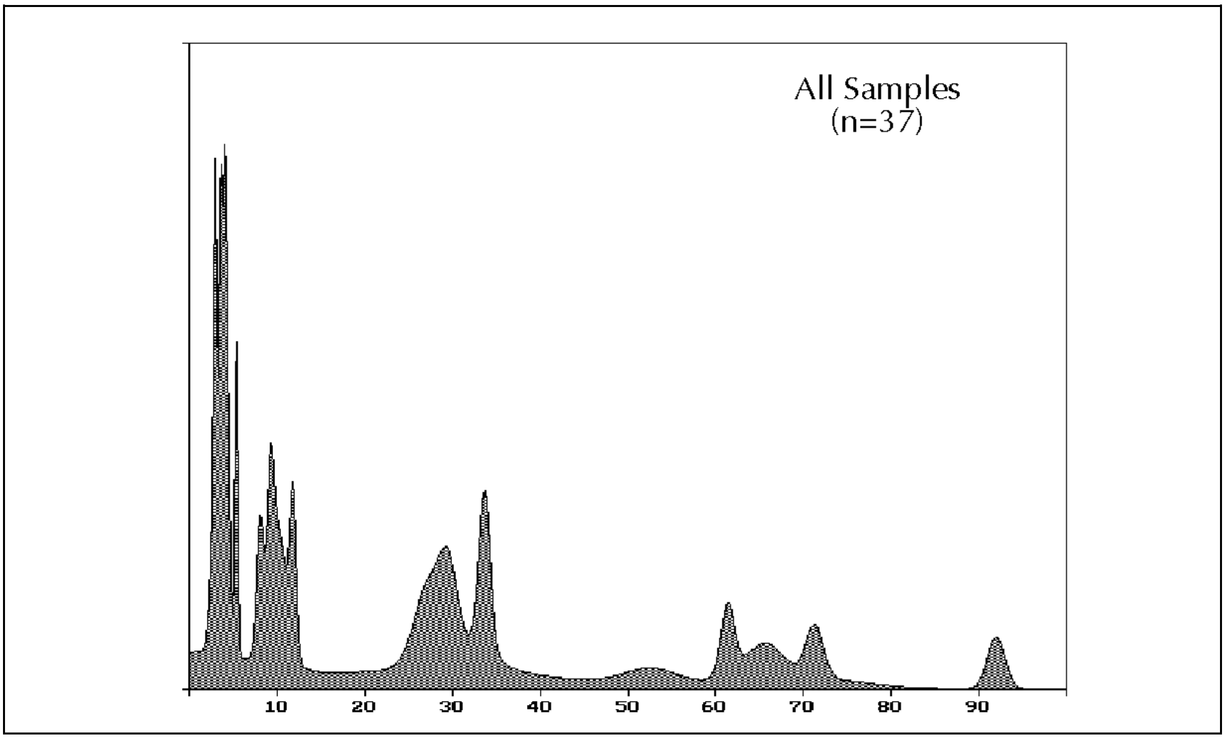

Figure 29 - Summary Histogram of Ages in Figures 25-28. Age Interpretation as for Figure 14. Horizontal Scale as for Figure 25.

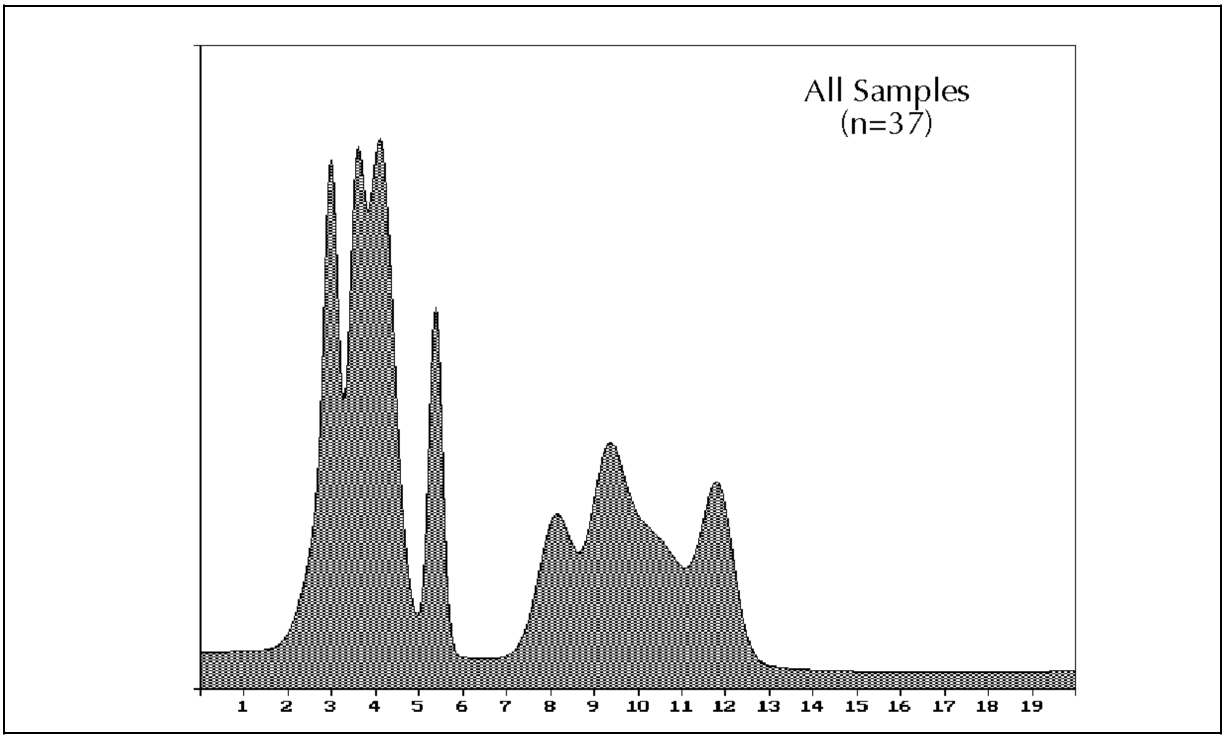

Figure 30 - Detail of Figure 29 Showing 0-20 Ma Region of Horizontal Axis. Age Interpretation as for Figure 14. Note Clusters of Ages at c.3-4 Ma and c.10 Ma.

Table of Contents
Table of Contents
Table of Contents
Table of Contents

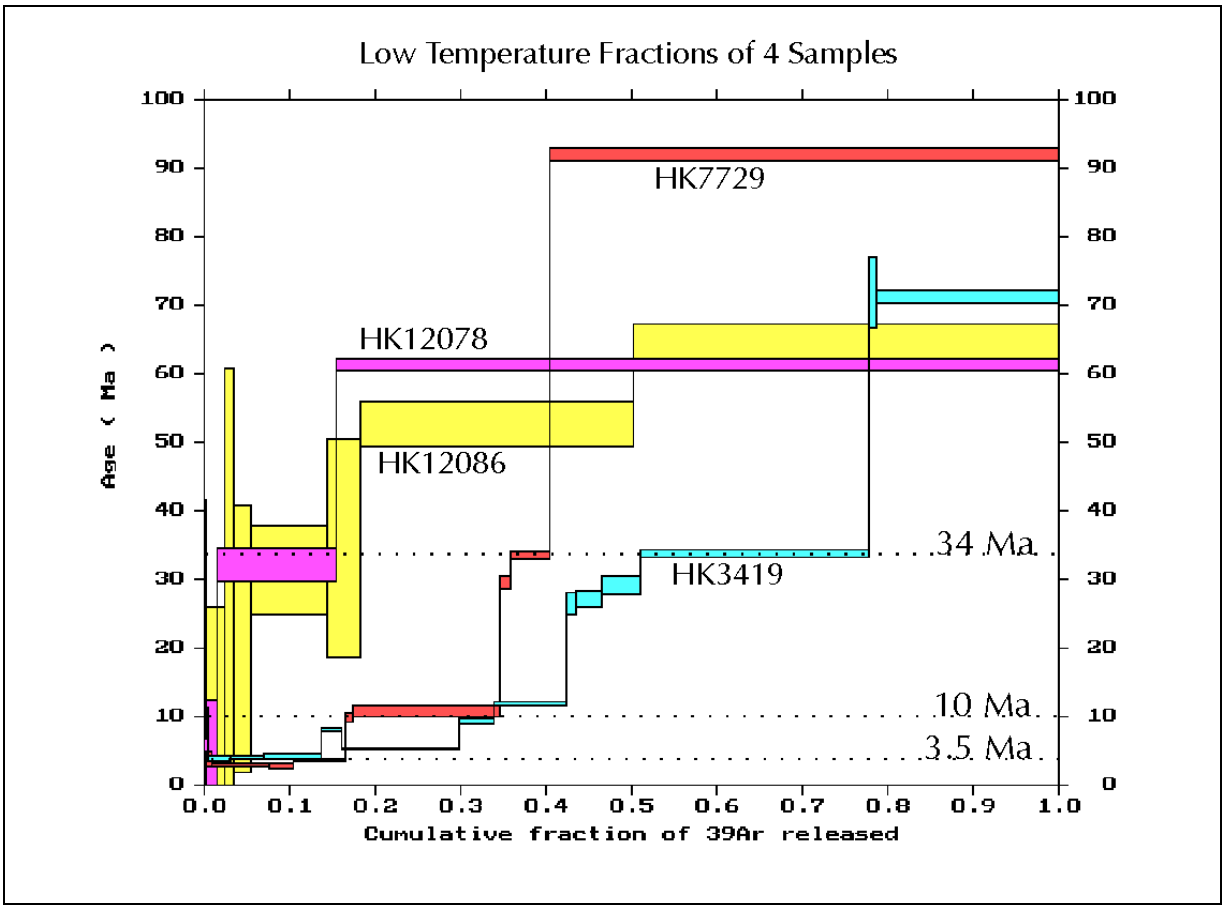

Figure 31 - Low-temperature Portions of Age Spectra of Fault Rock Samples. Horizontal Axes Vary but Emphasise Parallel Behaviour and Clustering at Ages of c.3.5 Ma, 10 Ma and 34 Ma, and 6-70 Ma in General.

Table of Contents
Table of Contents
Table of Contents
Table of Contents

Table of Contents

Table of Contents

APPENDIX A

RAW DATA FOR ANALYSES OF DYKE SAMPLES

Table of Contents

Table of Contents

P22-107 HK9842 mica

NewAge 981201 AgeParams 990623 (Fractionation relative to 40Ar/36Ar = 286.97)

Fractions:

No	Name	Temp	Cum 39K	Age	40Ar* / 39K
1	107-1 0.20W 10s	1	0.09426	97.210 ± 6.039 Ma	9.417 ± 0.60
2	107-2 0.20W 30s	2	0.19253	110.055 ± 5.340 Ma	10.700 ± 0.54
3	107-3 0.30W 20-	3	0.45690	107.924 ± 1.975 Ma	10.486 ± 0.20
4	107-4 0.40W 20-	4	0.72309	107.964 ± 2.302 Ma	10.491 ± 0.23
5	107-5 0.50w 20-	5	0.81206	86.226 ± 5.124 Ma	8.328 ± 0.51
6	107-6 0.70w 20-	6	0.90701	114.353 ± 6.721 Ma	11.131 ± 0.68
7	107-7 0.90W 20-	7	0.93840	124.070 ± 20.875 Ma	12.110 ± 2.11
8	107-8 1.20W 20-	8	1.00000	105.330 ± 10.151 Ma	10.227 ± 1.01

No	Name	Cum 36S	40Ar / 36Ar	40ArAcc/g	37Ca / 39K
1	107-1 0.20W 10s	0.82428	566.98 ± 33.08	1.8E-0011	728.815 ± 18.226 m
2	107-2 0.20W 30s	0.85491	8950.47 ± 13047.54	6.9E-0013	158.722 ± 17.757 m
3	107-3 0.30W 20-	0.86021	132291.46 ±1104036.48	1.2E-0013	109.625 ± 5.930 m
4	107-4 0.40W 20-	0.85415	-115940.29 ± 991536.50	-1.4E-0013	170.826 ± 7.317 m
5	107-5 0.50w 20-	1.00035	1573.15 ± 412.75	3.3E-0012	404.206 ± 27.651 m
6	107-6 0.70w 20-	1.00349	85144.60 ±1477804.80	7.0E-0014	262.666 ± 28.745 m
7	107-7 0.90W 20-	0.96673	-2312.28 ± 3544.93	-8.2E-0013	152.538 ± 58.783 m
8	107-8 1.20W 20-	1.00000	5069.46 ± 8112.35	7.4E-0013	156.952 ± 31.182 m

No	Name	40Ar* Vol ccNTP/g	Atm Cont	F1	F2
1	107-1 0.20W 10s	16.95 ± 1.08 E-12 (6.4%)	52.1182%	-5.2E-0004	5.3E-0003
2	107-2 0.20W 30s	20.09 ± 1.01 E-12 (5.0%)	3.3015%	-1.1E-0004	3.5E-0002
3	107-3 0.30W 20-	52.95 ± 1.03 E-12 (1.9%)	0.2234%	-7.8E-0005	2.8E-0001
4	107-4 0.40W 20-	53.34 ± 1.19 E-12 (2.2%)	-0.2549%	-1.2E-0004	-1.1E+0000
5	107-5 0.50w 20-	14.15 ± 0.86 E-12 (6.1%)	18.7840%	-2.9E-0004	1.7E-0002
6	107-6 0.70w 20-	20.19 ± 1.23 E-12 (6.1%)	0.3471%	-1.9E-0004	3.6E-0001
7	107-7 0.90W 20-	7.26 ± 1.26 E-12 (17.4%)	-12.7796%	-1.1E-0004	-9.4E-0003
8	107-8 1.20W 20-	12.03 ± 1.19 E-12 (9.9%)	5.8290%	-1.1E-0004	2.0E-0002

Integrated Results:

Age = 106.179 ± 1.699 Ma

40Ar* / 39K = 10.312 ± 0.165

Total 39K Vol = 1.9101E-0011 ccNTP/g

Total 40Ar* Vol = 1.970 ± 0.031 E-10

(40Ar / 36Ar)sam = 2895.20 ± 403.17

Total Atm 40Ar Vol = 2.2389E-0011 ccNTP/g

(36Ar / 40Ar)sam = 0.00034540 ±0.00006464
(37Ar / 40Ar)sam = 0.02038543 ±0.00057566
(39Ar / 40Ar)sam = 0.08707773 ±0.00124470

Corr 36/40 & 39/40 ratios =-0.664171
Corr 36/40 & 37/40 ratios =-0.338051
Corr 37/40 & 39/40 ratios = 0.501158

37Ca / 39K = 2.341 ± 0.057 E-1

Mass = 1.000 g

F1 = -1.670 E-4

F2 = 1.606 E-2

Table of Contents
Table of Contents
Table of Contents
Table of Contents

P22-108 HK9842 WR

NewAge 981201 AgeParams 990623 (Fractionation relative to 40Ar/36Ar = 286.97)

Fractions:

No	Name	Temp	Cum 39K	Age				40Ar* / 39K		
1	108-01 0.20w 30	2	0.00036	278.545	±	8.056	Ma	28.429	±	0.89
2	108-02 0.21w 2	3	0.00039	28.751	±	175.721	Ma	2.735	±	16.85
3	108-03 0.24w 25	3	0.00067	336.768	±	10.874	Ma	34.947	±	1.24
4	108-04 0.28w 25	4	0.00098	310.203	±	12.146	Ma	31.947	±	1.36
5	108-05 0.35w 25	5	0.00124	195.316	±	12.203	Ma	19.470	±	1.28
6	108-06 0.40w 25	6	0.00202	197.993	±	4.086	Ma	19.752	±	0.43
7	108-07 0.45w 25	7	0.00288	92.057	±	3.865	Ma	8.915	±	0.38
8	108-08 0.52W 25	8	0.00579	80.834	±	1.886	Ma	7.803	±	0.19
9	108-09 0.60W 25	9	0.00883	67.633	±	1.165	Ma	6.505	±	0.11
10	108-10 0.68w 26	10	0.01762	60.246	±	0.730	Ma	5.782	±	0.07
11	108-11 0.72w 26	11	0.02249	62.622	±	1.954	Ma	6.014	±	0.19
12	108-12 0.76w 26	12	0.03018	79.876	±	1.242	Ma	7.709	±	0.12
13	108-13 0.80W 26	13	0.03602	74.408	±	2.204	Ma	7.170	±	0.22
14	108-14 0.86W 26	14	0.04416	87.346	±	3.376	Ma	8.447	±	0.33
15	108-15 0.94W 26	15	0.05521	79.199	±	0.340	Ma	7.642	±	0.03
16	108-16 1.00w 27	16	0.06714	85.227	±	0.723	Ma	8.237	±	0.07
17	108-17 1.10w 27	17	0.07954	85.171	±	0.732	Ma	8.232	±	0.07
18	108-18 1.20w 27	18	0.09724	87.294	±	0.611	Ma	8.442	±	0.06
19	108-19 1.30w 27	19	0.12189	89.423	±	0.457	Ma	8.653	±	0.05
20	108-20 1.40w 27	20	0.15041	91.105	±	0.617	Ma	8.820	±	0.06
21	108-21 1.50W 27	21	0.18538	90.100	±	0.335	Ma	8.720	±	0.03
22	108-22 1.60w 28	22	0.24945	92.555	±	0.302	Ma	8.964	±	0.03
23	108-23 1.65w 28	23	0.31564	93.400	±	0.301	Ma	9.048	±	0.03
24	108-24 1.70w 28	24	0.35615	94.771	±	0.168	Ma	9.184	±	0.02
25	108-25 1.75w 28	25	0.39865	96.205	±	0.179	Ma	9.327	±	0.02
26	108-26 1.80W 28	26	0.42823	96.580	±	0.219	Ma	9.364	±	0.02
27	108-27 1.86W 28	27	0.46362	96.109	±	0.141	Ma	9.317	±	0.01
28	108-28 2.0W 28-	28	0.49499	95.390	±	0.217	Ma	9.246	±	0.02
29	108-29 2.20W 28	29	0.54288	93.284	±	0.168	Ma	9.036	±	0.02
30	108-30 2.40W 28	30	0.59253	89.942	±	0.133	Ma	8.705	±	0.01
31	108-31 2.60W 28	31	0.64423	87.206	±	0.243	Ma	8.433	±	0.02
32	108-32 2.80W 28	32	0.69321	86.290	±	0.256	Ma	8.343	±	0.03
33	108-33 3.00W 28	33	0.73571	86.297	±	0.248	Ma	8.343	±	0.02
34	108-34 3.30W 28	34	0.77522	86.775	±	0.243	Ma	8.391	±	0.02
35	108-35 4.00W 28	35	0.82450	91.145	±	0.115	Ma	8.824	±	0.01
36	108-36 6.00W 28	36	0.89393	94.238	±	0.116	Ma	9.131	±	0.01
37	108-37 fuse 28-	37	0.98262	93.158	±	0.107	Ma	9.024	±	0.01
38	108-38 refuse (	38	0.99464	93.127	±	0.622	Ma	9.021	±	0.06
39	108-39 re2fuse	39	0.99908	86.069	±	1.670	Ma	8.321	±	0.17
40	108-40 re3fuse	40	1.00000	88.926	±	10.642	Ma	8.604	±	1.06

Table of Contents

Table of Contents

Table of Contents

Table of Contents

P22-108 HK9842 WR

No	Name	Cum 36S	40Ar / 36Ar		40ArAcc/g	37Ca / 39K		
1	108-01 0.20w 30	0.06827	339.96 ±	1.54	2.4E-0010	564.545 ±	36.518	m
2	108-02 0.21w 2	0.07437	298.30 ±	17.43	2.2E-0011	356.145 ±	589.044	m
3	108-03 0.24w 25	0.09627	426.97 ±	6.53	7.7E-0011	418.616 ±	54.130	m
4	108-04 0.28w 25	0.11171	487.75 ±	13.14	5.4E-0011	380.228 ±	41.309	m
5	108-05 0.35w 25	0.11993	473.45 ±	18.63	2.9E-0011	456.284 ±	61.841	m
6	108-06 0.40w 25	0.13523	590.37 ±	12.56	5.4E-0011	344.989 ±	20.482	m
7	108-07 0.45w 25	0.14408	549.16 ±	19.91	3.1E-0011	342.427 ±	16.438	m
8	108-08 0.52W 25	0.16190	668.60 ±	18.25	6.3E-0011	447.135 ±	9.796	m
9	108-09 0.60W 25	0.17637	695.05 ±	15.35	5.1E-0011	668.747 ±	12.541	m
10	108-10 0.68w 26	0.20933	747.06 ±	11.42	1.2E-0010	1.129 ±	0.011	
11	108-11 0.72w 26	0.22684	785.70 ±	39.66	6.2E-0011	1.549 ±	0.021	
12	108-12 0.76w 26	0.25280	964.36 ±	29.84	9.2E-0011	1.588 ±	0.014	
13	108-13 0.80W 26	0.26934	1036.75 ±	68.18	5.8E-0011	1.519 ±	0.024	
14	108-14 0.86W 26	0.28760	1397.89 ±	172.04	6.4E-0011	1.562 ±	0.027	
15	108-15 0.94W 26	0.30675	1587.14 ±	26.44	6.8E-0011	1.729 ±	0.005	
16	108-16 1.00w 27	0.33535	1301.59 ±	30.05	1.0E-0010	1.799 ±	0.015	
17	108-17 1.10w 27	0.36094	1463.89 ±	44.60	9.0E-0011	2.158 ±	0.010	
18	108-18 1.20w 27	0.39684	1513.92 ±	26.57	1.3E-0010	2.360 ±	0.015	
19	108-19 1.30w 27	0.44694	1542.25 ±	23.25	1.8E-0010	2.418 ±	0.007	
20	108-20 1.40w 27	0.49857	1722.21 ±	26.95	1.8E-0010	2.422 ±	0.012	
21	108-21 1.50W 27	0.53263	2916.30 ±	52.35	1.2E-0010	2.183 ±	0.006	
22	108-22 1.60w 28	0.57793	4008.38 ±	85.37	1.6E-0010	1.142 ±	0.004	
23	108-23 1.65w 28	0.58492	25367.69 ±	1563.08	2.5E-0011	546.238 ±	2.208	m
24	108-24 1.70w 28	0.58954	23888.67 ±	2065.72	1.6E-0011	195.554 ±	3.630	m
25	108-25 1.75w 28	0.60012	11273.17 ±	355.29	3.7E-0011	147.444 ±	0.820	m
26	108-26 1.80W 28	0.65024	1913.47 ±	15.24	1.8E-0010	158.339 ±	1.047	m
27	108-27 1.86W 28	0.65841	12108.14 ±	460.37	2.9E-0011	178.943 ±	0.915	m
28	108-28 2.0W 28-	0.66411	15197.49 ±	1062.28	2.0E-0011	211.317 ±	1.381	m
29	108-29 2.20W 28	0.67280	14886.99 ±	597.88	3.1E-0011	260.777 ±	0.947	m
30	108-30 2.40W 28	0.68373	11866.43 ±	386.80	3.9E-0011	298.889 ±	1.132	m
31	108-31 2.60W 28	0.69444	12219.35 ±	512.34	3.8E-0011	354.951 ±	1.399	m
32	108-32 2.80W 28	0.70290	14443.06 ±	732.79	3.0E-0011	406.111 ±	1.242	m
33	108-33 3.00W 28	0.70936	16366.94 ±	999.73	2.3E-0011	470.115 ±	2.423	m
34	108-34 3.30W 28	0.71537	16433.48 ±	980.76	2.1E-0011	513.526 ±	1.999	m
35	108-35 4.00W 28	0.72362	15735.59 ±	765.46	2.9E-0011	705.760 ±	0.853	m
36	108-36 6.00W 28	0.73480	16902.11 ±	573.73	3.9E-0011	570.241 ±	1.166	m
37	108-37 fuse 28-	0.78634	4842.48 ±	44.10	1.8E-0010	584.546 ±	1.241	m
38	108-38 refuse (	0.80925	1681.46 ±	29.49	8.1E-0011	645.133 ±	3.961	m
39	108-39 re2fuse	0.88099	446.39 ±	3.73	2.5E-0010	650.355 ±	9.665	m
40	108-40 re3fuse	1.00000	314.88 ±	2.41	4.2E-0010	649.968 ±	46.704	m

Table of Contents
Table of Contents
Table of Contents

P22-108 HK9842 WR

No	Name	40Ar*	Vol ccNTP/g		Atm Cont	F1	F2
1	108-01 0.20w 30	36.25 ±	1.11 E-12	(3.1%)	86.9214%	-4.0E-0004	-1.6E-0004
2	108-02 0.21w 2	0.20 ±	1.26 E-12	(616.0%)	99.0606%	-2.5E-0004	-1.5E-0004
3	108-03 0.24w 25	34.38 ±	1.20 E-12	(3.5%)	69.2092%	-3.0E-0004	1.4E-0004
4	108-04 0.28w 25	35.45 ±	1.48 E-12	(4.2%)	60.5844%	-2.7E-0004	3.7E-0004
5	108-05 0.35w 25	17.46 ±	1.15 E-12	(6.6%)	62.4148%	-3.3E-0004	8.4E-0004
6	108-06 0.40w 25	53.89 ±	1.19 E-12	(2.2%)	50.0536%	-2.5E-0004	1.2E-0003
7	108-07 0.45w 25	26.82 ±	1.16 E-12	(4.3%)	53.8093%	-2.4E-0004	2.5E-0003
8	108-08 0.52W 25	79.40 ±	1.87 E-12	(2.4%)	44.1968%	-3.2E-0004	5.6E-0003
9	108-09 0.60W 25	69.08 ±	1.24 E-12	(1.8%)	42.5149%	-4.8E-0004	1.1E-0002
10	108-10 0.68w 26	177.76 ±	2.26 E-12	(1.3%)	39.5552%	-8.0E-0004	2.3E-0002
11	108-11 0.72w 26	102.52 ±	3.25 E-12	(3.2%)	37.6099%	-1.1E-0003	3.3E-0002
12	108-12 0.76w 26	207.38 ±	3.37 E-12	(1.6%)	30.6422%	-1.1E-0003	3.6E-0002
13	108-13 0.80W 26	146.38 ±	4.24 E-12	(2.9%)	28.5026%	-1.1E-0003	4.1E-0002
14	108-14 0.86W 26	240.51 ±	9.29 E-12	(3.9%)	21.1390%	-1.1E-0003	5.3E-0002
15	108-15 0.94W 26	295.37 ±	1.94 E-12	(0.7%)	18.6184%	-1.2E-0003	7.4E-0002
16	108-16 1.00w 27	343.72 ±	3.31 E-12	(1.0%)	22.7030%	-1.3E-0003	5.7E-0002
17	108-17 1.10w 27	357.00 ±	3.50 E-12	(1.0%)	20.1860%	-1.5E-0003	7.7E-0002
18	108-18 1.20w 27	522.43 ±	4.25 E-12	(0.8%)	19.5189%	-1.7E-0003	8.5E-0002
19	108-19 1.30w 27	746.09 ±	5.26 E-12	(0.7%)	19.1603%	-1.7E-0003	8.7E-0002
20	108-20 1.40w 27	879.75 ±	6.91 E-12	(0.8%)	17.1582%	-1.7E-0003	9.7E-0002
21	108-21 1.50W 27	1.07 ±	0.01 E-9	(0.6%)	10.1327%	-1.6E-0003	1.5E-0001
22	108-22 1.60w 28	2.01 ±	0.01 E-9	(0.6%)	7.3721%	-8.1E-0004	1.2E-0001
23	108-23 1.65w 28	2.09 ±	0.01 E-9	(0.6%)	1.1649%	-3.9E-0004	3.0E-0001
24	108-24 1.70w 28	1.30 ±	0.01 E-9	(0.5%)	1.2370%	-1.4E-0004	1.2E-0001
25	108-25 1.75w 28	1.39 ±	0.01 E-9	(0.5%)	2.6213%	-1.1E-0004	4.6E-0002
26	108-26 1.80W 28	968.56 ±	5.16 E-12	(0.5%)	15.4431%	-1.1E-0004	7.5E-0003
27	108-27 1.86W 28	1.15 ±	0.01 E-9	(0.5%)	2.4405%	-1.3E-0004	5.9E-0002
28	108-28 2.0W 28-	1.01 ±	0.01 E-9	(0.5%)	1.9444%	-1.5E-0004	8.7E-0002
29	108-29 2.20W 28	1.51 ±	0.01 E-9	(0.5%)	1.9850%	-1.9E-0004	1.1E-0001
30	108-30 2.40W 28	1.51 ±	0.01 E-9	(0.5%)	2.4902%	-2.1E-0004	1.0E-0001
31	108-31 2.60W 28	1.52 ±	0.01 E-9	(0.5%)	2.4183%	-2.5E-0004	1.2E-0001
32	108-32 2.80W 28	1.43 ±	0.01 E-9	(0.5%)	2.0460%	-2.9E-0004	1.6E-0001
33	108-33 3.00W 28	1.24 ±	0.01 E-9	(0.5%)	1.8055%	-3.4E-0004	2.0E-0001
34	108-34 3.30W 28	1.16 ±	0.01 E-9	(0.5%)	1.7982%	-3.7E-0004	2.2E-0001
35	108-35 4.00W 28	1.52 ±	0.01 E-9	(0.5%)	1.8779%	-5.0E-0004	2.6E-0001
36	108-36 6.00W 28	2.22 ±	0.01 E-9	(0.5%)	1.7483%	-4.1E-0004	2.2E-0001
37	108-37 fuse 28-	2.80 ±	0.01 E-9	(0.5%)	6.1022%	-4.2E-0004	7.6E-0002
38	108-38 refuse (	379.35 ±	2.99 E-12	(0.8%)	17.5740%	-4.6E-0004	2.7E-0002
39	108-39 re2fuse	129.28 ±	2.58 E-12	(2.0%)	66.1976%	-4.6E-0004	2.8E-0003
40	108-40 re3fuse	27.55 ±	3.32 E-12	(12.0%)	93.8440%	-4.6E-0004	-5.4E-0005

Table of Contents
Table of Contents
Table of Contents
Table of Contents

P22-108 HK9842 WR

Integrated Results:

Age = 91.020 ± 0.350 Ma

40Ar* / 39K = 8.812 ± 0.012	Total 39K Vol = 3.4974E-0009 ccNTP/g
	Total 40Ar* Vol = 3.082 ± 0.004 E-8
(40Ar / 36Ar)sam = 2875.71 ± 11.56	Total Atm 40Ar Vol = 3.5294E-0009 ccNTP/g
(36Ar / 40Ar)sam = 0.00034774 ±0.00000187	Corr 36/40 & 39/40 ratios =-0.366285
(37Ar / 40Ar)sam = 0.07680711 ±0.00007895	Corr 36/40 & 37/40 ratios =-0.247375
(39Ar / 40Ar)sam = 0.10182620 ±0.00006831	Corr 37/40 & 39/40 ratios = 0.464814
37Ca / 39K = 7.543 ± 0.007 E-1	Mass = 1.000 g
F1 = -5.381 E-4	F2 = 5.762 E-2

Table of Contents
Table of Contents
Table of Contents
Table of Contents

P22-116 HK9728 WR

NewAge 981201 AgeParams 990623 (Fractionation relative to 40Ar/36Ar = 286.97)

Fractions:

No	Name	Temp	Cum 39K	Age	40Ar* / 39K
1	116-1 0.20W 8-	1	0.00094	50.843 ± 37.044 Ma	4.862 ± 3.59
2	116-2 0.40W 8-	2	0.01894	58.226 ± 1.947 Ma	5.580 ± 0.19
3	116-3 0.50W 8-	3	0.03065	97.596 ± 2.593 Ma	9.456 ± 0.26
4	116-4 0.70W 8-	4	0.09205	99.742 ± 2.743 Ma	9.669 ± 0.27
5	116-05 0.90w 8	5	0.21331	101.046 ± 0.658 Ma	9.799 ± 0.07
6	116-06 1.20w 9	6	0.40356	104.178 ± 0.279 Ma	10.112 ± 0.03
7	116-07 1.4w 9-	7	0.54483	99.745 ± 0.373 Ma	9.670 ± 0.04
8	116-08 1.6w 9-	8	0.63202	99.960 ± 0.557 Ma	9.691 ± 0.06
9	116-09 2.0w 9-	9	0.76105	107.115 ± 0.413 Ma	10.406 ± 0.04
10	pay up to here!	10	0.83171	110.269 ± 0.625 Ma	10.721 ± 0.06
11	116-11 2.7w 9-	11	0.88323	113.172 ± 0.611 Ma	11.013 ± 0.06
12	116-12 3.2w 9-	12	0.92465	117.175 ± 0.852 Ma	11.415 ± 0.09
13	116-13 3.5w 9-	13	0.97003	121.931 ± 0.682 Ma	11.894 ± 0.07
14	116-14 4.0w 9-	14	0.99188	134.586 ± 1.137 Ma	13.175 ± 0.12
15	116-15 6w 9-Ju	15	0.99735	156.990 ± 4.434 Ma	15.465 ± 0.46
16	116-16 10w 10-J	16	1.00000	180.831 ± 10.360 Ma	17.934 ± 1.08

No	Name	Cum 36S	40Ar / 36Ar	40ArAcc/g	37Ca / 39K
1	116-1 0.20W 8-	0.02940	313.51 ± 14.11	2.5E-0011	556.720 ± 193.700 m
2	116-2 0.40W 8-	0.29582	339.00 ± 1.69	2.3E-0010	936.785 ± 12.075 m
3	116-3 0.50W 8-	0.34802	540.30 ± 12.13	4.5E-0011	2.714 ± 0.017
4	116-4 0.70W 8-	0.51646	702.20 ± 17.34	1.5E-0010	3.287 ± 0.045
5	116-05 0.90w 8	0.64518	1360.68 ± 24.85	1.1E-0010	2.225 ± 0.010
6	116-06 1.20w 9	0.72201	3184.90 ± 72.20	6.6E-0011	783.085 ± 2.400 m
7	116-07 1.4w 9-	0.75394	5232.56 ± 200.04	2.8E-0011	510.538 ± 3.811 m
8	116-08 1.6w 9-	0.78512	3422.41 ± 187.91	2.7E-0011	685.781 ± 3.309 m
9	116-09 2.0w 9-	0.83550	3370.34 ± 117.66	4.4E-0011	1.128 ± 0.004
10	pay up to here!	0.86592	3169.94 ± 160.25	2.6E-0011	885.760 ± 5.928 m
11	116-11 2.7w 9-	0.89146	2859.05 ± 129.34	2.2E-0011	783.225 ± 6.022 m
12	116-12 3.2w 9-	0.91458	2654.69 ± 152.78	2.0E-0011	859.523 ± 6.594 m
13	116-13 3.5w 9-	0.94880	2115.27 ± 69.47	3.0E-0011	640.694 ± 7.494 m
14	116-14 4.0w 9-	0.97587	1523.12 ± 53.10	2.3E-0011	694.622 ± 14.371 m
15	116-15 6w 9-Ju	0.99398	834.73 ± 44.01	1.6E-0011	705.221 ± 31.842 m
16	116-16 10w 10-J	1.00000	1205.35 ± 221.76	5.2E-0012	732.391 ± 77.705 m

No	Name	40Ar* Vol ccNTP/g		Atm Cont	F1	F2
1	116-1 0.20W 8-	1.55 ± 1.14 E-12	(73.9%)	94.2553%	-4.0E-0004	1.8E-0004
2	116-2 0.40W 8-	33.88 ± 1.16 E-12	(3.4%)	87.1693%	-6.7E-0004	1.4E-0003
3	116-3 0.50W 8-	37.35 ± 1.03 E-12	(2.8%)	54.6914%	-1.9E-0003	1.7E-0002
4	116-4 0.70W 8-	200.26 ± 5.31 E-12	(2.6%)	42.0820%	-2.3E-0003	3.5E-0002
5	116-05 0.90w 8	400.82 ± 3.21 E-12	(0.8%)	21.7170%	-1.6E-0003	6.2E-0002
6	116-06 1.20w 9	648.93 ± 3.62 E-12	(0.6%)	9.2781%	-5.6E-0004	5.8E-0002
7	116-07 1.4w 9-	460.80 ± 2.74 E-12	(0.6%)	5.6473%	-3.6E-0004	6.8E-0002
8	116-08 1.6w 9-	285.03 ± 2.09 E-12	(0.7%)	8.6343%	-4.9E-0004	5.8E-0002
9	116-09 2.0w 9-	452.88 ± 2.82 E-12	(0.6%)	8.7677%	-8.0E-0004	8.4E-0002
10	pay up to here!	255.57 ± 1.91 E-12	(0.7%)	9.3219%	-6.3E-0004	6.2E-0002
11	116-11 2.7w 9-	191.38 ± 1.39 E-12	(0.7%)	10.3356%	-5.6E-0004	4.8E-0002
12	116-12 3.2w 9-	159.47 ± 1.41 E-12	(0.9%)	11.1313%	-6.1E-0004	4.7E-0002
13	116-13 3.5w 9-	182.06 ± 1.35 E-12	(0.7%)	13.9698%	-4.6E-0004	2.6E-0002
14	116-14 4.0w 9-	97.13 ± 0.96 E-12	(1.0%)	19.4009%	-5.0E-0004	1.7E-0002
15	116-15 6w 9-Ju	28.55 ± 0.84 E-12	(2.9%)	35.4005%	-5.0E-0004	6.3E-0003
16	116-16 10w 10-J	16.01 ± 0.96 E-12	(6.0%)	24.5157%	-5.2E-0004	9.8E-0003

Table of Contents
Table of Contents
Table of Contents
Table of Contents

P22-116 HK9728 WR

Integrated Results:

Age = 105.386 ± 0.480 Ma

40Ar* / 39K = 10.233 ± 0.029	Total 39K Vol = 3.3732E-0010 ccNTP/g
	Total 40Ar* Vol = 3.452 ± 0.009 E-9
(40Ar / 36Ar)sam = 1476.25 ± 9.90	Total Atm 40Ar Vol = 8.6383E-0010 ccNTP/g
(36Ar / 40Ar)sam = 0.00067739 ±0.00000578	Corr 36/40 & 39/40 ratios =-0.353008
(37Ar / 40Ar)sam = 0.08877576 ±0.00023670	Corr 36/40 & 37/40 ratios =-0.262641
(39Ar / 40Ar)sam = 0.07816519 ±0.00015102	Corr 37/40 & 39/40 ratios = 0.568640
37Ca / 39K = 1.136 ± 0.003	Mass = 1.000 g
F1 = -8.101 E-4	F2 = 3.454 E-2

Table of Contents
Table of Contents
Table of Contents
Table of Contents

P22-327 HK10981 WR

NewAge 981201 AgeParams 990623 (Fractionation relative to 40Ar/36Ar = 286.97)

Fractions:

No	Name	Temp	Cum 39K	Age				40Ar* / 39K		
1	27-01 0.20w 11-	1	0.00844	537.654	±	5.674	Ma	59.058	±	0.72
2	27-02 0.25w 11-	2	0.04184	91.788	±	2.422	Ma	8.878	±	0.24
3	27-03 0.30W 11-	3	0.07359	88.176	±	1.581	Ma	8.520	±	0.16
4	27-04 0.40W 11-	4	0.14706	91.704	±	0.710	Ma	8.870	±	0.07
5	27-05 0.50W 11-	5	0.23177	90.952	±	0.568	Ma	8.796	±	0.06
6	27-06 0.60w 12-	6	0.28412	89.560	±	0.592	Ma	8.658	±	0.06
7	27-07 0.70w 12-	7	0.36130	88.295	±	0.501	Ma	8.532	±	0.05
8	27-08 0.80w 12-	8	0.43855	88.792	±	0.326	Ma	8.582	±	0.03
9	27-09 0.90w 12-	9	0.51274	90.255	±	0.507	Ma	8.726	±	0.05
10	27-10 1.00w 13-	10	0.57536	91.827	±	0.555	Ma	8.882	±	0.06
11	27-11 1.10w 13-	11	0.68028	91.582	±	0.320	Ma	8.858	±	0.03
12	27-12 1.20w 13-	12	0.72350	90.741	±	0.710	Ma	8.775	±	0.07
13	27-13 1.40W 13-	13	0.79493	93.151	±	0.410	Ma	9.014	±	0.04
14	27-14 1.60W 13-	14	0.83231	93.271	±	0.815	Ma	9.026	±	0.08
15	27-15 2.0W 13-A	15	0.87718	97.207	±	0.554	Ma	9.417	±	0.06
16	27-16 2.50W 13-	16	0.93114	97.312	±	0.472	Ma	9.427	±	0.05
17	27-17 5.00W 13-	17	0.97580	97.909	±	0.501	Ma	9.487	±	0.05
18	27-18 10w 14-Au	18	1.00000	98.861	±	1.225	Ma	9.582	±	0.12

No	Name	Cum 36S	40Ar / 36Ar			40ArAcc/g	37Ca / 39K			
1	27-01 0.20w 11-	0.43504	694.66	±	9.69	1.4E-0010	219.876	±	46.780	m
2	27-02 0.25w 11-	0.57942	1010.70	±	51.28	4.5E-0011	808.965	±	30.499	m
3	27-03 0.30W 11-	0.63465	2000.95	±	167.41	1.7E-0011	650.154	±	21.576	m
4	27-04 0.40W 11-	0.69637	3972.30	±	249.27	1.9E-0011	724.577	±	10.175	m
5	27-05 0.50W 11-	0.73691	6695.09	±	574.84	1.3E-0011	946.899	±	10.397	m
6	27-06 0.60w 12-	0.74455	20941.09	±	9693.47	2.4E-0012	621.620	±	10.431	m
7	27-07 0.70w 12-	0.76934	9549.87	±	1635.00	7.8E-0012	663.188	±	9.121	m
8	27-08 0.80w 12-	0.79444	9491.68	±	1044.70	7.9E-0012	866.596	±	6.816	m
9	27-09 0.90w 12-	0.81925	9379.12	±	1599.92	7.8E-0012	759.761	±	10.317	m
10	27-10 1.00w 13-	0.83279	14605.28	±	4243.10	4.2E-0012	599.337	±	9.264	m
11	27-11 1.10w 13-	0.85804	13114.03	±	1770.70	7.9E-0012	688.002	±	7.034	m
12	27-12 1.20w 13-	0.87270	9302.62	±	2210.32	4.6E-0012	597.565	±	13.718	m
13	27-13 1.40W 13-	0.89436	10642.93	±	1611.20	6.8E-0012	1.165	±	0.009	
14	27-14 1.60W 13-	0.90745	9274.19	±	2466.22	4.1E-0012	1.148	±	0.013	
15	27-15 2.0W 13-A	0.92706	7797.15	±	1122.16	6.1E-0012	1.475	±	0.011	
16	27-16 2.50W 13-	0.95640	6333.79	±	617.69	9.2E-0012	1.218	±	0.014	
17	27-17 5.00W 13-	0.98144	6188.43	±	616.24	7.8E-0012	695.965	±	11.695	m
18	27-18 10w 14-Au	1.00000	4644.73	±	862.45	5.8E-0012	578.853	±	25.143	m

Table of Contents
Table of Contents
Table of Contents
Table of Contents

P22-327 HK10981 WR

No	Name	40Ar* Vol ccNTP/g		Atm Cont	F1	F2
1	27-01 0.20w 11-	183.95 ± 2.16 E-12 (	1.2%)	42.5386%	-1.6E-0004	2.6E-0004
2	27-02 0.25w 11-	109.39 ± 2.97 E-12 (	2.7%)	29.2371%	-5.8E-0004	1.7E-0002
3	27-03 0.30W 11-	99.78 ± 1.86 E-12 (	1.9%)	14.7680%	-4.6E-0004	3.5E-0002
4	27-04 0.40W 11-	240.38 ± 2.16 E-12 (	0.9%)	7.4390%	-5.2E-0004	7.7E-0002
5	27-05 0.50W 11-	274.84 ± 2.17 E-12 (	0.8%)	4.4137%	-6.8E-0004	1.6E-0001
6	27-06 0.60w 12-	167.16 ± 1.39 E-12 (	0.8%)	1.4111%	-4.4E-0004	2.9E-0001
7	27-07 0.70w 12-	242.93 ± 1.82 E-12 (	0.7%)	3.0943%	-4.7E-0004	1.7E-0001
8	27-08 0.80w 12-	244.52 ± 1.50 E-12 (	0.6%)	3.1133%	-6.2E-0004	2.1E-0001
9	27-09 0.90w 12-	238.80 ± 1.80 E-12 (	0.8%)	3.1506%	-5.4E-0004	1.8E-0001
10	27-10 1.00w 13-	205.18 ± 1.61 E-12 (	0.8%)	2.0232%	-4.3E-0004	2.1E-0001
11	27-11 1.10w 13-	342.83 ± 2.04 E-12 (	0.6%)	2.2533%	-4.9E-0004	2.2E-0001
12	27-12 1.20w 13-	139.87 ± 1.30 E-12 (	0.9%)	3.1765%	-4.3E-0004	1.5E-0001
13	27-13 1.40W 13-	237.50 ± 1.58 E-12 (	0.7%)	2.7765%	-8.3E-0004	2.7E-0001
14	27-14 1.60W 13-	124.45 ± 1.26 E-12 (	1.0%)	3.1863%	-8.2E-0004	2.4E-0001
15	27-15 2.0W 13-A	155.86 ± 1.18 E-12 (	0.8%)	3.7898%	-1.1E-0003	2.5E-0001
16	27-16 2.50W 13-	187.63 ± 1.30 E-12 (	0.7%)	4.6655%	-8.7E-0004	1.8E-0001
17	27-17 5.00W 13-	156.30 ± 1.11 E-12 (	0.7%)	4.7750%	-5.0E-0004	1.1E-0001
18	27-18 10w 14-Au	85.52 ± 1.16 E-12 (	1.4%)	6.3621%	-4.1E-0004	6.8E-0002

Integrated Results:

Age = 96.207 ± 0.405 Ma

40Ar* / 39K = 9.317 ± 0.021

Total 39K Vol = 3.6887E-0010 ccNTP/g

Total 40Ar* Vol = 3.437 ± 0.007 E-9

(40Ar / 36Ar)sam = 3540.00 ± 60.07

Total Atm 40Ar Vol = 3.1302E-0010 ccNTP/g

(36Ar / 40Ar)sam = 0.00028249 ±0.00000650
(37Ar / 40Ar)sam = 0.08151392 ±0.00030548
(39Ar / 40Ar)sam = 0.09836702 ±0.00016546

Corr 36/40 & 39/40 ratios =-0.551907
Corr 36/40 & 37/40 ratios =-0.258413
Corr 37/40 & 39/40 ratios = 0.415052

37Ca / 39K = 8.287 ± 0.028 E-1

Mass = 1.000 g

F1 = -5.911 E-4

F2 = 7.406 E-2

Table of Contents
Table of Contents
Table of Contents
Table of Contents

P22-413 HK1651 WR

NewAge 981201 AgeParams 990623 (Fractionation relative to 40Ar/36Ar = 286.97)

Fractions:

No	Name	Temp	Cum 39K	Age	40Ar* / 39K
1	413-01 0.13w 13	1	0.00017	159.413 ± 41.570 Ma	15.715 ± 4.28
2	413-02 0.20w 13	2	0.00210	150.377 ± 11.018 Ma	14.786 ± 1.13
3	413-03 0.25w 13	3	0.00328	105.491 ± 11.206 Ma	10.243 ± 1.12
4	413-04 0.30W 13	4	0.00509	101.595 ± 5.945 Ma	9.854 ± 0.59
5	413-05 0.40W 13	5	0.00938	89.363 ± 3.352 Ma	8.638 ± 0.33
6	413-06 0.50W 13	6	0.02356	77.138 ± 1.112 Ma	7.431 ± 0.11
7	413-07 0.55w 14	7	0.04348	93.092 ± 1.354 Ma	9.008 ± 0.13
8	413-08 0.60w 14	8	0.06002	91.125 ± 1.321 Ma	8.813 ± 0.13
9	413-09 0.65w 14	9	0.07944	83.408 ± 2.078 Ma	8.049 ± 0.21
10	413-10 0.70w 14	10	0.09885	72.175 ± 0.561 Ma	6.943 ± 0.06
11	413-11 0.70w re	11	0.10980	67.473 ± 0.638 Ma	6.482 ± 0.06
12	413-12 0.75w 15	12	0.12244	70.519 ± 0.747 Ma	6.781 ± 0.07
13	413-13 0.80w 15	13	0.13742	69.735 ± 0.570 Ma	6.704 ± 0.06
14	413-14 0.85w 15	14	0.15492	69.871 ± 0.426 Ma	6.717 ± 0.04
15	413-15 0.90w 15	15	0.17149	69.949 ± 0.360 Ma	6.725 ± 0.04
16	413-16 0.95W 15	16	0.18845	70.474 ± 0.498 Ma	6.776 ± 0.05
17	413-17 1.00W 15	17	0.20362	68.892 ± 0.428 Ma	6.621 ± 0.04
18	413-18 1.10W 15	18	0.22308	67.263 ± 0.533 Ma	6.462 ± 0.05
19	413-19 1.20W 15	19	0.24829	68.640 ± 0.305 Ma	6.597 ± 0.03
20	413-20 1.30W 15	20	0.28789	69.998 ± 0.295 Ma	6.730 ± 0.03
21	413-21 1.40W 16	21	0.32317	71.592 ± 0.233 Ma	6.886 ± 0.02
22	413-22 1.50w 16	22	0.37981	71.967 ± 0.199 Ma	6.923 ± 0.02
23	413-23 1.55w 16	23	0.41510	72.998 ± 0.244 Ma	7.024 ± 0.02
24	413-24 1.60w 16	24	0.45037	73.365 ± 0.265 Ma	7.060 ± 0.03
25	413-25 1.65w 16	25	0.48495	73.805 ± 0.290 Ma	7.103 ± 0.03
26	413-26 1.70w su	26	0.51836	73.977 ± 0.303 Ma	7.120 ± 0.03
27	413-27 1.75w 17	27	0.54490	74.523 ± 0.271 Ma	7.174 ± 0.03
28	413-28 1.80w 17	28	0.57287	74.909 ± 0.282 Ma	7.212 ± 0.03
29	413-29 1.90w 17	29	0.60252	74.092 ± 0.493 Ma	7.131 ± 0.05
30	413-30 2.00w 17	30	0.64339	75.853 ± 0.202 Ma	7.305 ± 0.02
31	413-31 2.10w 17	31	0.67502	75.030 ± 0.282 Ma	7.224 ± 0.03
32	413-32 2.20w 17	32	0.70613	74.711 ± 0.322 Ma	7.192 ± 0.03
33	413-33 2.30w 17	33	0.73603	73.507 ± 0.415 Ma	7.074 ± 0.04
34	413-34 2.50w 17	34	0.77190	75.609 ± 0.270 Ma	7.281 ± 0.03
35	413-35 2.70W 17	35	0.80328	75.544 ± 0.287 Ma	7.274 ± 0.03
36	413-36 3.00W 17	36	0.85005	75.863 ± 0.198 Ma	7.305 ± 0.02
37	413-37 3.40W 17	37	0.91693	76.605 ± 0.171 Ma	7.379 ± 0.02
38	413-38 3.70W 17	38	0.96297	75.631 ± 0.208 Ma	7.283 ± 0.02
39	413-39 4.20W 17	39	0.98232	75.419 ± 0.317 Ma	7.262 ± 0.03
40	413-40 5.00W 17	40	0.99220	77.077 ± 0.560 Ma	7.425 ± 0.06
41	413-41 5.00w na	41	0.99571	78.830 ± 2.486 Ma	7.597 ± 0.24
42	413-42 5.00w pi	42	1.00000	81.749 ± 1.321 Ma	7.885 ± 0.13

Table of Contents
Table of Contents
Table of Contents
Table of Contents

P22-413 HK1651 WR

No	Name	Cum 36S	40Ar / 36Ar	±	40ArAcc/g	37Ca / 39K	±	
1	413-01 0.13w 13	0.00682	402.36	39.33	1.1E-0011	0.785	1.442	
2	413-02 0.20w 13	0.04396	501.17	22.66	5.8E-0011	827.930	271.104	m
3	413-03 0.25w 13	0.06442	453.08	25.56	3.2E-0011	1.697	0.360	
4	413-04 0.30W 13	0.08982	483.92	17.61	4.0E-0011	926.012	219.833	m
5	413-05 0.40W 13	0.12628	567.41	18.76	5.7E-0011	833.916	97.094	m
6	413-06 0.50W 13	0.20837	638.91	8.93	1.3E-0010	693.601	23.307	m
7	413-07 0.55w 14	0.32603	703.60	10.06	1.8E-0010	808.423	36.870	m
8	413-08 0.60w 14	0.41442	736.84	12.57	1.4E-0010	626.453	27.308	m
9	413-09 0.65w 14	0.49909	789.79	18.49	1.3E-0010	388.840	26.098	m
10	413-10 0.70w 14	0.56411	850.00	11.19	1.0E-0010	285.666	19.412	m
11	413-11 0.70w re	0.59752	864.20	15.78	5.2E-0011	310.529	18.864	m
12	413-12 0.75w 15	0.63064	988.20	24.68	5.2E-0011	299.397	18.741	m
13	413-13 0.80w 15	0.66046	1196.66	29.98	4.7E-0011	219.144	14.461	m
14	413-14 0.85w 15	0.67991	1912.74	63.02	3.1E-0011	258.281	13.904	m
15	413-15 0.90w 15	0.69140	2889.88	126.62	1.8E-0011	237.684	12.095	m
16	413-16 0.95W 15	0.69555	7706.99	1352.87	6.5E-0012	246.429	10.183	m
17	413-17 1.00W 15	0.70311	3854.69	280.73	1.2E-0011	281.101	15.590	m
18	413-18 1.10W 15	0.71653	2801.20	186.67	2.1E-0011	307.231	13.784	m
19	413-19 1.20W 15	0.72925	3797.16	187.70	2.0E-0011	294.355	12.277	m
20	413-20 1.30W 15	0.74660	4405.77	243.65	2.7E-0011	315.729	5.840	m
21	413-21 1.40W 16	0.75955	5316.45	271.82	2.0E-0011	323.242	7.195	m
22	413-22 1.50w 16	0.78389	4605.35	125.63	3.8E-0011	357.338	5.326	m
23	413-23 1.55w 16	0.79680	5434.09	282.90	2.0E-0011	365.850	8.503	m
24	413-24 1.60w 16	0.81086	5035.70	250.49	2.2E-0011	409.688	8.793	m
25	413-25 1.65w 16	0.82694	4384.77	196.42	2.5E-0011	476.543	9.349	m
26	413-26 1.70w su	0.84257	4368.62	227.22	2.5E-0011	525.030	13.089	m
27	413-27 1.75w 17	0.85499	4397.51	197.54	1.9E-0011	546.693	11.800	m
28	413-28 1.80w 17	0.86674	4891.74	271.95	1.8E-0011	567.545	9.846	m
29	413-29 1.90w 17	0.88006	4543.29	255.44	2.1E-0011	622.715	10.563	m
30	413-30 2.00w 17	0.89747	4883.59	163.33	2.7E-0011	732.927	10.680	m
31	413-31 2.10w 17	0.90971	5290.96	304.87	1.9E-0011	685.020	9.619	m
32	413-32 2.20w 17	0.92189	5212.49	336.44	1.9E-0011	684.951	12.376	m
33	413-33 2.30w 17	0.93298	5395.98	322.83	1.7E-0011	654.515	11.662	m
34	413-34 2.50w 17	0.94449	6369.87	420.33	1.8E-0011	657.532	8.372	m
35	413-35 2.70W 17	0.95276	7686.26	712.86	1.3E-0011	607.602	9.446	m
36	413-36 3.00W 17	0.96684	6789.56	317.68	2.2E-0011	587.051	6.773	m
37	413-37 3.40W 17	0.98326	8336.87	346.71	2.6E-0011	481.197	4.952	m
38	413-38 3.70W 17	0.99276	9745.38	703.05	1.5E-0011	395.831	5.892	m
39	413-39 4.20W 17	0.99691	9358.82	1142.84	6.5E-0012	398.773	13.225	m
40	413-40 5.00W 17	0.99841	13357.02	4199.81	2.4E-0012	422.932	24.037	m
41	413-41 5.00w na	0.99924	8859.81	8243.92	1.3E-0012	326.408	96.460	m
42	413-42 5.00w pi	1.00000	12236.56	8023.64	1.2E-0012	468.874	86.458	m

Table of Contents
Table of Contents
Table of Contents
Table of Contents

P22-413 HK1651 WR

No	Name	40Ar* Vol ccNTP/g		Atm Cont	F1	F2
1	413-01 0.13w 13	3.87 ± 1.05 E-12	(27.2%)	73.4416%	-5.6E-0004	9.3E-0004
2	413-02 0.20w 13	40.56 ± 2.99 E-12	(7.4%)	58.9615%	-5.9E-0004	2.6E-0003
3	413-03 0.25w 13	17.11 ± 1.86 E-12	(10.9%)	65.2197%	-1.2E-0003	6.0E-0003
4	413-04 0.30W 13	25.42 ± 1.51 E-12	(5.9%)	61.0639%	-6.6E-0004	4.3E-0003
5	413-05 0.40W 13	52.63 ± 2.02 E-12	(3.8%)	52.0789%	-5.9E-0004	6.7E-0003
6	413-06 0.50W 13	149.65 ± 2.28 E-12	(1.5%)	46.2505%	-4.9E-0004	8.4E-0003
7	413-07 0.55w 14	254.95 ± 3.88 E-12	(1.5%)	41.9982%	-5.8E-0004	9.6E-0003
8	413-08 0.60w 14	207.11 ± 3.19 E-12	(1.5%)	40.1037%	-4.5E-0004	8.2E-0003
9	413-09 0.65w 14	222.18 ± 5.75 E-12	(2.6%)	37.4152%	-2.8E-0004	6.4E-0003
10	413-10 0.70w 14	191.41 ± 1.78 E-12	(0.9%)	34.7645%	-2.0E-0004	6.1E-0003
11	413-11 0.70w re	100.89 ± 1.09 E-12	(1.1%)	34.1934%	-2.2E-0004	7.3E-0003
12	413-12 0.75w 15	121.81 ± 1.44 E-12	(1.2%)	29.9028%	-2.1E-0004	8.3E-0003
13	413-13 0.80w 15	142.67 ± 1.38 E-12	(1.0%)	24.6937%	-1.6E-0004	8.0E-0003
14	413-14 0.85w 15	166.99 ± 1.31 E-12	(0.8%)	15.4491%	-1.8E-0004	1.7E-0002
15	413-15 0.90w 15	158.33 ± 1.13 E-12	(0.7%)	10.2253%	-1.7E-0004	2.5E-0002
16	413-16 0.95W 15	163.27 ± 1.41 E-12	(0.9%)	3.8342%	-1.8E-0004	7.0E-0002
17	413-17 1.00W 15	142.79 ± 1.13 E-12	(0.8%)	7.6660%	-2.0E-0004	4.0E-0002
18	413-18 1.10W 15	178.61 ± 1.67 E-12	(0.9%)	10.5490%	-2.2E-0004	3.2E-0002
19	413-19 1.20W 15	236.33 ± 1.56 E-12	(0.7%)	7.7821%	-2.1E-0004	4.2E-0002
20	413-20 1.30W 15	378.67 ± 2.44 E-12	(0.6%)	6.7071%	-2.3E-0004	5.1E-0002
21	413-21 1.40W 16	345.16 ± 2.03 E-12	(0.6%)	5.5582%	-2.3E-0004	6.2E-0002
22	413-22 1.50w 16	557.15 ± 3.08 E-12	(0.6%)	6.4164%	-2.5E-0004	5.8E-0002
23	413-23 1.55w 16	352.19 ± 2.09 E-12	(0.6%)	5.4379%	-2.6E-0004	6.9E-0002
24	413-24 1.60w 16	353.75 ± 2.12 E-12	(0.6%)	5.8681%	-2.9E-0004	7.1E-0002
25	413-25 1.65w 16	349.01 ± 2.13 E-12	(0.6%)	6.7392%	-3.4E-0004	7.1E-0002
26	413-26 1.70w su	337.99 ± 2.16 E-12	(0.6%)	6.7642%	-3.7E-0004	7.7E-0002
27	413-27 1.75w 17	270.60 ± 1.65 E-12	(0.6%)	6.7197%	-3.9E-0004	8.0E-0002
28	413-28 1.80w 17	286.60 ± 1.78 E-12	(0.6%)	6.0408%	-4.0E-0004	9.1E-0002
29	413-29 1.90w 17	300.39 ± 2.50 E-12	(0.8%)	6.5041%	-4.4E-0004	9.4E-0002
30	413-30 2.00w 17	424.16 ± 2.36 E-12	(0.6%)	6.0509%	-5.2E-0004	1.1E-0001
31	413-31 2.10w 17	324.66 ± 2.00 E-12	(0.6%)	5.5850%	-4.9E-0004	1.2E-0001
32	413-32 2.20w 17	317.86 ± 2.05 E-12	(0.6%)	5.6691%	-4.9E-0004	1.2E-0001
33	413-33 2.30w 17	300.52 ± 2.27 E-12	(0.8%)	5.4763%	-4.7E-0004	1.2E-0001
34	413-34 2.50w 17	371.07 ± 2.24 E-12	(0.6%)	4.6390%	-4.7E-0004	1.3E-0001
35	413-35 2.70W 17	324.35 ± 2.03 E-12	(0.6%)	3.8445%	-4.3E-0004	1.5E-0001
36	413-36 3.00W 17	485.53 ± 2.67 E-12	(0.6%)	4.3523%	-4.2E-0004	1.3E-0001
37	413-37 3.40W 17	701.13 ± 3.73 E-12	(0.5%)	3.5445%	-3.4E-0004	1.3E-0001
38	413-38 3.70W 17	476.41 ± 2.66 E-12	(0.6%)	3.0322%	-2.8E-0004	1.3E-0001
39	413-39 4.20W 17	199.65 ± 1.29 E-12	(0.6%)	3.1574%	-2.8E-0004	1.2E-0001
40	413-40 5.00W 17	104.24 ± 0.91 E-12	(0.9%)	2.2123%	-3.0E-0004	1.7E-0001
41	413-41 5.00w na	37.85 ± 1.23 E-12	(3.3%)	3.3353%	-2.3E-0004	9.3E-0002
42	413-42 5.00w pi	48.07 ± 0.82 E-12	(1.7%)	2.4149%	-3.3E-0004	1.7E-0001

Table of Contents
Table of Contents
Table of Contents
Table of Contents

P22-413 HK1651 WR

Integrated Results:

Age = 74.743 ± 0.293 Ma

40Ar* / 39K = 7.195 ± 0.010	Total 39K Vol = 1.4208E-0009 ccNTP/g
	Total 40Ar* Vol = 1.022 ± 0.001 E-8
(40Ar / 36Ar)sam = 2221.15 ± 12.28	Total Atm 40Ar Vol = 1.5689E-0009 ccNTP/g
(36Ar / 40Ar)sam = 0.00045022 ±0.00000329	Corr 36/40 & 39/40 ratios =-0.428023
(37Ar / 40Ar)sam = 0.05802619 ±0.00027296	Corr 36/40 & 37/40 ratios =-0.112706
(39Ar / 40Ar)sam = 0.12048802 ±0.00011974	Corr 37/40 & 39/40 ratios = 0.192960
37Ca / 39K = 4.816 ± 0.022 E-1	Mass = 1.000 g
F1 = -3.435 E-4	F2 = 3.443 E-2

Standards:

Weighted Average of J from standards = 5.879 ± 0.022 E-3

APPENDIX B

RAW DATA FOR ANALYSES OF FAULT ROCK SAMPLES

Table of Contents
Table of Contents
Table of Contents
Table of Contents

P23-20 HK12078 K-feldspar
NewAge 981201 AgeParams 990623 Cd liner (Fractionation relative to 40Ar/36Ar = 286.97)

Fractions:

No	Name	Temp	Cum 39K	Age			40Ar* / 39K	
1	20-01 0.13w 15-	1	0.00088	4.002 ±	8.305	Ma	44.985 ±	93.45
2	20-02 0.13w 20s	2	0.00838	32.186 ±	2.499	Ma	364.600 ±	28.56
3	20-03 0.20w 30s	5	0.05458	61.381 ±	0.747	Ma	700.985 ±	8.68
4	20-04 0.20w 35s	6	0.07128	65.844 ±	2.010	Ma	752.893 ±	23.40
5	20-05 0.25w 18-	7	0.10099	65.205 ±	1.520	Ma	745.454 ±	17.69
6	20-06 0.30w 18-	8	0.12761	63.645 ±	1.163	Ma	727.302 ±	13.53
7	20-07 0.40w 18-	9	0.18740	65.889 ±	0.649	Ma	753.410 ±	7.56
8	20-08 0.50w 18-	10	0.24713	63.018 ±	0.616	Ma	720.005 ±	7.16
9	20-09 0.60w 18-	11	0.29765	63.239 ±	0.882	Ma	722.577 ±	10.25
10	20-10 0.70w 18-	12	0.33391	64.148 ±	1.149	Ma	733.145 ±	13.36
11	20-11 0.80w 19-	13	0.36182	65.973 ±	1.353	Ma	754.388 ±	15.76
12	20-12 1.00w 19-	14	0.39268	63.843 ±	0.856	Ma	729.595 ±	9.95
13	20-13 1.4w 19-A	15	0.43403	63.302 ±	0.839	Ma	723.310 ±	9.76
14	20-14 1.80w 19-	16	0.51130	66.924 ±	0.656	Ma	765.465 ±	7.65
15	20-15 2.3w 19-A	17	0.73227	67.088 ±	0.312	Ma	767.374 ±	3.63
16	20-16 2.50w 19-	18	0.81561	68.392 ±	0.795	Ma	782.581 ±	9.27
17	20-17 2.70w 19-	19	0.84937	68.727 ±	1.313	Ma	786.482 ±	15.31
18	20-18 3.00w 19-	20	0.89841	68.891 ±	0.894	Ma	788.398 ±	10.42
19	20-19 3.50W 19-	21	0.94195	70.041 ±	0.804	Ma	801.821 ±	9.39
20	20-20 5.00W 19-	22	0.97958	69.352 ±	1.087	Ma	793.778 ±	12.68
21	20-21 7.00W 19-	23	0.99280	72.371 ±	2.758	Ma	829.028 ±	32.23
22	20-22 10.0W 19-	24	0.99671	75.668 ±	8.460	Ma	867.598 ±	99.05
23	20-23 fuse 19-A	25	1.00000	64.714 ±	9.854	Ma	739.732 ±	114.67

No	Name	Cum 36S	40Ar / 36Ar		40ArAcc/g	37Ca / 39K		
1	20-01 0.13w 15-	0.03629	296.82 ±	2.67	8.9E-0011	1.858 ±	1.407	
2	20-02 0.13w 20s	0.12938	331.18 ±	2.03	2.3E-0010	-48.989 ±	123.830	m
3	20-03 0.20w 30s	0.21146	774.67 ±	4.15	2.0E-0010	32.865 ±	17.174	m
4	20-04 0.20w 35s	0.22389	1523.73 ±	40.16	3.1E-0011	-111.364 ±	55.410	m
5	20-05 0.25w 18-	0.23950	2018.21 ±	40.95	3.8E-0011	59.716 ±	32.227	m
6	20-06 0.30w 18-	0.24685	3493.53 ±	128.28	1.8E-0011	40.268 ±	39.466	m
7	20-07 0.40w 18-	0.25999	4460.34 ±	143.11	3.2E-0011	58.844 ±	23.483	m
8	20-08 0.50w 18-	0.26559	9613.57 ±	961.90	1.4E-0011	26.560 ±	14.346	m
9	20-09 0.60w 18-	0.26703	31110.22 ±	8153.33	3.5E-0012	48.989 ±	19.449	m
10	20-10 0.70w 18-	0.26879	18592.67 ±	4879.20	4.3E-0012	47.749 ±	29.834	m
11	20-11 0.80w 19-	0.26989	23714.43 ±	7546.06	2.7E-0012	48.487 ±	32.429	m
12	20-12 1.00w 19-	0.27178	14731.55 ±	3185.64	4.7E-0012	25.220 ±	39.257	m
13	20-13 1.4w 19-A	0.27707	7154.46 ±	624.06	1.3E-0011	17.453 ±	26.511	m
14	20-14 1.80w 19-	0.32438	1814.03 ±	16.12	1.2E-0010	2.507 ±	16.664	m
15	20-15 2.3w 19-A	0.60222	1036.64 ±	4.08	6.8E-0010	0.029 ±	5.100	m
16	20-16 2.50w 19-	0.71870	975.47 ±	6.28	2.9E-0010	5.203 ±	9.353	m
17	20-17 2.70w 19-	0.76810	948.17 ±	10.00	1.2E-0010	-9.835 ±	46.379	m
18	20-18 3.00w 19-	0.84576	900.14 ±	5.18	1.9E-0010	-4.347 ±	20.646	m
19	20-19 3.50W 19-	0.91339	922.27 ±	5.65	1.7E-0010	41.810 ±	22.599	m
20	20-20 5.00W 19-	0.96812	958.25 ±	7.16	1.3E-0010	49.688 ±	29.055	m
21	20-21 7.00W 19-	0.98920	927.04 ±	18.22	5.2E-0011	77.514 ±	63.998	m
22	20-22 10.0W 19-	0.99554	944.34 ±	65.59	1.6E-0011	167.560 ±	328.331	m
23	20-23 fuse 19-A	1.00000	958.82 ±	79.34	1.1E-0011	-66.648 ±	280.491	m

Table of Contents
Table of Contents
Table of Contents
Table of Contents

P23-20 HK12078 K-feldspar

No	Name	40Ar* Vol ccNTP/g	Atm Cont	F1	F2
1	20-01 0.13w 15-	398.59 ± 800.60 E-15 (200.9%)	99.5556%	-1.3E-0003	-1.3E-0003
2	20-02 0.13w 20s	27.65 ± 1.41 E-12 (5.1%)	89.2268%	3.5E-0005	3.4E-0005
3	20-03 0.20w 30s	327.45 ± 1.98 E-12 (0.6%)	38.1450%	-2.3E-0005	-1.7E-0005
4	20-04 0.20w 35s	127.14 ± 1.04 E-12 (0.8%)	19.3932%	7.9E-0005	2.9E-0005
5	20-05 0.25w 18-	223.90 ± 1.38 E-12 (0.6%)	14.6417%	-4.3E-0005	-4.0E-0006
6	20-06 0.30w 18-	195.75 ± 1.19 E-12 (0.6%)	8.4585%	-2.9E-0005	2.1E-0005
7	20-07 0.40w 18-	455.52 ± 2.55 E-12 (0.6%)	6.6251%	-4.2E-0005	4.9E-0005
8	20-08 0.50w 18-	434.81 ± 2.67 E-12 (0.6%)	3.0738%	-1.9E-0005	7.7E-0005
9	20-09 0.60w 18-	369.09 ± 2.08 E-12 (0.6%)	0.9498%	-3.5E-0005	5.5E-0004
10	20-10 0.70w 18-	268.82 ± 1.78 E-12 (0.7%)	1.5893%	-3.4E-0005	3.0E-0004
11	20-11 0.80w 19-	212.88 ± 1.38 E-12 (0.6%)	1.2461%	-3.5E-0005	3.9E-0004
12	20-12 1.00w 19-	227.67 ± 1.53 E-12 (0.7%)	2.0059%	-1.8E-0005	1.2E-0004
13	20-13 1.4w 19-A	302.34 ± 1.92 E-12 (0.6%)	4.1303%	-1.2E-0005	3.4E-0005
14	20-14 1.80w 19-	598.06 ± 3.27 E-12 (0.5%)	16.2897%	-1.8E-0006	-4.0E-0007
15	20-15 2.3w 19-A	1.71 ± 0.01 E -9 (0.5%)	28.5055%	-2.1E-0008	-1.3E-0008
16	20-16 2.50w 19-	659.42 ± 4.03 E-12 (0.6%)	30.2932%	-3.7E-0006	-2.4E-0006
17	20-17 2.70w 19-	268.44 ± 1.90 E-12 (0.7%)	31.1654%	7.0E-0006	4.7E-0006
18	20-18 3.00w 19-	390.96 ± 2.33 E-12 (0.6%)	32.8283%	3.1E-0006	2.2E-0006
19	20-19 3.50W 19-	352.92 ± 2.12 E-12 (0.6%)	32.0404%	-3.0E-0005	-2.1E-0005
20	20-20 5.00W 19-	302.02 ± 1.86 E-12 (0.6%)	30.8373%	-3.5E-0005	-2.4E-0005
21	20-21 7.00W 19-	110.86 ± 1.17 E-12 (1.1%)	31.8755%	-5.5E-0005	-3.9E-0005
22	20-22 10.0W 19-	34.26 ± 1.10 E-12 (3.2%)	31.2917%	-1.2E-0004	-8.5E-0005
23	20-23 fuse 19-A	24.61 ± 0.92 E-12 (3.7%)	30.8190%	4.8E-0005	3.1E-0005

Integrated Results:

Age = 65.989 ± 0.546 Ma

40Ar* / 39K = 754.579 ± 2.548

Total 39K Vol = 1.0111E-0011 ccNTP/g

Total 40Ar* Vol = 7.630 ± 0.013 E-9

(40Ar / 36Ar)sam = 1211.84 ± 2.83

Total Atm 40Ar Vol = 2.4604E-0009 ccNTP/g

(36Ar / 40Ar)sam = 0.00082519 ±0.00000241
(37Ar / 40Ar)sam = 0.00002121 ±0.00000509
(39Ar / 40Ar)sam = 0.00100209 ±0.00000298

Corr 36/40 & 39/40 ratios =-0.101121
Corr 36/40 & 37/40 ratios =-0.001843
Corr 37/40 & 39/40 ratios =-0.000620

37Ca / 39K = 2.117 ± 0.508 E-2

Mass = 1.000 g

F1 = -1.510 E-5

F2 = -7.917 E-6

Weighted Average of J from standards = 4.937 ± 0.038 E-5

Table of Contents
Table of Contents
Table of Contents
Table of Contents

P23-37 HK12078 Rambler Channel Fault: 14

```
NewAge  981201  AgeParams 990623 Cd liner (Fractionation relative to 40Ar/36Ar =286.97)
 1  37-01 0.2w  5-A     10    0.09471 122.227 ±  27.174 Ma      1419.795 ±   326.46
 2  37-02 fuse 4 w      11    1.00000  89.262 ±   2.202 Ma      1027.349 ±    25.98

No       Name         Cum 36S      40Ar / 36Ar          40ArAcc/g        37Ca / 39K
 1  37-01 0.2w  5-A   0.65511      410.43 ±      5.35    8.3E-0011  -179.134 ± 494.632 m
 2  37-02 fuse 4 w    1.00000     1805.44 ±     33.83    4.4E-0011   -34.552 ±  28.754 m

No     Name              40Ar* Vol ccNTP/g             Atm Cont       F1           F2
 1  37-01 0.2w  5-A  32.18 ±   1.09 E-12 (   3.4% )      71.9972%    1.3E-0004    1.2E-0004
 2  37-02 fuse 4 w  222.57 ±   1.39 E-12 (   0.6% )      16.3672%    2.5E-0005    1.0E-0005


40Ar* / 39K =    1.065 ±   0.034 E 3           Total 39K Vol      =  2


Integrated Results:

Age  =  92.410 ±   2.966 Ma

40Ar* / 39K =    1.065 ±   0.034 E 3           Total 39K Vol      =  2.3931E-0013 ccNTP/g

                                               Total 40Ar* Vol    =  2.548 ± 018 E-10

(40Ar / 36Ar)sam =   891.56 ±    9.55          Total Atm 40Ar Vol =  1.2630E-0010 ccNTP/g

(36Ar / 40Ar)sam = 0.00112163 ±0.00001445      Corr 36/40 & 39/40 ratios =-0.062139
(37Ar / 40Ar)sam =-0.00003030 ±0.00003357      Corr 36/40 & 37/40 ratios = 0.001115
(39Ar / 40Ar)sam = 0.00062804 ±0.00001976      Corr 37/40 & 39/40 ratios =-0.001579

37Ca / 39K = -4.825 ± 5.347 E-2                Mass =    1.000  g

F1 =  3.441 E-5                                F2 =  2.687 E-5

Weighted Average of J from standards =  4.937 ± 0.038 E-5
```

Table of Contents
Table of Contents
Table of Contents
Table of Contents

P23-39 HK12078 Rambler Channel Fault: 14
NewAge 981201 AgeParams 990623 Cd liner (Fractionation relative to 40Ar/36Ar =286.97)

Fractions:

No	Name	Temp	Cum 39K	Age	40Ar* / 39K
1	39-01 0.20w 10-	21	0.02328	47.173 ± 85.768 Ma	536.600 ± 988.43
2	39-02 0.20w 30s	22	0.03248	96.224 ± 329.476 Ma	1109.640 ± 3901.69
3	39-03 0.50w 10-	23	0.19787	46.736 ± 8.470 Ma	531.562 ± 97.59
4	39-04 0.80w 10-	24	0.36303	98.252 ± 21.436 Ma	1133.663 ± 254.14
5	39-05 fuse 8w 1	25	1.00000	106.562 ± 6.108 Ma	1232.415 ± 72.75

No	Name	Cum 36S	40Ar / 36Ar	40ArAcc/g	37Ca / 39K
1	39-01 0.20w 10-	0.47356	306.14 ± 5.89	4.5E-0011	0.346 ± 2.794
2	39-02 0.20w 30s	0.50431	429.38 ± 161.10	2.9E-0012	-6.805 ± 24.119
3	39-03 0.50w 10-	0.88084	389.66 ± 9.84	3.6E-0011	-213.106 ± 311.852 m
4	39-04 0.80w 10-	0.95160	1362.65 ± 210.49	6.8E-0012	232.810 ± 408.953 m
5	39-05 fuse 8w 1	1.00000	6836.09 ± 1370.73	4.6E-0012	17.285 ± 96.643 m

No	Name	40Ar* Vol ccNTP/g	Atm Cont	F1	F2
1	39-01 0.20w 10-	1.64 ± 0.88 E-12 (53.6%)	96.5243%	-2.5E-0004	-2.4E-0004
2	39-02 0.20w 30s	1.34 ± 1.01 E-12 (75.6%)	68.8204%	4.9E-0003	4.6E-0003
3	39-03 0.50w 10-	11.51 ± 0.91 E-12 (7.9%)	75.8351%	1.5E-0004	1.4E-0004
4	39-04 0.80w 10-	24.51 ± 1.06 E-12 (4.3%)	21.6857%	-1.7E-0004	-1.0E-0004
5	39-05 fuse 8w 1	102.75 ± 1.06 E-12 (1.0%)	4.3226%	-1.2E-0005	1.3E-0005

Integrated Results:

Age = 93.962 ± 7.340 Ma

40Ar* / 39K = 1.083 ± 0.086 E 3

Total 39K Vol = 1.3089E-0013 ccNTP/g

Total 40Ar*Vol = 1.417 ± 0.022 E-10

(40Ar / 36Ar)sam = 732.21 ± 16.69

Total Atm 40Ar Vol = 9.5903E-0011 ccNTP/g

(36Ar / 40Ar)sam = 0.00136572 ±0.00003625
(37Ar / 40Ar)sam =-0.00002221 ±0.00007476
(39Ar / 40Ar)sam = 0.00055079 ±0.00004340

Corr 36/40 & 39/40 ratios =-0.059731
Corr 36/40 & 37/40 ratios = 0.000822
Corr 37/40 & 39/40 ratios =-0.001548

37Ca / 39K = -0.403 ± 1.358 E-1

Mass = 1.000 g

F1 = 2.876 E-5

F2 = 2.422 E-5

Weighted Average of J from standards = 4.937 ± 0.038 E-5

Table of Contents
Table of Contents
Table of Contents
Table of Contents

P23-40 HK12078 Rambler Channel Fault: 14

NewAge 981201 AgeParams 990623 Cd liner (Fractionation relative to 40Ar/36Ar = 286.97)

Fractions:

No	Name	Temp	Cum 39K	Age	40Ar* / 39K
1	40-01 0.20w 5s	12	0.00945	11.318 ± 12.820 Ma	127.467 ± 144.83
2	40-02 0.20w 30s	13	0.09363	34.695 ± 3.732 Ma	393.293 ± 42.71
3	40-03 0.25w 6-	14	0.13215	38.788 ± 8.769 Ma	440.192 ± 100.59
4	40-04 0.35w 6-	15	0.16261	72.797 ± 20.713 Ma	834.002 ± 242.13
5	40-05 0.80w 6-	16	0.18731	64.887 ± 21.481 Ma	741.748 ± 250.00
6	40-06 3.00w 6-	17	0.35538	62.122 ± 3.160 Ma	709.597 ± 36.72
7	40-07 4.00w 10-	18	0.57527	88.500 ± 3.208 Ma	1018.364 ± 37.83
8	40-08 5.00w 10-	19	0.65930	83.085 ± 8.359 Ma	954.611 ± 98.26
9	40-09 fuse 10w	20	1.00000	74.309 ± 1.725 Ma	851.688 ± 20.18

No	Name	Cum 36S	40Ar / 36Ar	40ArAcc/g	37Ca / 39K
1	40-01 0.20w 5s	0.06018	316.82 ± 21.81	9.7E-0012	0.728 ± 1.182
2	40-02 0.20w 30s	0.25251	478.80 ± 13.00	3.1E-0011	302.586 ± 166.995 m
3	40-03 0.25w 6-	0.33711	508.96 ± 37.62	1.4E-0011	-52.226 ± 297.933 m
4	40-04 0.35w 6-	0.50210	459.42 ± 17.01	2.7E-0011	411.438 ± 499.378 m
5	40-05 0.80w 6-	0.59597	503.36 ± 34.17	1.5E-0011	-167.590 ± 392.429 m
6	40-06 3.00w 6-	0.70218	1491.20 ± 58.16	1.7E-0011	122.145 ± 57.417 m
7	40-07 4.00w 10-	0.75637	4696.03 ± 469.53	8.8E-0012	73.279 ± 59.422 m
8	40-08 5.00w 10-	0.78957	2868.73 ± 418.73	5.4E-0012	-85.742 ± 128.968 m
9	40-09 fuse 10w	1.00000	1763.89 ± 59.43	3.4E-0011	45.027 ± 38.258 m

No	Name	40Ar* Vol ccNTP/g	Atm Cont	F1	F2
1	40-01 0.20w 5s	701.39 ± 669.32 E-15 (95.4%)	93.2710%	-5.2E-0004	-4.9E-0004
2	40-02 0.20w 30s	19.27 ± 0.85 E-12 (4.4%)	61.7174%	-2.2E-0004	-1.8E-0004
3	40-03 0.25w 6-	9.87 ± 1.01 E-12 (10.2%)	58.0591%	3.7E-0005	3.0E-0005
4	40-04 0.35w 6-	14.79 ± 1.00 E-12 (6.7%)	64.3202%	-2.9E-0004	-2.7E-0004
5	40-05 0.80w 6-	10.67 ± 1.03 E-12 (9.7%)	58.7053%	1.2E-0004	1.1E-0004
6	40-06 3.00w 6-	69.43 ± 0.76 E-12 (1.1%)	19.8163%	-8.7E-0005	-3.0E-0005
7	40-07 4.00w 10-	130.36 ± 1.10 E-12 (0.8%)	6.2925%	-5.2E-0005	3.6E-0005
8	40-08 5.00w 10-	46.70 ± 0.82 E-12 (1.7%)	10.3007%	6.1E-0005	-3.4E-0006
9	40-09 fuse 10w	168.93 ± 1.43 E-12 (0.8%)	16.7528%	-3.2E-0005	-1.0E-0005

Integrated Results:

Age = 70.619 ± 1.796 Ma

40Ar* / 39K = 808.568 ± 20.020

Total 39K Vol = 5.8215E-0013 ccNTP/g

Total 40Ar* Vol = 4.707 ± 0.030 E-10

(40Ar / 36Ar)sam = 1156.52 ± 19.41

Total Atm 40Ar Vol = 1.6155E-0010 ccNTP/g

(36Ar / 40Ar)sam = 0.00086466 ±0.00001809
(37Ar / 40Ar)sam = 0.00007689 ±0.00003306
(39Ar / 40Ar)sam = 0.00092075 ±0.00002241

Corr 36/40 & 39/40 ratios =-0.105004
Corr 36/40 & 37/40 ratios =-0.006453
Corr 37/40 & 39/40 ratios = 0.000713

37Ca / 39K = 8.350 ± 3.597 E-2

Mass = 1.000 g

F1 = -5.957 E-5

F2 = -3.472 E-5

Weighted Average of J from standards = 4.937 ± 0.038 E-5

Table of Contents
Table of Contents
Table of Contents
Table of Contents

P23-124 HK3419 fd. Tuen Mun Fault mylonite
NewAge 981201 AgeParams 990623 Cd liner (Fractionation relative to 40Ar/36Ar = 286.97)

Fractions:

No	Name	Temp	Cum 39K	Age				40Ar* / 39K		
1	124-01 0.50w	7	0.00020	23.812	±	17.995	Ma	269.110	±	204.72
2	124-02 0.60w 8	8	0.00056	28.695	±	12.899	Ma	324.736	±	147.14
3	124-03 0.70w 8	9	0.00180	9.126	±	2.297	Ma	102.720	±	25.92
4	124-04 0.80w 8	10	0.01042	3.996	±	0.434	Ma	44.917	±	4.89
5	124-05 0.90W 8	11	0.02327	4.084	±	0.255	Ma	45.901	±	2.87
6	124-06 1.00W 8	12	0.04614	4.191	±	0.295	Ma	47.104	±	3.32
7	124-07 1.10w 9	13	0.05394	8.127	±	0.383	Ma	91.450	±	4.31
8	124-08 1.10w r	14	0.09964	5.380	±	0.151	Ma	60.493	±	1.71
9	124-09 1.20 w	16	0.11376	9.286	±	0.361	Ma	104.520	±	4.08
10	124-10 2.30w 9	18	0.14171	11.833	±	0.338	Ma	133.289	±	3.82
11	124-11 2.50w 9	19	0.14569	26.546	±	1.572	Ma	300.231	±	17.91
12	124-12 2.70W 9	20	0.15588	27.246	±	1.231	Ma	308.209	±	14.03
13	124-13 2.90W 9	21	0.17107	29.309	±	1.347	Ma	331.745	±	15.37
14	124-14 3.00W 10	22	0.26078	33.833	±	0.590	Ma	383.423	±	6.75
15	124-15 3.20w 10	23	0.26345	71.874	±	5.237	Ma	823.216	±	61.19
16	124-16 5.0w 26-	24	0.33475	71.268	±	0.986	Ma	816.143	±	11.51
17	124-17 5.00w 26	25	0.37244	81.189	±	0.698	Ma	932.337	±	8.20
18	124-18 7.0w 26-	26	0.48161	78.891	±	0.686	Ma	905.366	±	8.04
19	124-19 8.0w 26-	27	0.61896	79.617	±	0.654	Ma	913.883	±	7.67
20	124-20 8.0w 26	28	0.69785	78.813	±	0.536	Ma	904.448	±	6.29
21	124-21 9.0w 27-	29	0.78230	82.770	±	0.605	Ma	950.912	±	7.11
22	124-22 9.0w 60s	30	0.83322	82.110	±	0.547	Ma	943.150	±	6.43
23	124-23 9.0w nb	31	0.85942	80.185	±	0.932	Ma	920.543	±	10.94
24	124-24 nb 9 27-	32	0.89842	79.882	±	0.681	Ma	916.985	±	8.00
25	124-25 9w 60 27	33	0.93848	80.716	±	0.636	Ma	926.777	±	7.47
26	124-26 9w nb 60	34	0.96816	80.233	±	0.590	Ma	921.114	±	6.93
27	124-27 10w 120s	35	0.97977	81.756	±	1.930	Ma	938.994	±	22.67
28	124-28 12w 27-O	36	0.98973	83.167	±	2.396	Ma	955.578	±	28.17
29	124-29 narrbe 2	37	0.99389	75.137	±	3.202	Ma	861.375	±	37.48
30	124-30 rere-try	38	1.00000	51.185	±	2.950	Ma	582.885	±	34.07

Table of Contents
Table of Contents
Table of Contents
Table of Contents

P23-124 HK3419 fd. Tuen Mun Fault myloni

No	Name	Cum 36S	40Ar / 36Ar	±	40ArAcc/g	37Ca / 39K	±	
1	124-01 0.50w	0.00072	548.68	202.16	2.0E-0012	2.128	2.534	
2	124-02 0.60w 8	0.00270	494.97	77.92	5.5E-0012	1.998	1.479	
3	124-03 0.70w 8	0.00675	402.55	34.21	1.1E-0011	26.781	324.940	m
4	124-04 0.80w 8	0.01969	396.73	13.59	3.6E-0011	272.067	71.515	m
5	124-05 0.90W 8	0.03419	433.34	11.13	4.0E-0011	126.734	58.615	m
6	124-06 1.00W 8	0.05611	461.98	15.76	6.1E-0011	187.531	35.033	m
7	124-07 1.10w 9	0.07476	425.06	7.44	5.2E-0011	287.002	56.987	m
8	124-08 1.10w r	0.12552	479.98	4.92	1.4E-0010	191.750	13.302	m
9	124-09 1.20 w	0.15179	485.78	7.28	7.3E-0011	280.295	39.806	m
10	124-10 2.30w 9	0.20522	531.74	6.71	1.5E-0010	341.838	27.626	m
11	124-11 2.50w 9	0.21793	614.07	18.45	3.5E-0011	878.065	97.398	m
12	124-12 2.70W 9	0.24807	648.31	7.89	8.4E-0011	657.762	47.683	m
13	124-13 2.90W 9	0.28310	782.77	8.30	9.7E-0011	617.783	38.496	m
14	124-14 3.00W 10	0.39070	1378.25	9.88	3.0E-0010	585.392	15.175	m
15	124-15 3.20w 10	0.39546	1862.95	139.07	1.3E-0011	607.241	177.339	m
16	124-16 5.0w 26-	0.44615	4183.86	48.93	1.4E-0010	356.160	22.999	m
17	124-17 5.00w 26	0.46299	7361.72	148.12	4.7E-0011	167.761	32.223	m
18	124-18 7.0w 26-	0.53780	4770.92	56.40	2.1E-0010	193.377	15.783	m
19	124-19 8.0w 26-	0.62646	5091.55	111.08	2.5E-0010	218.756	9.877	m
20	124-20 8.0w 26	0.67767	5014.89	139.35	1.4E-0010	245.241	30.600	m
21	124-21 9.0w 27-	0.73691	4887.27	72.66	1.6E-0010	228.160	14.766	m
22	124-22 9.0w 60s	0.78261	3855.08	64.89	1.3E-0010	255.832	28.145	m
23	124-23 9.0w nb	0.80754	3573.21	105.02	6.9E-0011	327.299	78.570	m
24	124-24 nb 9 27-	0.84431	3589.91	44.71	1.0E-0010	154.663	42.927	m
25	124-25 9w 60 27	0.87902	3919.22	46.19	9.6E-0011	299.019	57.886	m
26	124-26 9w nb 60	0.91353	2978.88	58.48	9.6E-0011	430.337	80.695	m
27	124-27 10w 120s	0.93610	1931.18	52.64	6.3E-0011	676.319	164.678	m
28	124-28 12w 27-O	0.95724	1820.06	30.79	5.9E-0011	416.438	138.895	m
29	124-29 narrbe 2	0.97145	1150.90	37.08	3.9E-0011	1.424	0.295	
30	124-30 rere-try	1.00000	717.92	22.72	7.9E-0011	1.504	0.264	

Table of Contents
Table of Contents
Table of Contents
Table of Contents

P23-124 HK3419 fd. Tuen Mun Fault myloni

No	Name	40Ar*	Vol ccNTP/g		Atm Cont	F1	F2
1	124-01 0.50w	1.72 ±	0.74 E-12	(43.2%)	53.8563%	-1.5E-0003	-9.6E-0004
2	124-02 0.60w 8	3.71 ±	0.87 E-12	(23.4%)	59.7003%	-1.4E-0003	-1.1E-0003
3	124-03 0.70w 8	4.07 ±	0.96 E-12	(23.5%)	73.4076%	-1.9E-0005	-1.1E-0005
4	124-04 0.80w 8	12.31 ±	1.24 E-12	(10.1%)	74.4843%	-1.9E-0004	-2.3E-0005
5	124-05 0.90W 8	18.76 ±	1.08 E-12	(5.7%)	68.1920%	-9.0E-0005	1.6E-0005
6	124-06 1.00W 8	34.28 ±	2.17 E-12	(6.3%)	63.9633%	-1.3E-0004	5.1E-0005
7	124-07 1.10w 9	22.70 ±	0.92 E-12	(4.0%)	69.5193%	-2.0E-0004	-9.1E-0005
8	124-08 1.10w r	87.94 ±	1.80 E-12	(2.0%)	61.5651%	-1.4E-0004	2.7E-0005
9	124-09 1.20 w	46.94 ±	1.15 E-12	(2.5%)	60.8301%	-2.0E-0004	-5.7E-0005
10	124-10 2.30w 9	118.55 ±	2.17 E-12	(1.8%)	55.5720%	-2.4E-0004	-7.5E-0005
11	124-11 2.50w 9	38.04 ±	1.10 E-12	(2.9%)	48.1218%	-6.3E-0004	-3.7E-0004
12	124-12 2.70W 9	99.87 ±	1.27 E-12	(1.3%)	45.5800%	-4.7E-0004	-2.6E-0004
13	124-13 2.90W 9	160.30 ±	1.64 E-12	(1.0%)	37.7503%	-4.4E-0004	-1.9E-0004
14	124-14 3.00W 10	1.09 ±	0.01 E -9	(0.6%)	21.4402%	-4.2E-0004	4.4E-0005
15	124-15 3.20w 10	69.93 ±	1.06 E-12	(1.5%)	15.8620%	-4.3E-0004	-1.1E-0004
16	124-16 5.0w 26-	1.85 ±	0.01 E -9	(0.5%)	7.0629%	-2.5E-0004	2.2E-0004
17	124-17 5.00w 26	1.12 ±	0.01 E -9	(0.5%)	4.0140%	-1.2E-0004	2.4E-0004
18	124-18 7.0w 26-	3.14 ±	0.02 E -9	(0.6%)	6.1938%	-1.4E-0004	1.3E-0004
19	124-19 8.0w 26-	3.99 ±	0.02 E -9	(0.6%)	5.8037%	-1.6E-0004	1.6E-0004
20	124-20 8.0w 26	2.27 ±	0.01 E -9	(0.5%)	5.8925%	-1.7E-0004	1.8E-0004
21	124-21 9.0w 27-	2.55 ±	0.01 E -9	(0.5%)	6.0463%	-1.6E-0004	1.5E-0004
22	124-22 9.0w 60s	1.53 ±	0.01 E -9	(0.6%)	7.6652%	-1.8E-0004	8.7E-0005
23	124-23 9.0w nb	767.45 ±	4.69 E-12	(0.6%)	8.2699%	-2.3E-0004	9.2E-0005
24	124-24 nb 9 27-	1.14 ±	0.01 E -9	(0.5%)	8.2314%	-1.1E-0004	4.5E-0005
25	124-25 9w 60 27	1.18 ±	0.01 E -9	(0.6%)	7.5398%	-2.1E-0004	1.1E-0004
26	124-26 9w nb 60	869.72 ±	5.03 E-12	(0.6%)	9.9198%	-3.1E-0004	4.3E-0005
27	124-27 10w 120s	346.75 ±	2.54 E-12	(0.7%)	15.3015%	-4.8E-0004	-1.5E-0004
28	124-28 12w 27-O	302.72 ±	1.92 E-12	(0.6%)	16.2357%	-3.0E-0004	-1.1E-0004
29	124-29 narrbe 2	114.12 ±	1.42 E-12	(1.2%)	25.6755%	-1.0E-0003	-6.2E-0004
30	124-30 rere-try	113.27 ±	2.59 E-12	(2.3%)	41.1608%	-1.1E-0003	-7.7E-0004

Table of Contents
Table of Contents
Table of Contents
Table of Contents

P23-124 HK3419 fd. Tuen Mun Fault myloni

Integrated Results:

Age = 63.558 ± 0.532 Ma

40Ar* / 39K = 726.287 ± 2.608

Total 39K Vol = 3.1812E-0011 ccNTP/g

Total 40Ar* Vol = 2.310 ± 0.004 E-8

(40Ar / 36Ar)sam = 2755.69 ± 10.49

Total Atm 40Ar Vol = 2.7752E-0009 ccNTP/g

(36Ar / 40Ar)sam = 0.00036289 ±0.00000184
(37Ar / 40Ar)sam = 0.00037941 ±0.00000876
(39Ar / 40Ar)sam = 0.00122922 ±0.00000397

Corr 36/40 & 39/40 ratios =-0.064490
Corr 36/40 & 37/40 ratios =-0.010347
Corr 37/40 & 39/40 ratios = 0.004655

37Ca / 39K = 3.087 ± 0.072 E-1

Mass = 1.000 g

F1 = -2.202 E-4

F2 = 7.194 E-5

Standards:

Weighted Average of J from standards = 4.937 ± 0.038 E-5

Name	F1	F2	40Ar* / 39K	Age	J
p23-16 TCR3 n=2	-1.6E-0005	5.9E-0004	3.156 ± 0.037 E 2	27.920 Ma	4.94142E-0005
p23-29 TCR3 N=3	-1.2E-0005	2.9E-0004	3.190 ± 0.043 E 2	27.920 Ma	4.88962E-0005
p23-28 TCR3 n=3	-2.2E-0005	6.8E-0004	3.120 ± 0.050 E 2	27.920 Ma	4.99960E-0005

Table of Contents
Table of Contents
Table of Contents
Table of Contents

P23-125 HK7284 Schist..unfinished: 6 ste
NewAge 981201 AgeParams 990623 Cd liner (Fractionation relative to 40Ar/36Ar = 286.97)

Fractions:

No	Name	Temp	Cum.39K	Age	40Ar* / 39K
1	125-01 0.14w 23	1	0.05828	58.387 ± 73.194 Ma	666.232 ± 848.78
2	125-02 0.18w 23	2	0.26634	111.512 ± 47.504 Ma	1291.450 ± 567.33
3	125-03 0.20w 23	3	0.46335	102.035 ± 33.685 Ma	1178.568 ± 400.19
4	125-04 0.23W 23	4	0.53368	46.981 ± 46.869 Ma	534.381 ± 540.08
5	125-05 0.26W 23	5	0.68585	164.490 ± 66.431 Ma	1933.540 ± 817.02
6	125-06 0.30W 23	6	1.00000	86.003 ± 17.378 Ma	988.946 ± 204.63

No	Name	Cum 36S	40Ar / 36Ar	40ArAcc/g	37Ca / 39K
1	125-01 0.14w 23	0.09086	435.68 ± 68.48	5.8E-0012	0.547 ± 5.566
2	125-02 0.18w 23	0.42837	556.64 ± 28.18	2.1E-0011	-0.329 ± 1.323
3	125-03 0.20w 23	0.55778	884.05 ± 79.52	8.2E-0012	1.454 ± 1.489
4	125-04 0.23W 23	0.59795	602.34 ± 187.31	2.5E-0012	-3.510 ± 4.444
5	125-05 0.26W 23	0.78327	816.27 ± 70.43	1.2E-0011	-0.339 ± 1.857
6	125-06 0.30W 23	1.00000	765.71 ± 30.62	1.4E-0011	-31.604 ± 568.039 m

No	Name	40Ar* Vol ccNTP/g	Atm Cont	F1	F2
1	125-01 0.14w 23	2.73 ± 0.91 E-12 (33.3%)	67.8253%	-3.9E-0004	-3.6E-0004
2	125-02 0.18w 23	18.91 ± 1.07 E-12 (5.7%)	53.0868%	2.3E-0004	2.2E-0004
3	125-03 0.20w 23	16.34 ± 0.78 E-12 (4.8%)	33.4256%	-1.0E-0003	-8.3E-0004
4	125-04 0.23W 23	2.64 ± 0.77 E-12 (29.2%)	49.0586%	2.5E-0003	1.9E-0003
5	125-05 0.26W 23	20.71 ± 1.00 E-12 (4.8%)	36.2013%	2.4E-0004	2.2E-0004
6	125-06 0.30W 23	21.86 ± 0.56 E-12 (2.6%)	38.5919%	2.3E-0005	1.8E-0005

Integrated Results:

Age = 102.341 ± 17.604 Ma

40Ar* / 39K = 1.182 ± 0.209 E 3

Total 39K Vol = 7.0376E-0014 ccNTP/g

Total 40Ar* Vol = 8.320 ± 0.212 E-11

(40Ar / 36Ar)sam = 683.28 ± 22.85

Total Atm 40Ar Vol = 6.3400E-0011 ccNTP/g

(36Ar / 40Ar)sam = 0.00146353 ±0.00005627
(37Ar / 40Ar)sam =-0.00002806 ±0.00030647
(39Ar / 40Ar)sam = 0.00048006 ±0.00008426

Corr 36/40 & 39/40 ratios =-0.040591
Corr 36/40 & 37/40 ratios =-0.000869
Corr 37/40 & 39/40 ratios =-0.002704

37Ca / 39K = -0.585 ± 6.385 E-1

Mass = 1.000 g

F1 = 4.170 E-5

F2 = 3.634 E-5

Weighted Average of J from standards = 4.937 ± 0.038 E-5

Table of Contents
Table of Contents
Table of Contents
Table of Contents

P23-126 HK7729 WR(rusty stain) Pat Sin L
NewAge 981201 AgeParams 990623 Cd liner (Fractionation relative to 40Ar/36Ar = 286.97)

Fractions:

No	Name	Temp	Cum 39K	Age			40Ar* / 39K	
1	126-01c 0.80w 1	3	0.00018	0.206 ±	2.110	Ma	2.309 ±	23.70
2	126-02 0.90W 10	4	0.00056	3.821 ±	1.117	Ma	42.941 ±	12.57
3	126-03 1.00W 10	5	0.00544	2.989 ±	0.152	Ma	33.587 ±	1.71
4	126-04 1.10W 10	6	0.00756	2.869 ±	0.402	Ma	32.239 ±	4.52
5	126-05 1.20W 10	7	0.01193	3.572 ±	0.161	Ma	40.147 ±	1.81
6	126-06 1.20w re	8	0.01249	9.956 ±	0.695	Ma	112.091 ±	7.84
7	126-07 1.20w 45	9	0.02476	10.711 ±	0.826	Ma	120.611 ±	9.33
8	126-08 1.20w 30	10	0.02571	29.492 ±	0.931	Ma	333.833 ±	10.62
9	126-09 1.20w 13	11	0.02905	33.495 ±	0.655	Ma	379.557 ±	7.50
10	126-10 3.0w 27-	12	0.07184	91.972 ±	0.988	Ma	1059.347 ±	11.68
11	126-11 4.0W 27-	13	0.10304	94.790 ±	0.608	Ma	1092.661 ±	7.19
12	126-12 5.0W 27-	14	0.18764	77.185 ±	1.109	Ma	885.364 ±	12.99
13	126-13 6.0w 28-	15	0.36405	49.694 ±	1.298	Ma	565.671 ±	14.97
14	126-14 6.5w 28-	16	0.54470	46.501 ±	1.311	Ma	528.852 ±	15.10
15	126-15 7.0w 28-	17	0.66140	57.933 ±	1.109	Ma	660.972 ±	12.86
16	126-16 8.0w 28-	18	0.83320	55.592 ±	0.833	Ma	633.848 ±	9.64
17	126-17 9.0W 28-	19	0.88575	84.396 ±	0.810	Ma	970.023 ±	9.53
18	126-18 11.0W 28	20	0.93806	86.982 ±	0.417	Ma	1000.474 ±	4.92
19	126-19 14.0W 28	21	0.97930	88.869 ±	0.405	Ma	1022.712 ±	4.78
20	126-20 18.0W 28	22	0.99726	92.855 ±	0.677	Ma	1069.778 ±	8.00
21	126-21 10.0W, n	23	0.99848	129.860 ±	17.441	Ma	1511.693 ±	210.42
22	126-22 naerbe 1	24	1.00000	170.732 ±	38.106	Ma	2010.442 ±	470.28

No	Name	Cum 36S	40Ar / 36Ar		40ArAcc/g	37Ca / 39K		
1	126-01c 0.80w 1	0.00150	312.51 ±	184.45	1.8E-0012	120.112 ±	388.700	m
2	126-02 0.90W 10	0.00234	1455.62 ±	1639.03	1.0E-0012	-114.179 ±	176.554	m
3	126-03 1.00W 10	0.01787	932.60 ±	63.81	1.9E-0011	125.695 ±	22.519	m
4	126-04 1.10W 10	0.02814	697.73 ±	126.79	1.2E-0011	128.204 ±	42.789	m
5	126-05 1.20W 10	0.04483	930.77 ±	43.32	2.0E-0011	75.823 ±	24.146	m
6	126-06 1.20w re	0.05146	863.13 ±	93.24	7.9E-0012	19.705 ±	139.571	m
7	126-07 1.20w 45	0.09254	2470.78 ±	135.19	4.9E-0011	82.115 ±	9.670	m
8	126-08 1.20w 30	0.09727	4379.82 ±	731.07	5.7E-0012	10.445 ±	64.498	m
9	126-09 1.20w 13	0.11120	5778.92 ±	301.31	1.7E-0011	97.013 ±	21.413	m
10	126-10 3.0w 27-	0.18876	35600.62 ±	2826.07	9.3E-0011	-29.000 ±	39.746	m
11	126-11 4.0W 27-	0.23888	41368.76 ±	7681.27	6.0E-0011	79.927 ±	37.953	m
12	126-12 5.0W 27-	0.29676	78450.21 ±	8613.30	6.9E-0011	33.994 ±	10.691	m
13	126-13 6.0w 28-	0.47993	33198.89 ±	2085.94	2.2E-0010	52.534 ±	12.431	m
14	126-14 6.5w 28-	0.56676	66744.46 ±	10424.81	1.0E-0010	43.242 ±	12.467	m
15	126-15 7.0w 28-	0.67538	43183.93 ±	5223.20	1.3E-0010	51.234 ±	25.238	m
16	126-16 8.0w 28-	0.77188	68445.81 ±	8555.47	1.2E-0010	23.747 ±	13.980	m
17	126-17 9.0W 28-	0.79483	134473.11 ±	35134.36	2.7E-0011	2.446 ±	32.067	m
18	126-18 11.0W 28	0.80677	265009.88 ±	160150.51	1.4E-0011	-9.112 ±	27.821	m
19	126-19 14.0W 28	0.82457	143383.96 ±	61258.08	2.1E-0011	12.384 ±	29.061	m
20	126-20 18.0W 28	0.88092	20884.76 ±	1763.37	6.7E-0011	-44.226 ±	60.066	m
21	126-21 10.0W, n	0.86358	-6154.82 ±	2120.29	-2.1E-0011	-1.576 ±	0.774	
22	126-22 naerbe 1	1.00000	1647.19 ±	107.84	1.6E-0010	-0.502 ±	1.555	

Table of Contents
Table of Contents
Table of Contents
Table of Contents

P23-126 HK7729 WR(rusty stain) Pat Sin L

No	Name	40Ar*		Vol ccNTP/g		Atm Cont	F1	F2
1	126-01c 0.80w 1	0.10	±	1.06 E-12	(1026.0%)	94.5573%	-8.6E-0005	1.6E-0004
2	126-02 0.90W 10	3.95	±	1.14 E-12	(28.9%)	20.3006%	8.1E-0005	-7.8E-0004
3	126-03 1.00W 10	40.05	±	1.74 E-12	(4.3%)	31.6858%	-9.0E-0005	5.8E-0004
4	126-04 1.10W 10	16.72	±	2.30 E-12	(13.8%)	42.3514%	-9.1E-0005	3.6E-0004
5	126-05 1.20W 10	42.94	±	1.54 E-12	(3.6%)	31.7478%	-5.4E-0005	2.8E-0004
6	126-06 1.20w re	15.23	±	0.87 E-12	(5.7%)	34.2358%	-1.4E-0005	1.4E-0005
7	126-07 1.20w 45	361.86	±	11.95 E-12	(3.3%)	11.9598%	-5.9E-0005	3.6E-0004
8	126-08 1.20w 30	78.19	±	1.13 E-12	(1.4%)	6.7469%	-7.5E-0006	2.8E-0005
9	126-09 1.20w 13	309.30	±	2.04 E-12	(0.7%)	5.1134%	-6.9E-0005	3.2E-0004
10	126-10 3.0w 27-	11.09	±	0.07 E -9	(0.6%)	0.8300%	2.1E-0005	-2.5E-0004
11	126-11 4.0W 27-	8.34	±	0.04 E -9	(0.5%)	0.7143%	-5.7E-0005	7.8E-0004
12	126-12 5.0W 27-	18.32	±	0.12 E -9	(0.6%)	0.3767%	-2.4E-0005	8.1E-0004
13	126-13 6.0w 28-	24.40	±	0.17 E -9	(0.7%)	0.8901%	-3.7E-0005	8.2E-0004
14	126-14 6.5w 28-	23.36	±	0.17 E -9	(0.7%)	0.4427%	-3.1E-0005	1.5E-0003
15	126-15 7.0w 28-	18.86	±	0.13 E -9	(0.7%)	0.6843%	-3.7E-0005	8.9E-0004
16	126-16 8.0w 28-	26.63	±	0.17 E -9	(0.6%)	0.4317%	-1.7E-0005	7.0E-0004
17	126-17 9.0W 28-	12.46	±	0.07 E -9	(0.6%)	0.2197%	-1.7E-0006	9.3E-0005
18	126-18 11.0W 28	12.80	±	0.07 E -9	(0.5%)	0.1115%	6.5E-0006	-6.7E-0004
19	126-19 14.0W 28	10.31	±	0.05 E -9	(0.5%)	0.2061%	-8.8E-0006	4.8E-0004
20	126-20 18.0W 28	4.70	±	0.02 E -9	(0.5%)	1.4149%	3.2E-0005	-2.1E-0004
21	126-21 10.0W, n	452.93	±	6.90 E-12	(1.5%)	-4.8011%	1.1E-0003	3.0E-0003
22	126-22 naerbe 1	746.64	±	10.36 E-12	(1.4%)	17.9396%	3.6E-0004	2.6E-0004

Integrated Results:

Age = 62.057 ± 0.682 Ma

40Ar* / 39K = 708.836 ± 5.735

Total 39K Vol = 2.4454E-0010 ccNTP/g

Total 40Ar* Vol = 1.733 ± 0.004 E-7

(40Ar / 36Ar)sam = 43105.70 ± 1426.81

Total Atm 40Ar Vol = 1.1965E-0009 ccNTP/g

(36Ar / 40Ar)sam = 0.00002320 ±0.00000108
(37Ar / 40Ar)sam = 0.00004272 ±0.00000922
(39Ar / 40Ar)sam = 0.00140109 ±0.00001110

Corr 36/40 & 39/40 ratios =-0.015141
Corr 36/40 & 37/40 ratios =-0.002937
Corr 37/40 & 39/40 ratios = 0.000520

37Ca / 39K = 3.049 ± 0.659 E-2

Mass = 1.000 g

F1 = -2.175 E-5

F2 = 4.925 E-4

Weighted Average of J from standards = 4.937 ± 0.038 E-5

Table of Contents
Table of Contents
Table of Contents
Table of Contents

P23-137 HK12086 fd

NewAge 981201 AgeParams 990623 Cd liner (Fractionation relative to 40Ar/36Ar = 286.97)

Fractions:

No	Name	Temp	Cum 39K	Age	40Ar* / 39K
1	137-01 0.20w 20	1	0.00309	12.474 ± 13.508 Ma	140.526 ± 152.71
2	137-02 0.20w 20	2	0.00439	20.794 ± 39.973 Ma	234.802 ± 453.98
3	137-04 0.25w 20	5	0.00682	21.328 ± 19.545 Ma	240.868 ± 222.04
4	137-04 0.30w 20	6	0.01829	31.375 ± 6.424 Ma	355.331 ± 73.39
5	137-05 0.30w re	7	0.02310	34.613 ± 16.062 Ma	392.350 ± 183.83
6	137-06 0.50w 21	10	0.06365	52.694 ± 3.123 Ma	600.325 ± 36.10
7	137-07 0.60w 21	11	0.12686	64.067 ± 3.198 Ma	732.201 ± 37.20
8	137-08 0.80w 21	12	0.32403	65.620 ± 1.307 Ma	750.280 ± 15.22
9	137-09 1.00w 21	13	0.49597	54.194 ± 2.035 Ma	617.667 ± 23.54
10	137-10 1.20w 21	14	0.56165	73.236 ± 3.173 Ma	839.137 ± 37.10
11	137-11 1.40W 21	15	0.64299	80.825 ± 2.788 Ma	928.055 ± 32.74
12	137-12 1.60W 22	16	0.69298	78.237 ± 2.362 Ma	897.695 ± 27.70
13	137-13 1.80W 22	17	0.74309	77.464 ± 3.206 Ma	888.631 ± 37.57
14	137-14 2.20W 22	18	0.79386	82.145 ± 3.007 Ma	943.560 ± 35.33
15	137-15 2.60W 22	19	0.83070	74.620 ± 3.771 Ma	855.332 ± 44.12
16	137-16 3.00w 23	20	0.85019	74.882 ± 8.653 Ma	858.391 ± 101.27
17	137-17 5.00w 23	21	0.89503	80.999 ± 2.715 Ma	930.096 ± 31.89
18	137-18 10w 23-S	22	1.00000	181.871 ± 3.660 Ma	2148.343 ± 45.45

No	Name	Cum 36S	40Ar / 36Ar	40ArAcc/g	37Ca / 39K
1	137-01 0.20w 20	0.02358	324.98 ± 30.03	9.8E-0012	1.848 ± 2.194
2	137-02 0.20w 20	0.03714	331.37 ± 54.77	5.6E-0012	-5.751 ± 9.398
3	137-04 0.25w 20	0.04071	558.05 ± 379.29	1.5E-0012	-3.341 ± 4.284
4	137-04 0.30w 20	0.06647	548.64 ± 41.61	1.1E-0011	310.980 ± 602.261 m
5	137-05 0.30w re	0.07587	616.47 ± 134.10	3.9E-0012	-1.712 ± 1.788
6	137-06 0.50w 21	0.13388	966.72 ± 23.61	2.4E-0011	707.746 ± 200.031 m
7	137-07 0.60w 21	0.18140	1853.61 ± 81.21	2.0E-0011	346.774 ± 114.139 m
8	137-08 0.80w 21	0.32365	1959.07 ± 32.54	5.9E-0011	341.644 ± 41.404 m
9	137-09 1.00w 21	0.36530	4374.62 ± 339.07	1.7E-0011	706.695 ± 61.452 m
10	137-10 1.20w 21	0.37468	9692.27 ± 1669.37	3.9E-0012	1.100 ± 0.171
11	137-11 1.40W 21	0.38553	11422.07 ± 2019.01	4.5E-0012	2.578 ± 0.130
12	137-12 1.60W 22	0.39711	6496.11 ± 1239.16	4.8E-0012	2.557 ± 0.182
13	137-13 1.80W 22	0.40481	9545.21 ± 2825.98	3.2E-0012	1.795 ± 0.213
14	137-14 2.20W 22	0.41206	10861.00 ± 3428.93	3.0E-0012	-0.034 ± 129.411 m
15	137-15 2.60W 22	0.42447	4357.79 ± 696.73	5.2E-0012	155.922 ± 191.391 m
16	137-16 3.00w 23	0.42987	5247.70 ± 1822.94	2.2E-0012	1.016 ± 0.432
17	137-17 5.00w 23	0.45560	2889.33 ± 214.20	1.1E-0011	631.365 ± 267.989 m
18	137-18 10w 23-S	1.00000	958.13 ± 5.03	2.3E-0010	345.727 ± 73.529 m

Table of Contents
Table of Contents
Table of Contents
Table of Contents

P23-137 HK12086 fd

No	Name	40Ar* Vol ccNTP/g	Atm Cont	F1	F2
1	137-01 0.20w 20	978.76 ± 906.99 E-15 (92.7%)	90.9289%	-1.3E-0003	-1.2E-0003
2	137-02 0.20w 20	684.87 ± 928.38 E-15 (135.6%)	89.1765%	4.1E-0003	3.9E-0003
3	137-04 0.25w 20	1.32 ± 1.01 E-12 (76.4%)	52.9524%	2.4E-0003	1.4E-0003
4	137-04 0.30w 20	9.18 ± 0.82 E-12 (8.9%)	53.8602%	-2.2E-0004	-1.6E-0004
5	137-05 0.30w re	4.25 ± 0.85 E-12 (19.9%)	47.9341%	1.2E-0003	8.3E-0004
6	137-06 0.50w 21	54.83 ± 0.66 E-12 (1.2%)	30.5672%	-5.0E-0004	-2.8E-0004
7	137-07 0.60w 21	104.26 ± 1.03 E-12 (1.0%)	15.9419%	-2.5E-0004	-4.1E-0005
8	137-08 0.80w 21	333.24 ± 1.95 E-12 (0.6%)	15.0837%	-2.4E-0004	-3.2E-0005
9	137-09 1.00w 21	239.23 ± 1.84 E-12 (0.8%)	6.7549%	-5.0E-0004	8.0E-0004
10	137-10 1.20w 21	124.15 ± 0.95 E-12 (0.8%)	3.0488%	-7.8E-0004	2.6E-0003
11	137-11 1.40W 21	170.05 ± 1.23 E-12 (0.7%)	2.5871%	-1.8E-0003	6.7E-0003
12	137-12 1.60W 22	101.09 ± 1.07 E-12 (1.1%)	4.5489%	-1.8E-0003	3.1E-0003
13	137-13 1.80W 22	100.31 ± 1.11 E-12 (1.1%)	3.0958%	-1.3E-0003	3.9E-0003
14	137-14 2.20W 22	107.91 ± 1.13 E-12 (1.1%)	2.7207%	2.4E-0008	-8.1E-0008
15	137-15 2.60W 22	70.97 ± 0.90 E-12 (1.3%)	6.7810%	-1.1E-0004	9.6E-0005
16	137-16 3.00w 23	37.69 ± 0.82 E-12 (2.2%)	5.6310%	-7.3E-0004	9.1E-0004
17	137-17 5.00w 23	93.96 ± 0.94 E-12 (1.0%)	10.2273%	-4.5E-0004	4.2E-0005
18	137-18 10w 23-S	507.98 ± 2.85 E-12 (0.6%)	30.8415%	-2.5E-0004	-2.2E-0004

Integrated Results:

Age = 79.748 ± 1.098 Ma

40Ar* / 39K = 915.414 ± 10.781

Total 39K Vol = 2.2526E-0012 ccNTP/g

Total 40Ar* Vol = 2.062 ± 0.005 E-9

(40Ar / 36Ar)sam = 1759.86 ± 16.40

Total Atm 40Ar Vol = 4.1612E-0010 ccNTP/g

(36Ar / 40Ar)sam = 0.00056823 ±0.00000689
(37Ar / 40Ar)sam = 0.00074066 ±0.00003220
(39Ar / 40Ar)sam = 0.00090898 ±0.00001054

Corr 36/40 & 39/40 ratios =-0.085678
Corr 36/40 & 37/40 ratios =-0.024150
Corr 37/40 & 39/40 ratios = 0.002845

37Ca / 39K = 8.148 ± 0.366 E-1

Mass = 1.000 g

F1 = -5.812 E-4

F2 = -2.170 E-4

Weighted Average of J from standards = 4.937 ± 0.038 E-5

Table of Contents
Table of Contents
Table of Contents
Table of Contents

P23 HK12078 Rambler Channel Fault: 146 M
NewAge 981201 AgeParams 990623 Cd liner (Fractionation relative to 40Ar/36Ar = 286.97)

No	Name		Temp	Cum 39K	Age	40Ar* / 39K
1	p23-06 ms	3-Au	1	0.02066	87.627 ± 14.039 Ma	1008.080 ± 165.46
2	p23-08 ms	3-Au	2	0.02846	84.924 ± 37.116 Ma	976.239 ± 436.79
3	p23-22 ms	3-Au	3	0.04510	74.221 ± 12.919 Ma	850.662 ± 151.13
4	p23-21 m	3-Aug	4	0.15916	44.188 ± 2.060 Ma	502.230 ± 23.70
5	p23-36 ms	5-Au	5	0.17959	77.910 ± 8.095 Ma	893.857 ± 94.90
6	p23-25 ms	5-Au	6	0.19786	66.455 ± 9.305 Ma	760.008 ± 108.39
7	p23-24 m	5-Aug	7	0.23067	77.266 ± 6.278 Ma	886.309 ± 73.57
8	p23-23 l	5-Aug	8	0.29460	77.523 ± 3.857 Ma	889.328 ± 45.21
9	p23-38 l	5-Aug	9	0.38893	84.878 ± 2.800 Ma	975.705 ± 32.95

No	Name		Cum 36S	40Ar / 36Ar	40ArAcc/g	37Ca / 39K
1	p23-06 ms	3-Au	0.03790	691.04 ± 24.59	2.4E-0011	-195.370 ± 198.589 m
2	p23-08 ms	3-Au	0.07432	446.10 ± 18.64	2.3E-0011	-145.739 ± 475.696 m
3	p23-22 ms	3-Au	0.09333	831.43 ± 77.52	1.2E-0011	-323.253 ± 231.656 m
4	p23-21 m	3-Aug	0.15278	989.23 ± 24.65	3.8E-0011	77.228 ± 38.815 m
5	p23-36 ms	5-Au	0.19585	600.89 ± 20.47	2.8E-0011	22.759 ± 199.471 m
6	p23-25 ms	5-Au	0.21553	803.12 ± 53.06	1.3E-0011	-96.542 ± 266.677 m
7	p23-24 m	5-Aug	0.25683	802.59 ± 26.18	2.6E-0011	16.774 ± 165.201 m
8	p23-23 l	5-Aug	0.31646	981.94 ± 20.90	3.8E-0011	39.860 ± 80.130 m
9	p23-38 l	5-Aug	0.40008	1087.96 ± 13.26	5.3E-0011	92.036 ± 34.802 m

No	Name		40Ar* Vol ccNTP/g		Atm Cont	F1	F2
1	p23-06 ms	3-Au	32.45 ± 0.87 E-12	(2.7%)	42.7615%	1.4E-0004	1.2E-0004
2	p23-08 ms	3-Au	11.87 ± 0.97 E-12	(8.2%)	66.2410%	1.0E-0004	9.8E-0005
3	p23-22 ms	3-Au	22.06 ± 1.14 E-12	(5.2%)	35.5412%	2.3E-0004	1.7E-0004
4	p23-21 m	3-Aug	89.28 ± 1.07 E-12	(1.2%)	29.8717%	-5.5E-0005	-2.5E-0005
5	p23-36 ms	5-Au	28.47 ± 0.95 E-12	(3.3%)	49.1770%	-1.6E-0005	-1.4E-0005
6	p23-25 ms	5-Au	21.63 ± 0.84 E-12	(3.9%)	36.7940%	6.9E-0005	5.1E-0005
7	p23-24 m	5-Aug	45.33 ± 0.89 E-12	(2.0%)	36.8183%	-1.2E-0005	-9.3E-0006
8	p23-23 l	5-Aug	88.61 ± 0.93 E-12	(1.0%)	30.0935%	-2.8E-0005	-2.0E-0005
9	p23-38 l	5-Aug	143.45 ± 0.98 E-12	(0.7%)	27.1610%	-6.6E-0005	-4.5E-0005

Integrated Results:

Age = 75.569 ± 1.315 Ma

40Ar* / 39K = 866.431 ± 13.867

(40Ar / 36Ar)sam = 919.31 ± 6.62

(36Ar / 40Ar)sam = 0.00108778 ±0.00000947
(37Ar / 40Ar)sam = 0.00002282 ±0.00001832
(39Ar / 40Ar)sam = 0.00078317 ±0.00001233

37Ca / 39K = 2.914 ± 2.340 E-2

F1 = -2.078 E-5

Total 39K Vol = 1.5585E-0012 ccNTP/g

Total 40Ar* Vol = 1.350 ± 0.005 E-9

Total Atm 40Ar Vol = 6.3966E-0010 ccNTP/g

Corr 36/40 & 39/40 ratios =-0.082245
Corr 36/40 & 37/40 ratios =-0.002153
Corr 37/40 & 39/40 ratios =-0.000633

Mass = 1.000 g

F2 = -1.492 E-5

Weighted Average of J from standards = 4.937 ± 0.038 E-5

Table of Contents
Table of Contents
Table of Contents
Table of Contents

GEO PUBLICATIONS AND ORDERING INFORMATION
土力工程處刊物及訂購資料

A selected list of major GEO publications is given in the next page. An up-to-date full list of GEO publications can be found at the CEDD Website http://www.cedd.gov.hk on the Internet under "Publications". Abstracts for the documents can also be found at the same website. Technical Guidance Notes are published on the CEDD Website from time to time to provide updates to GEO publications prior to their next revision.

部份土力工程處的主要刊物目錄刊載於下頁。而詳盡及最新的土力工程處刊物目錄，則登載於土木工程拓展署的互聯網網頁 http://www.cedd.gov.hk 的"刊物"版面之內。刊物的摘要及更新刊物內容的工程技術指引，亦可在這個網址找到。

Copies of GEO publications (except maps and other publications which are free of charge) can be purchased either by:

writing to
Publications Sales Section,
Information Services Department,
Room 402, 4th Floor, Murray Building,
Garden Road, Central, Hong Kong.
Fax: (852) 2598 7482

or
- Calling the Publications Sales Section of Information Services Department (ISD) at (852) 2537 1910
- Visiting the online Government Bookstore at http://bookstore.esdlife.com
- Downloading the order form from the ISD website at http://www.isd.gov.hk and submit the order online or by fax to (852) 2523 7195
- Placing order with ISD by e-mail at puborder@isd.gov.hk

讀者可採用以下方法購買土力工程處刊物(地質圖及免費刊物除外):

書面訂購
香港中環花園道
美利大廈4樓402室
政府新聞處
刊物銷售組
傳真: (852) 2598 7482

或
- 致電政府新聞處刊物銷售小組訂購 (電話：(852) 2537 1910)
- 進入網上「政府書店」選購，網址爲 http://bookstore.esdlife.com
- 透過政府新聞處的網站 (http://www.isd.gov.hk) 於網上遞交訂購表格，或將表格傳真至刊物銷售小組 (傳真：(852) 2523 7195)
- 以電郵方式訂購 (電郵地址：puborder@isd.gov.hk)

1:100 000, 1:20 000 and 1:5 000 maps can be purchased from:

Map Publications Centre/HK,
Survey & Mapping Office, Lands Department,
23th Floor, North Point Government Offices,
333 Java Road, North Point, Hong Kong.
Tel: 2231 3187
Fax: (852) 2116 0774

讀者可於下列地點購買1:100 000，1:20 000及1:5 000地質圖：

香港北角渣華道333號
北角政府合署23樓
地政總署測繪處
電話: 2231 3187
傳真: (852) 2116 0774

Requests for copies of Geological Survey Sheet Reports, publications and maps which are free of charge should be sent to:

For Geological Survey Sheet Reports and maps which are free of charge:
Chief Geotechnical Engineer/Planning,
(Attn: Hong Kong Geological Survey Section)
Geotechnical Engineering Office,
Civil Engineering and Development Department,
Civil Engineering and Development Building,
101 Princess Margaret Road,
Homantin, Kowloon, Hong Kong.
Tel: (852) 2762 5380
Fax: (852) 2714 0247
E-mail: jsewell@cedd.gov.hk

For other publications which are free of charge:
Chief Geotechnical Engineer/Standards and Testing,
Geotechnical Engineering Office,
Civil Engineering and Development Department,
Civil Engineering and Development Building,
101 Princess Margaret Road,
Homantin, Kowloon, Hong Kong.
Tel: (852) 2762 5346
Fax: (852) 2714 0275
E-mail: wmcheung@cedd.gov.hk

如欲索取地質調查報告、其他免費刊物及地質圖，請致函：

地質調查報告及地質圖:
香港九龍何文田公主道101號
土木工程拓展署大樓
土木工程拓展署
土力工程處
規劃部總土力工程師
(請交:香港地質調查組)
電話: (852) 2762 5380
傳真: (852) 2714 0247
電子郵件: jsewell@cedd.gov.hk

其他免費刊物:
香港九龍何文田公主道101號
土木工程拓展署大樓
土木工程拓展署
土力工程處
標準及測試部總土力工程師
電話: (852) 2762 5346
傳真: (852) 2714 0275
電子郵件: wmcheung@cedd.gov.hk

MAJOR GEOTECHNICAL ENGINEERING OFFICE PUBLICATIONS
土力工程處之主要刊物

GEOTECHNICAL MANUALS

Geotechnical Manual for Slopes, 2nd Edition (1984), 300 p. (English Version), (Reprinted, 2000).

斜坡岩土工程手冊(1998)，308頁(1984年英文版的中文譯本)。

Highway Slope Manual (2000), 114 p.

GEOGUIDES

Geoguide 1	Guide to Retaining Wall Design, 2nd Edition (1993), 258 p. (Reprinted, 2000).
Geoguide 2	Guide to Site Investigation (1987), 359 p. (Reprinted, 2000).
Geoguide 3	Guide to Rock and Soil Descriptions (1988), 186 p. (Reprinted, 2000).
Geoguide 4	Guide to Cavern Engineering (1992), 148 p. (Reprinted, 1998).
Geoguide 5	Guide to Slope Maintenance, 3rd Edition (2003), 132 p. (English Version).
岩土指南第五冊	斜坡維修指南，第三版(2003)，120頁(中文版)。
Geoguide 6	Guide to Reinforced Fill Structure and Slope Design (2002), 236 p.

GEOSPECS

Geospec 1	Model Specification for Prestressed Ground Anchors, 2nd Edition (1989), 164 p. (Reprinted, 1997).
Geospec 3	Model Specification for Soil Testing (2001), 340 p.

GEO PUBLICATIONS

GCO Publication No. 1/90	Review of Design Methods for Excavations (1990), 187 p. (Reprinted, 2002).
GEO Publication No. 1/93	Review of Granular and Geotextile Filters (1993), 141 p.
GEO Publication No. 1/2000	Technical Guidelines on Landscape Treatment and Bio-engineering for Man-made Slopes and Retaining Walls (2000), 146 p.
GEO Publication No. 1/2006	Foundation Design and Construction (2006), 376 p.

GEOLOGICAL PUBLICATIONS

The Quaternary Geology of Hong Kong, by J.A. Fyfe, R. Shaw, S.D.G. Campbell, K.W. Lai & P.A. Kirk (2000), 210 p. plus 6 maps.

The Pre-Quaternary Geology of Hong Kong, by R.J. Sewell, S.D.G. Campbell, C.J.N. Fletcher, K.W. Lai & P.A. Kirk (2000), 181 p. plus 4 maps.

TECHNICAL GUIDANCE NOTES

TGN 1	Technical Guidance Documents